UNIVERSITA' DEGLI STUDI DI ROMA
"LA SAPIENZA"

FACOLTA' DI SCIENZE MATEMATICHE,
FISICHE E NATURALI

Dottorato di Ricerca in Scienze Chimiche
- Curriculum "Chimica macromolecolare e biologica" –

XXIV CICLO

"*Perylene derivatives in biological systems: application as fluorescent probes in models for nanotechnology*"

Supervisore:

Dottorando:

Prof. Armandodoriano Bianco

Dott.ssa Silvia Borioni

Correlatore:
Dott.ssa Giovanna Mancini

INDEX

1. INTRODUCTION

In this thesis, the synthesis and the study of spectroscopic features of new perylene derivates are discussed, applied to biological systems. In particular, their fluorescence has been studied in two different fields: DNA aptamers and phospholipids bilayers. In the introduction of the thesis, the reasons for the choice of perylene dyes in our studies is explained (paragraph 1.1).

As a background of our studies on DNA aptamers, unusual G-quadruplex DNA secondary structures are described (paragraph 1.2.1). Then, the methods to study the conjugated aptamers with fluorescent probes are presented (paragraph 1.2.2).

In the second part of the introduction, lipid systems are discussed. In particular different fluorescent lipid analogues are described (paragraph 1.3.1), together with their current applications (paragraph 1.3.2).

1.1 Perylene dyes

Most of perylene pigments are solid and red, but other orange, bordeaux, bluish black and black derivatives are also known. Perylene pigments have received considerable attention in academic as well as industrial dye and pigment research. Several members of the perylene family found high grade industrial applications as pigments thanks to their clarity and transparency. One application is in the dyestuffs industry, especially in the production of water colour or acrylics.

Many perylene pigments show low solubility in organic solvents, however, all perylene pigments are soluble in concentrated sulphuric acid via protonation that causes a bathochromic shift of the absorption of 80 nm, with respect to the neutral free perylene pigment.

Different kinds of substituents can be introduced at the perylene core (Figure **1.1-1**). The nature of the substituents as well as the position at which they are attached to the perylene core has a strong impact on the resulting solubility as well as the optical properties, such as HOMO/LUMO energies, absorption wavelengths (λ_{max}), and the spatial properties of the molecular orbitals. (Langhals, 2005). In this way, the introduction of substituents offers access to a large portfolio of tailored functional perylene, which can be functionalized for the desired application.

Perylene diimide (PDI) (Figure **1.1-2)** are among the most valuable functional dyes and have numerous potential applications. Their application is possible thank to high chemical, thermal, and photochemical stability. Moreover, these compounds display high fluorescent quantum yields.

Moreover, the solubility of these derivates can be improved modifying the length and the nature of substituents in the N position. Perylene diimides are highly versatile molecules, which attract a great interest owing to their applications in diverse fields of physical organic chemistry, such as dye

lasers (Sadrai et al. 1992), light harvesting arrays (Tomizaki et al. 2002), organic electronic devices (Kraft et al. 1998, Würthner & Schmidt 2006) and liquid crystalline dyes (Zollinger 1991, Rohr et al. 1998, Rohr et al. 2001).

Moreover, the extended quadrupolar π system of this class of dyes has facilitated the construction of numerous supramolecular architectures with fascinating photophysical properties. However, the supramolecular approach to the formation of perylene bisimide aggregates has been restricted mostly to organic media. Pleasingly, considerable progress has been made in the last few years in developing water-soluble perylene bisimides and their application in aqueous media.

PDIs can be functionalized with water-solubility-mediating substituents at the imide as well as at the bay position (Figure **1.1-3**), thus offering versatile opportunities for structural variations that are

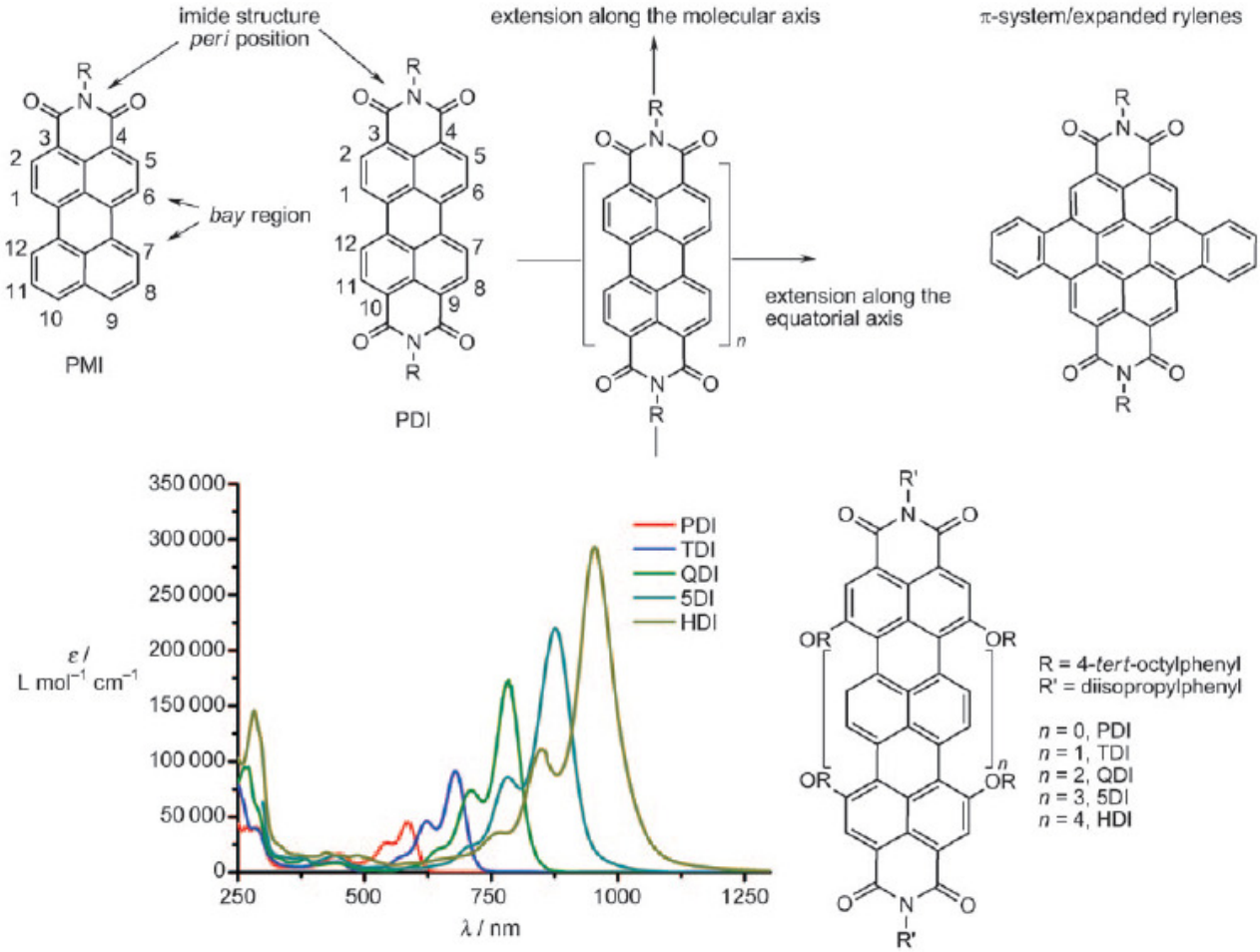

(Figure **1.1-1**): Top: Chemical structures of unsubstituted peryleneimide chromophores: Perylene-3,4-dicarboximide (PMI) and perylenebis(dicarboximide) (PDI), illustration of the bay and peri positions, as well as the concept of achieving higher order rylenes by extending the aromatic scaffold. Bottom: Absorption spectra of the entire tetraphenoxy-substituted rylenediimide series in $CHCl_3$: Perylenebis(dicarboximide) (PDI), terrylenebis(dicarboximide) (TDI), quaterrylenebis(dicarboximide) (QDI), pentarylenebis(dicarboximide) (5DI), hexarylenebis(dicarboximide) (HDI). (Langhals, 2005)

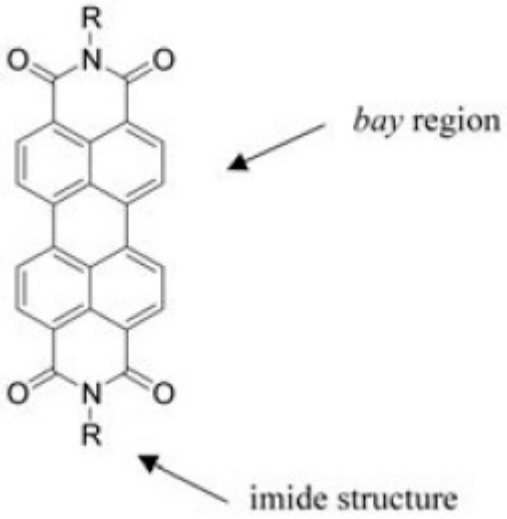

(Figure **1.1-2**): a lot of N,N'-disubstituted perylene diimides are present in literature.

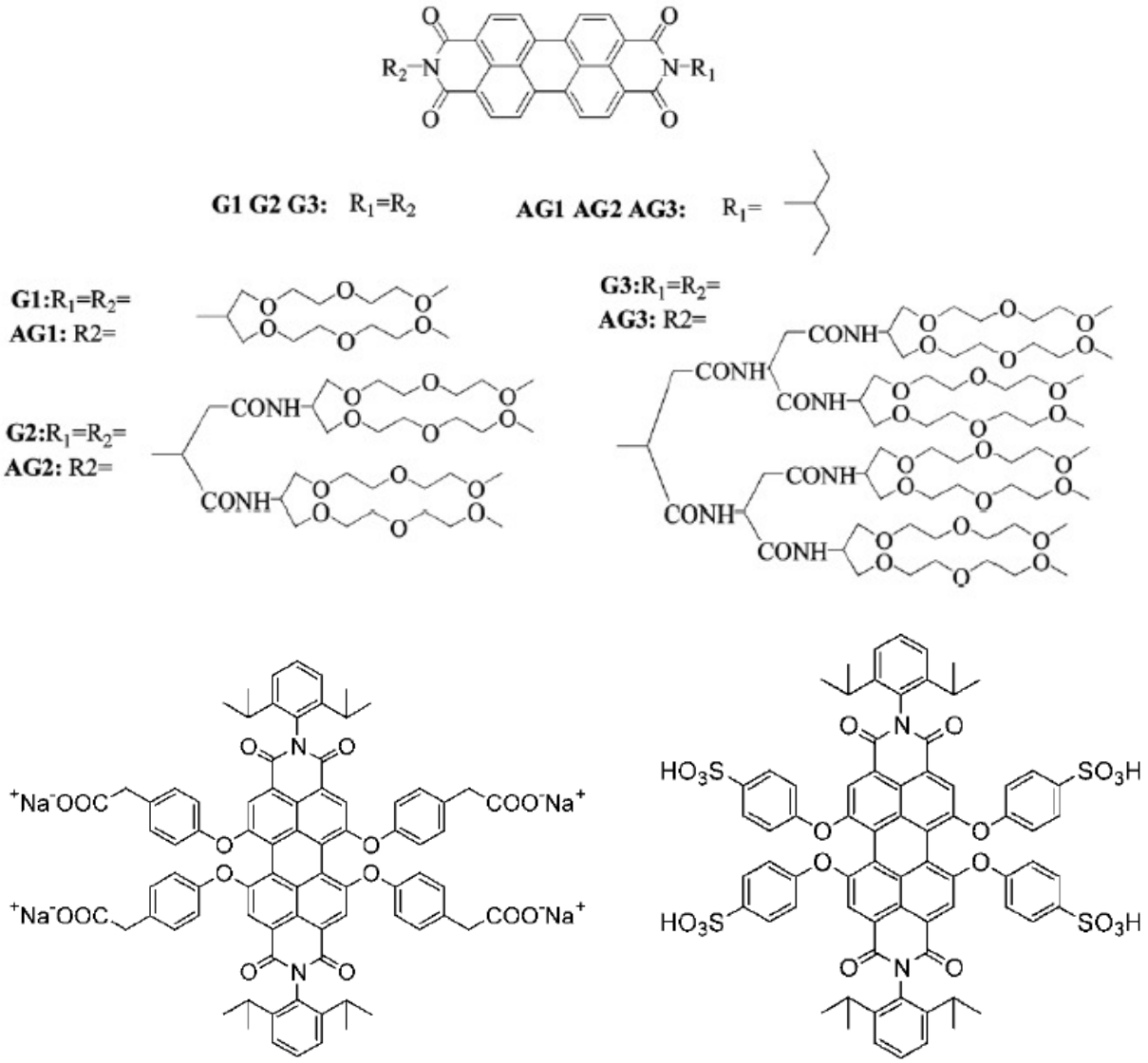

(Figure **1.1-3**): Examples of PDIs functionalized with substituents at the imide as well as at the bay position (Khol et al., 2004; Liu et al., 2012).

at best only rudimentarily explored so far. Water-soluble PDIs that are accessible by this approach possess strongly hydrophobic π surfaces, which can interact with themselves or with other π systems. It is quite encouraging that well-defined PDI dye aggregates and bilayer membranes can already be obtained in water, since the natural light-harvesting systems impressively illustrate the function and the benefit of highly organized membrane bound dye aggregates.

The hydrophobic effect plays a decisive role in many important phenomena, such as molecular self-assembly, formation of micelles and biological membranes, and protein folding (Blokzijl et al., 1993; Israelachvili, 1991) Although several noncovalent interactions, for example, hydrogen bonding, are specific and directional in the formation of supramolecular structures, this is usually not the case for hydrophobic interactions. Therefore, the structures of supramolecular aggregates formed in water can not be predicted as easily as in the case of organic media. Nevertheless, water offers many opportunities and advantages as a solvent for supramolecular chemistry compared with organic media.

In this regard, aggregates of π-conjugated dye molecules are, in particular, the focus of interest. Inspired by natural supramolecular structures such as, for example, the DNA double helix or (bacterio)chlorophyll arrays of the photosynthesis apparatus, numerous functional architectures based mainly on π -conjugated dye molecules have been synthesized through noncovalent interactions, particularly π – π interactions.

Supramolecular architectures with highly promising optical and electronic properties, which are not inherent to the respective individual molecules, could be generated by this approach, and thus facilitated, for example, efficient energy and electron transfer (Gonzàlez-Rodrìguez et al., 2011; Würthner et al., 2011). The π – π interactions between individual building blocks used for self-assembly reflect the sum of noncovalent interactions including electrostatic and dispersion interactions as well as attractive (charge transfer (CT)) and repulsive orbital interactions (Hunter, et al., 1990). Since the individual contributions are strongly solvent-dependent, especially in water, this may lead to large binding constants because the hydrophobic effect makes the largest contribution to the standard Gibbs free energy for aggregate formation. It turned out to be a great challenge to generate such molecular aggregates in aqueous media, as this requires the introduction of an adequate number of polar, water-solubility-mediating functionalities into the parent building blocks. This has been achieved for one-dimensional π –conjugated oligomers such as π –phenylenes (Ryu et al., 2008), π –oligophenylenevinylenes (Hoeben et al., 2006) and ligophenyleneethinylenes (Garcìa et al.,2010) as well as for two-dimensional, extended polycyclic aromatic compounds such as triphenylenes (Hughes et al., 2002) and hexabenzocoronenes (Zhang et al., 2007). Remarkably,

the prospect of using PDI dyes (Würthner, 2004; Langhals, 1995) to construct supramolecular aggregates in aqueous medium has been approached relatively late.

Recently, a library of N-N'-disubstituted perylene diimides having the same perylene core but differently functionalized side chains have been extensively studied by our research group (Alvino et al., 2007) (Figure **1.1-4**).

We have shown that the new three and four basic side chain perylene derivatives are characterized by excellent water solubility without aggregation, differently from the previously synthesized two-chained perylene diimides. Their colours range from blue to green in the solid state and in neutral and slightly acid solutions. Furthermore the broad absorption bands over 600 nm, due to charge transfer absorption, which characterize the UV–vis spectra of these compounds disappear or are greatly reduced in concentrated acid, when the conjugation of the N atom and the aromatic core of perylene is hindered.

Water-soluble PBIs with ionic substituents at the imide positions that exhibited intensive fluorescence in water were already known in the 1980s and 1990s (Ford, 1986; Schnurpfeil et al., 1995). Moreover, Ford showed that PBI containing two glycine residues forms aggregates in basic aqueous solutions whose fluorescence is quenched nearly completely compared to that of the respective monomers (fluorescence quantum yield, FQY $\Phi_f \approx 100\%$) (Ford, 1987).

Fluorescence is ideally suited for observation of the location and interaction of biologically active probes in vivo, since it is non-invasive and can be detected with high sensitivity and signal specificity (Bastiaens et al., 1999). In particular, in vivo investigations of biological targets require chromophores giving FQYs in water and displaying absorption and emission maxima in an area that does not interfere with the self-absorption wavelength of the cell: above 500 nm, for example (Hope-Ross et al., 1994). In recent years the investigation of individual biologically active macromolecules such as DNA and proteins has become very popular since it provides better insight into their dynamics and interaction partners than measurements made on ensembles (Moerner and Orrit, 1999).

For such measurements, however, the photostability of the chromophore plays a crucial role. Despite the large variety of water-soluble chromophores commercially available today (Haugland, 1989) there are almost no chromophores that meet all the following criteria: 1) water solubility, 2) high fluorescence intensities, 3) absorption and emission maxima above 500 nm, 4) no toxicity, and 5) high photostability. In organic solvents, perylene-3,4,9,10-tetracarboxylic acid diimide chromophores display exceptional chemical, thermal, and photochemical stability with high fluorescence quantum yields close to unity (Rademacher, 1982; Zollinger, 1987).

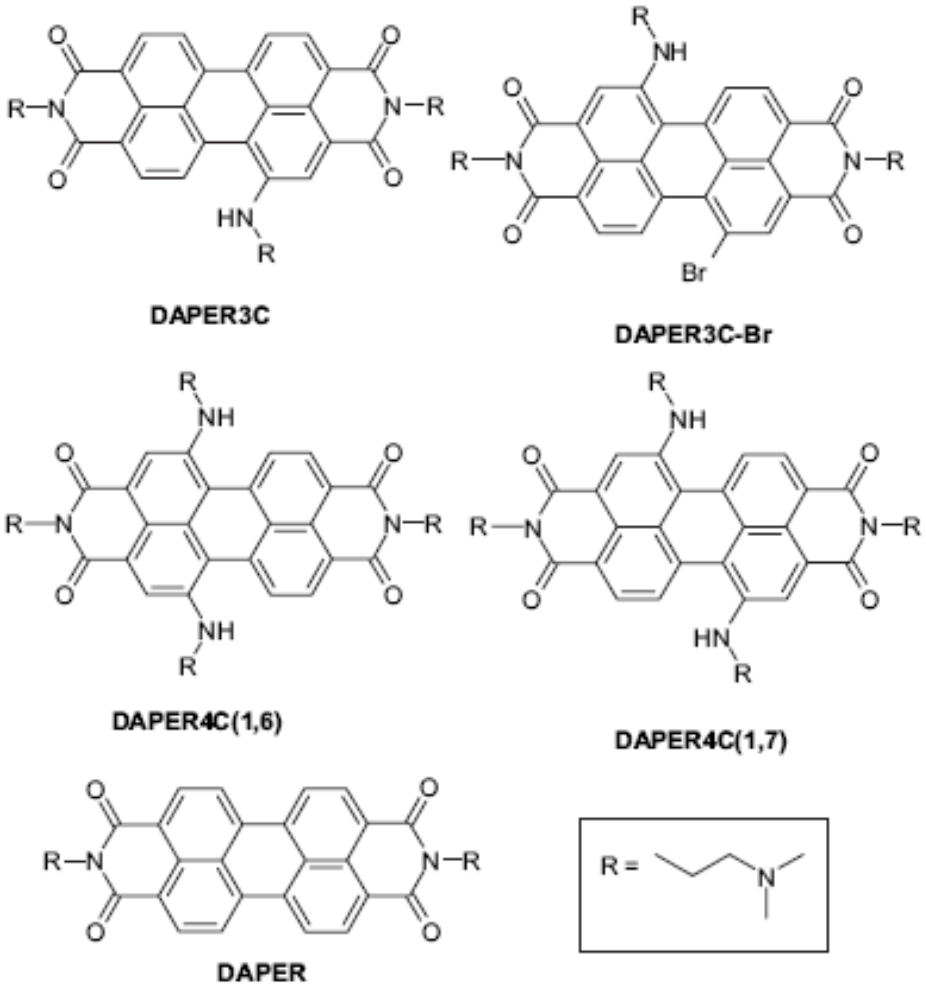

(Figure **1.1-4**): N-N'-disubstituted perylene diimides having different side chains (Alvino et al. 2007)

Therefore, thanks to these unique properties, PDI chromophores should also be ideally suited as high-performance fluorescent labels for biologically active probes.

Many approaches were made to obtain readily soluble perylene pigments by substitution with tert-butyl group or with long-chain second alkyl groups (Langhals, 1995). An intensely fluorescent perylenebis(dicarboximide) shows λ_{max} 526 nm, ε 95 000, and a FQY of 0.99 (Langhals, 1985). Whereas perylenebis(dicarboximide) containing trialkylamino groups in alkyl amino group are virtually non-fluorescent. But quaternization of the trialkylamino group with alkyl iodide resulted in an increase in the fluorescence (Deliggeorgiev et al., 1994, Schnurpfeil et al., 1995).
The excellent lightfastness of perylene pigments makes many application possible. Together with the photostability the perylene pigments are also very thermally stable with some derivatives able to sublimed at up to 550°C.
Recently, Kohl and co-workers (2004), have presented different synthetic approaches towards fluorescent, water-soluble perylenetetracarboxylic acid diimide chromophores. The introduction of hydrophilic substituents onto the bay region of the chromophore results in a loss in planarity of the aromatic scaffold, and water-soluble chromophores displaying low to moderate FQYs (7%–75%) were obtained. To suppress aggregation, the chromophore was further isolated within a dendritic shell. Such variation of structural features and a thorough investigation of the resulting optical properties facilitated the first synthesis of perylene-3,4:9,10-tetracarboxylic acid diimides combining the properties of water solubility and fluorescence quantum yields (FQYs) close to unity.

1.2 G-quadruplex: structures and application in nanotechnology

1.2.1 G-quadruplex DNA structures

The ability for DNA and RNA to form structures containing more than two strands has been known since the earliest physical studies of nucleic acids. In the past decade, interest in multistranded DNA

structures has been renewed for two principle reasons: 1) the potential use of nucleic acids as therapeutics; and 2) evidence that alternative DNA structures (i.e. non-B-form) may have specific functional roles in vivo.

G-quadruplex are a family of nucleic acid secondary structures, built upon the motif of the guanine quartet (Williamson 1993, Williamson 1994). Each quartet is composed of four guanines, held together by a cyclic arrangement of eight hydrogen bonds. Two or more guanine tetrads can stack upon each other to form four-stranded structures, these are collectively referred to as G-quadruplexes, or DNA tetraplexes. The presence of a central cation helps to the stability of the structure, which can be very stable under physiological conditions (Figure **1.2-1**).

Many structural studies (by X-ray crystallography and NMR) have shown a surprising structural polymorphism of G-quadruplexes. A classification is possible on the basis of:

1. Strand Stoichiometry: Intermolecular quadruplexes are formed by two or four separate strands associating together, intramolecular quadruplexes by the folding of either two or four consecutive repeats (Figure **1.2-2**)
2. Strand Polarity Polymorphism: the strand or strands that constitute a G-quadruplex can come together in four different ways. They can be all parallel (Aboul-ela et al., 1992, 1994; Wang and Patel 1992, 1993 ;Phillips et al., 1997), three parallel and one antiparallel (Wang and Patel 1994, Wang and Patel 1995), adjacent parallel (Smith and Feigon 1992; Wang and Patel 1993b; Catasti et al. 1996), or alternating antiparallel (Kang et al. 1992; Macaya et al. 1993; Wang et al. 1993; Schultze et al., 1994a, b) (Figure **1.2-3**)
3. Glycosidic Torsion Angle Variation: The bases in normal B-DNA are found exclusively in the anti conformation, whereas guanines involved in formation of guanine tetrads are observed both in syn and anti conformations (Figure **1.2-4**). However, restrictions apply to adjacent guanines involved in the same guanine tetrad. If they are on parallel strands, they must have the same glycosidic torsion angles, and conversely if they are on antiparallel strands they must have opposite glycosidic torsion angles. The glycosidic conformation changes the relative orientations of the bases in contiguous guanine tetrads, and affects the stacking energy. An additional feature that originates

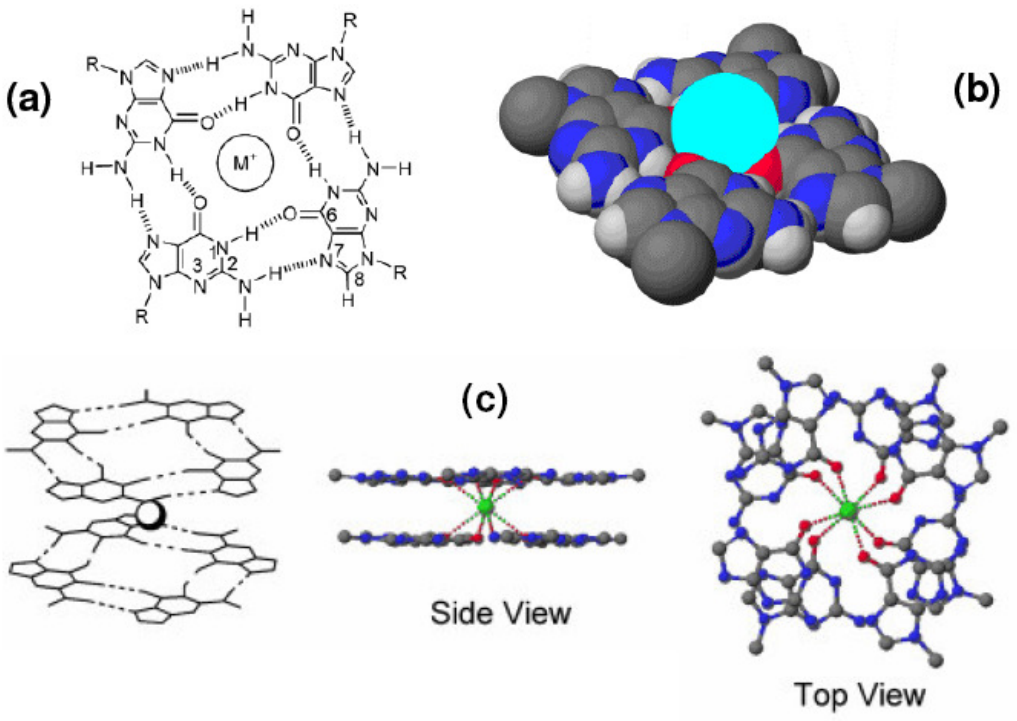

(Figure **1.2-1**): (a) the arrangement of hydrogen bonds in a G-tetrad. (b) X-ray derived model of a Gquartet; the central cation is coloured in cyano.(c) the presence of a central cation (typically potassium or sodium) helps to maintain the stability of the G-quadruplex structure.

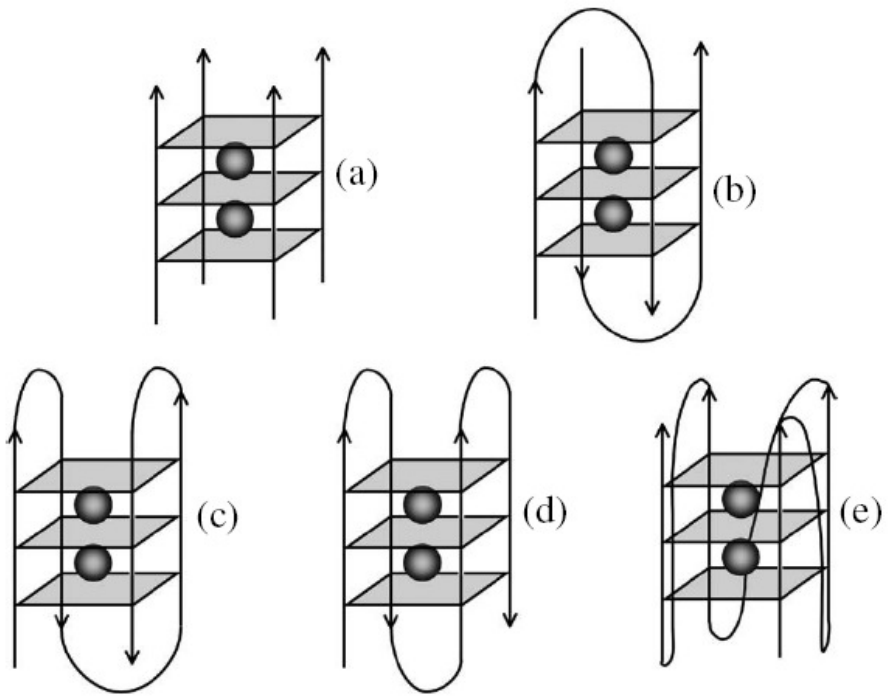

(Figure **1.2-2**): Schematic description of the different G-quadruplex topologies (a) tetrameric parallel; (b) dimeric antiparallel; (c) monomeric antiparallel; (d) monomeric antiparallel; (e) monomeric parallel. (Huppert et al 2007)

(Figure **1.2-3**): The possible orientations of four DNA strands (Neidle & Parkinson, 2002).

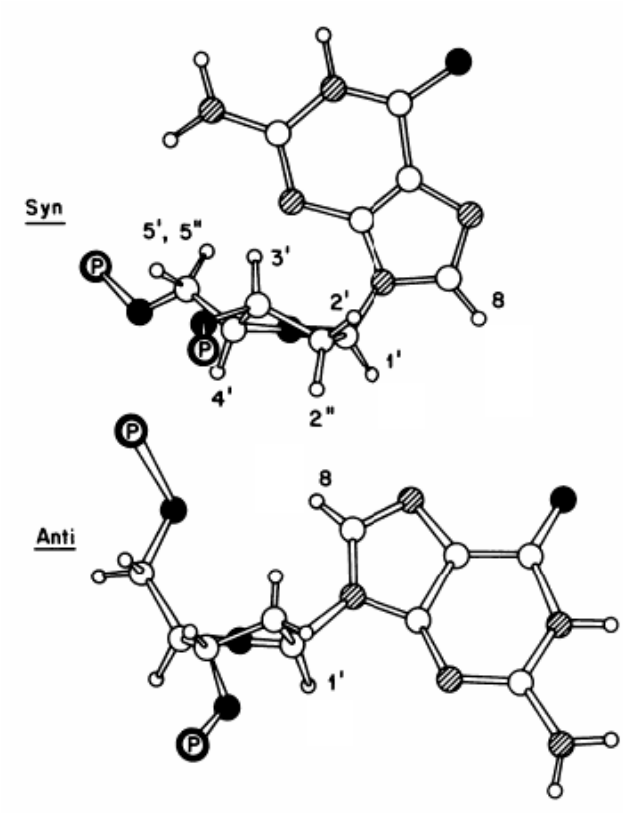

(Figure **1.2-4**): Syn and anti conformations of the glycosidic bond connecting the guanine base to the sugar-phosphate backbone (Williamson 1994).

from the glycosidic torsion angle pattern is the size of the four grooves produced by the stacking of guanine tetrads. Guanines that belong to adjacent strands and have the same glycosidic torsion angles produce medium grooves, whereas guanines that belong to adjacent antiparallel strands and have opposite glycosidic torsion angles produce one wide and one narrow groove .

4. Connecting Loops: The loops that connect guanine tracts participating in the formation of unimolecular or bimolecular G-quadruplexes can run in a number of different ways.

Sequences that exhibit G-quadruplex formation motifs are widely dispersed in eukaryotic genomes. G-quadruplex forming elements can be found in the telomeres (Blackburn, 1991), the immunoglobulin switch regions (Sen and Gilbert, 1988, 1990), the promoter regions of c-myc and other oncogenes (Simonsson et al., 1998; Simonsson and Sjöback, 1999), the retinoblastoma susceptibility gene (Murchie and Lilley, 1992), and upstream of the insulin gene (Bell et al., 1982). Whole genome studies have been performed to look at the occurrence of G-quadruplex motifs in human gene promoters (Huppert et al. 2007). This work showed that almost half (43%) of all known genes contained G-quadruplex motifs in their promoter regions (defined as a 1 kb region upstream of the annotated transcription start site (TSS)).

This is significantly more than would be expected by chance, suggesting a general functional role. There is a particular concentration of predicted G-quadruplexes in the few hundred bases immediately upstream of the TSS, where the overrepresentation exceeds an order of magnitude. Interestingly, the sequences found in this region are also predicted to be especially stable, by virtue of having single-base loops. The functions of genes predicted to have promoter G-quadruplexes are also highly non-random. Oncogenes are much more likely to have promoter G-quadruplex motifs than other genes, with 69% of them having such motifs. Some gene ontology categories are either much more or much less likely to have putative promoter G-quadruplexes; genes involved in transcription factor activity, development, neurogenesis and kinase activity are more likely to have putative promoter G-quadruplexes, and genes involved in olfaction, G-protein signalling, immune response, nucleic acid binding and protein biosynthesis are much less likely to have such structures, suggesting differential regulatory systems for these genes. Broadly, genes requiring high levels of regulatory control seem to be more likely to have promoter G-quadruplex motifs.

Although the structures of G-quadruplexes have been well studied in vitro, if, when and where they form in vivo and how they might affect cell biology have remained key questions. The structural heterogeneity of quadruplexes makes it difficult to obtain universal rules to predict their formation or probes to test for their presence. Nonetheless, a good deal of information demonstrating or strongly suggesting their functions in vivo has emerged in recent years (Johnson et al. 2008). For example, telomeric G4-DNA has been proven to exist in Stylonichia lemnae using highly specific

G4-DNA antibodies and immunofluorescence microscopy (Paeschke et al. 2005, Schaffitzel et al. 2001). Other observations suggest that G4-DNA might form at mammalian telomeres. These include demonstrations that loss of the Werner, Bloom or RTEL helicases results in defects in telomere maintenance in vivo (Crabbe et al 2004, Ding et al. 2004, Du et al. 2004). The Werner and Bloom helicases are particularly adapt at unwinding G-quadruplex substrates in vitro (Huber et al. 2002, Sun et al. 1998), while RTEL is homologous to the C. elegans DOG-1 protein that prevents deletions in G-rich sequences (Ding et al. 2004, Cheung et al. 2002). Further, the human telomere binding protein POT1, which binds the single stranded telomere overhang, inhibits G4-DNA formation in vitro (Zaug et al. 2005), while treatment of cells with the quadruplex-selective ligand telomestatin displaces POT1 and uncaps telomeres (i.e. causes them to be recognized as DNA breaks) (Gomez et al. 2006). Therefore, POT1 binding and G4-DNA formation at the telomere are likely mutually exclusive states. However, the distribution of telomeres between these states in untreated cells is currently unknown. Sequences with intramolecular quadruplex forming potential in the promoter regions of diverse organisms have been shown to be connected with control of gene expression. Infact, a number of small molecule ligands have been identified that bind to and stabilize quadruplexes, and some of these have been found to affect expression from intramolecular quadruplex forming potential containing loci, indicating that these sequences can adopt G4 conformations. A prominent example is c-MYC which has been particularly well characterized (Ambrus et al. 2005). This oncogene is an important transcription factor, which regulates a wide variety of genes, especially those involved with proliferation, differentiation and apoptosis (Marcu et al. 1992). It has a number of nuclease hypersensitive regions (regions of DNA that are especially susceptible to enzymatic cleavage) in its promoter, one of which is responsible for a large majority of the transcriptional activity, and contains the sequence d(GGG GAG GGT GGG GAG GGT GGG GAA GG), which forms a family of stable G-quadruplex sequences (Ambrus et al. 2005). Stabilization of these structures using the porphyrin-derived G-quadruplex ligand TMPyP4 resulted in down regulation of the c-myc oncogene in vivo (Siddiqui-Jain et al. 2002). Although TMPyP4 has little selectivity for binding G4-DNA in comparison to duplex DNA, repression of c-MYC by the ligand is abolished by point mutations that ought to abrogate quadruplex formation by the intramolecular quadruplex forming potential sequence. Similar inhibition of KRAS expression by TMPyP4 and of c-KIT by several selective trisubstituted alloisoxazines has been reported (Bejugam et al. 2007, Cogoi et al. 2006). This work stimulated considerable interest in Gquadruplexes in oncogenic promoters, and a number of individual examples have been studied and characterized, such as VEGF (Sun et al. 2005), HIF- 1a (de Armond et al. 2005), BCL2 (Dai et al. 2006), PDGF-A

(Qin et al. 2007), RET (Sun et al. 2003) and c-KIT (Rankin et al. 2005, Fernando et al 2006), which contains two such sequences.

One model for the effect of these sequences consists of an equilibrium between a folded and unfolded form of the G-quadruplex motif, resulting in transcriptional change (Figure **1.2-5**). One mechanism by which this could happen involves the G-quadruplex acting as a steric block to the transcription machinery (Huppert 2008). Quadruplex-interacting proteins may potentially mediate the equilibrium exchange. It should be noted that the formation of G-quadruplexes in promoters might result in either an increase or a decrease in expression.

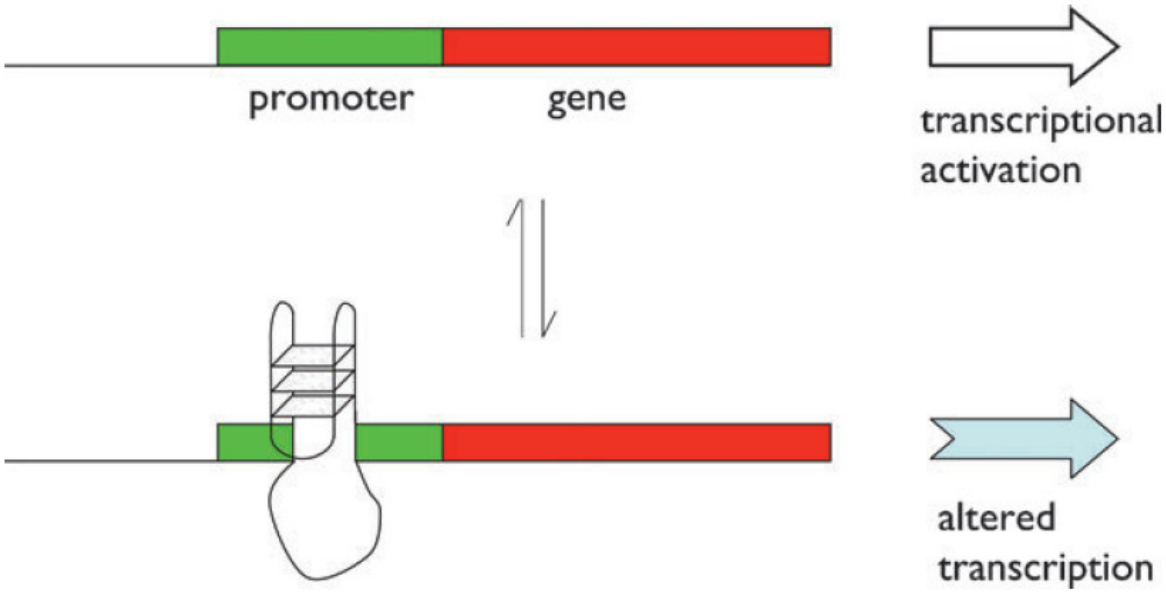

(Figure **1.2-5**): G-quadruplex structure formation in promoters could alter gene transcription. (Huppert 2008)

1.2.2 Fluorescent G-quadruplex DNA: supramolecular chemistry

G-rich synthetic oligonucleotides have shown promising biological and possibly pharmacological properties ranging from anticancer to anti-HIV activities; G-quadruplex formation has been shown to be essential in determining these biological effects in all cases (Dapic´ et al. 2003). When a specific target molecule is defined for the biochemical action of these oligonucleotides, the oligonucleotide is referred to as an "aptamer". The most widely studied G-quadruplex-forming aptamer class is that of the thrombin-binding aptamers (TBAs), which bind to α-thrombin, a fundamental protein involved in blood coagulation, preventing thrombosis (Bock et al. 1992, Wang et al. 1993b). G-quadruplex conformation and stability have been determined to be key parameters in defining the biophysical and biological properties of these aptamers (Pagano et al. 2008). Modified TBAs, including oligonucleotides containing an acyclic nucleotide (Coppola et al. 2008), have been reported to enhance G-quadruplex stability and anticoagulant activity.

Another bioactive quadruplex- forming oligonucleotide, a 26-mer nucleotide named "AS1411" (Antisoma, London, UK), has been shown specifically to inhibit cancer cell proliferation: the activity of this aptamer has been related to its binding to certain nucleolin containing complexes (Teng et al. 2007). AS1411 has completed phase I clinical trials, and phase II clinical trials have recently begun (Bates et al. 2007). Another family of guanine-rich oligonucleotides has been developed as potential anti-HIV therapeutic drugs (Held et al. 2006). These compounds have demonstrated strong interaction with HIV-1 integrase in vitro and the ability to inhibit the integration of viral DNA into host DNA (Jing et al. 2000a). Among several different G-quartet oligonucleotides proposed and studied for their ability to inhibit HIV, the most efficient was the 17-mer oligonucleotide 5'-GTGGTGGGTGGGTGGGT, referred to as Zintevir (AR177 or T30177), as well as two 16-mer oligonucleotides (T30695 and 93del) and the shorter sequence TTGGGGTT (ISIS 5320) (Jing et al. 2000a, Chou et al., 2005) Because of the importance of the structural stabilities of the G-quadruplexes formed by these aptamers for their activities (Jing et al. 2000b) several synthetic approaches to improving the stabilities of the G-quadruplexes formed by short G-rich sequences have been proposed, either through the introduction of large aromatic substituents at their 5'-ends (D'Onofrio et al. 2007) or by tethering them to a suitable linker to afford constrained quadruplexes (Figure **1.2-6**) (Oliviero et al., 2004; Oliviero et al., 2006; Murat et al., 2008).

G-quartets show molecular self-assembly features typical of supramolecular chemistry: these properties have awakened interest in the use of such structures in nanotechnology (Davis, 2004). Such self-organization of noncovalent assemblies of G-quartets, for instance, leads to liquid crystals

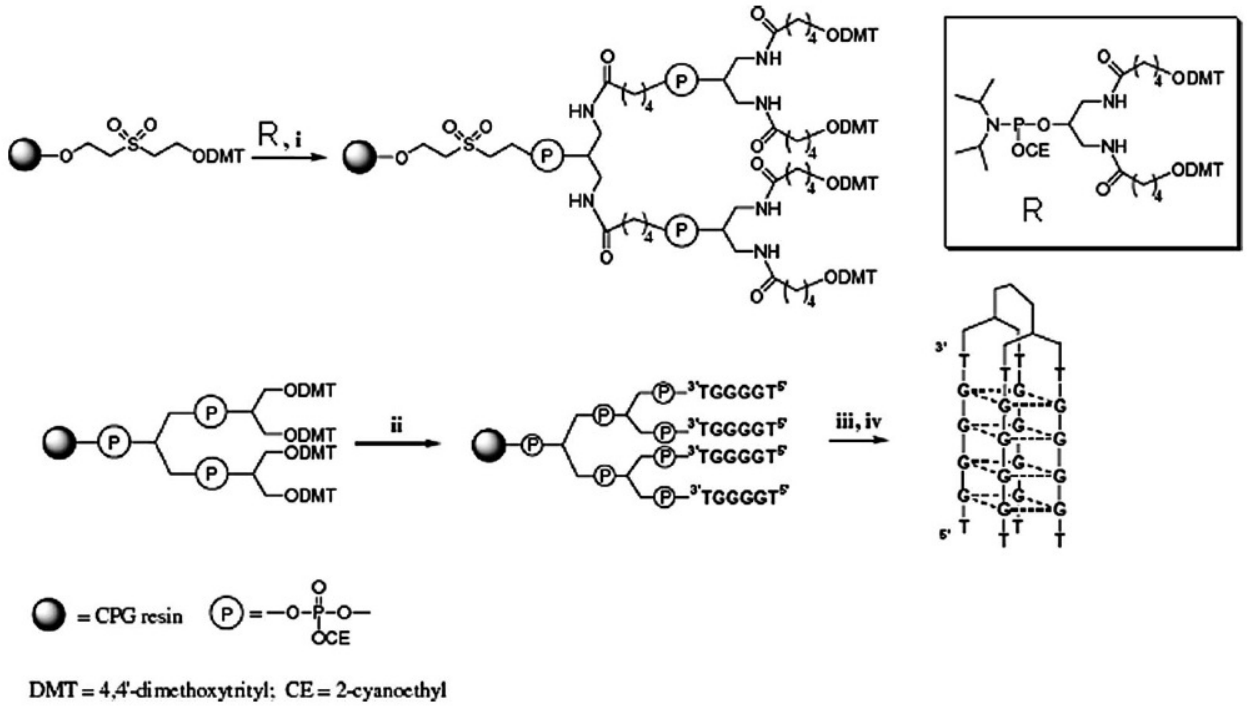

(Figure 1**.2-6**): Synthesis of G-quadruplex-forming bunch-oligonucleotides. i) Two coupling procedures with R, ii) ODN synthesis, iii) detachment and deprotection with NH_4OH conc. 32% (7 h, 55 °C), and iv) HPLC purification and annealing (Oliviero et al., 2004).

in water: even without any covalent bridge, G-quartets stack to give columnar structures with hydrophilic surfaces and lipophilic cores. Depending on the concentration and other physico-chemical parameters, these aggregates generate arrangements in the cholesteric phase and in the hexagonal liquid-crystalline phase (Figure **1.2-7**) (Davis et Spada, 2007). In another case, a lipophilic G-quadruplex is reported to act as a Na^+ ion transporter when inserted in a phospholipid membrane (Kaucher et al., 2006). In this case olefin metathesis was used to cross-link all 16 appropriately substituted guanosine subunits after self-assembly into a G-quadruplex structure in the presence of K^+ ions (Figure **1.2-8**). Because G-quadruplex-forming sequences combined with two fluorescent probes forming donor–acceptor systems have proven to be efficient FRET systems for study of G-quadruplex ligands (Mergny et Maurizot, 2001; De Cian et al., 2007), the same principle has been applied to obtain some nanodevices. This is the case with quadruplex molecular beacons, fluorescent nucleic acid probes with hairpin-shaped structures used for the diagnosis of single-stranded DNA or RNA with high mismatch discrimination (Bourdoncle et al., 2006), and of quadruplex probes for the fluorimetric detection of K^+ ions (Figure **1.2-9**) (Nagatoishi et al., 2007). Another intriguing potential application of quadruplex based nanodevices is represented by the so called G-wires. The term “G-wires” was coined by Marsh and Henderson to describe the continuous

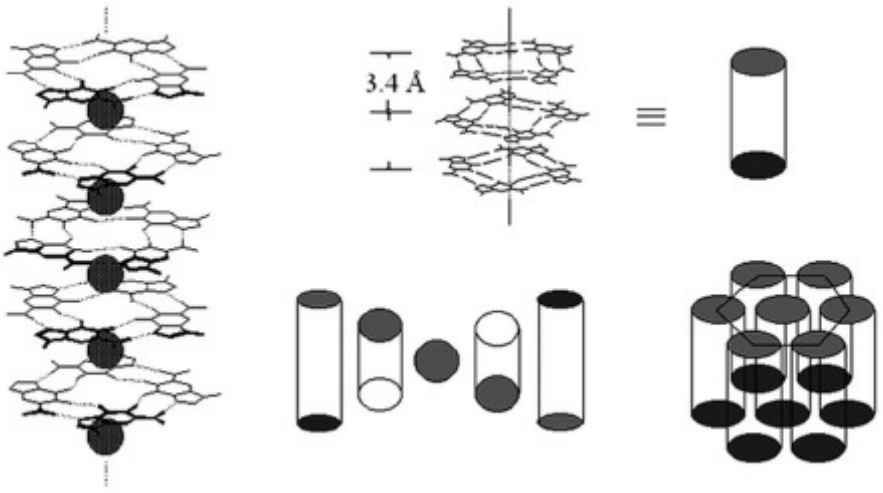

(Figure **1.2-7**): Formation of liquid crystals from self-assembled guanosines.

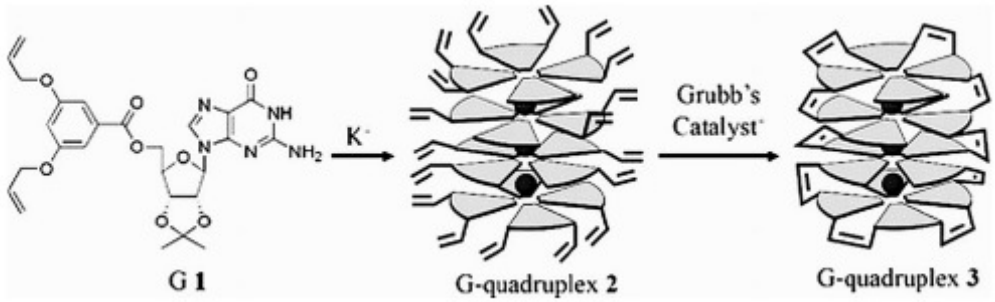

(Figure **1.2-8**): Two-step synthesis of a lipophilic G-quadruplex by olefin metathesis (Kaucher et al., 2006)

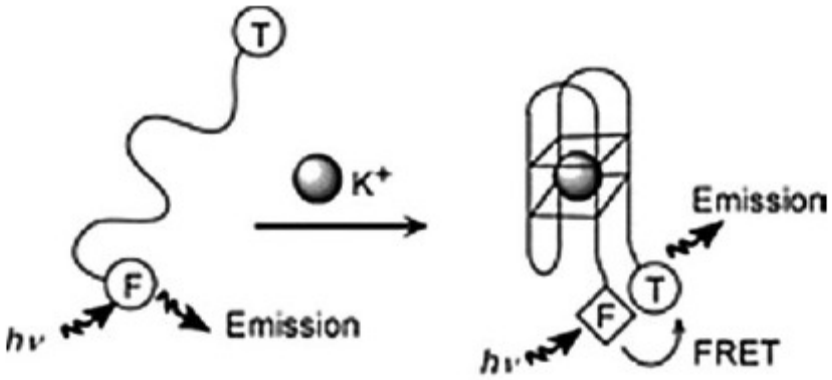

(Figure **1.2-9**): Effect of K^+ ions on the structures of fluorescence labelled G-rich oligonucleotides and consequent FRET detection (Nagatoishi et al., 2007).

parallel-stranded DNA superstructures formed by G4T2G4 self-assembly as a consequence of the slippage of chains, visualized by AFM imaging (Marsh et al., 1995). Guanine nanowires incorporating 2,2'-bipyridine units have been reported to be controllable and switchable by external signals (Figure **1.2-10**) (Miyoshi et al., 2007). Such G-wire switches present important properties that make them useful for the development of DNA-based functional nanomaterials (Karimata et al., 2007). Being controllable by chemical input signals – namely, divalent metal ions – they are important for the development of molecular electronic technologies: together with previously reported DNA logic gates based on the effect of monovalent ions on telomeric sequences (Miyoshi et al., 2006) they can constitute the basis of "liquid computing". Finally, it is worth reporting that G-wire assembly has very recently been proposed to have a role in prebiotic nucleic acid organization (Pisano et al., 2008).

The outstanding fluorescence and electron-acceptor properties of PDIs appear to be particularly interesting for a diagnostic application based on intercalation into ribonucleic acid (RNA) or deoxyribonucleic acid (DNA). In principle, there are two different possibilities by which PDIs can interact with DNA. On the one hand, these chromophores can be a part of DNA–PDI conjugates once they are covalently connected to oligonucleotides and, on the other hand, they may interact with DNA bases through noncovalent π-π interactions (upon intercalation). It has been known for long time that water-soluble PDIs undergo π-stacking interactions with DNA bases. Cationic PIs, in particular, showed enormous potential for the stabilization of DNA G-quartets.

Typically, conjugated molecules are characterized by the presence of a large aromatic core, (e.g porphyrine, pyrene, acridine, and pyrene), capable of interacting with G-tetrads by π-π forces.

Among the great number of molecules potentially suitable for conjugation to G-rich oligonucleotides, perylene bisimide and its derivatives are of particular interest because their presence could add desired features such as chemical resistance and the propensity to form higher-ordered aggregates, as well as favorable fluorescence and electronic properties (Würthner, 2004; Imahori et al., 2009; Chen et al., 2009). Furthermore, a member of this family, PIPER (N,N'-bis-[2-(1-piperidino)ethyl]-3,4,9,10-perylenetetracarboxylic bisimide) demonstrated the ability to drive the association of G-rich strands into G-quadruplexes (Han et al., 1999). This mechanism, known as "threading intercalation", has been extensively studied because of its potential involvement in the inhibition of human telomere elongation by telomerase (Franceschin et al., 2009; Han et al., 1999; Tuesuwan et al., 2008). Although a variety of DNA structures formed by linked perylene-oligonucleotides have been discussed extensively in many papers, to the best of our knowledge only one perylene bisimide-conjugated G-rich oligonucleotide has been reported to date (Saha et al., 2010).

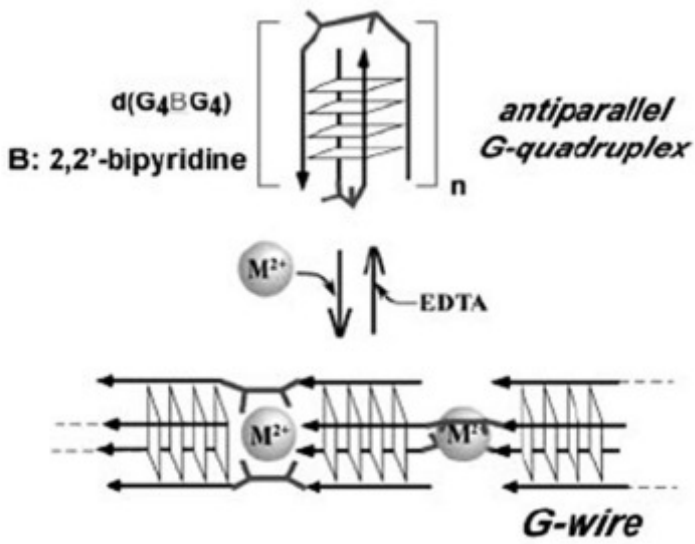

(Figure **1.2-10**): G-wire formation controlled by divalent cations (Miyoshi et al., 2007).

1.3. Lipid systems in aqueous solution

1.3.1 Fluorescent lipid analogues

Analogues of lipids are often used in studies and research such as, supported phospholipids bilayers (SLB)(Tamm, et McConnell, 1985), lipid monolayers (Maget-Dana, 1999) and liposome (Eytan, 1982).

In lipid research, the last two decades of the previous century were highlighted by rapid developments in the recognition of the role of lipids in a great variety of cellular processes, ranging from membrane fusion, involvement in microdomain formation and transport, to signal transduction (Hoekstra, 1994). Indeed, the appreciation that the specific intracellular localization of distinct proteins is mirrored by a similar sort of non-random distribution of lipids, has triggered numerous studies on the trafficking of lipids and raised such questions as whether lipids accompany membrane proteins as a necessary part of the lipid matrix, being an inherent part of the vesicular transport vehicle, or that proteins were recruited into domains, dictated by the lipids. Evidently, there is much more to lipids than that they only provide, in terms of composition, an appropriate matrix to proteins or a barrier that prevents free flow of extra- and intracellular compounds.

To study the dynamics of lipids, a variety of techniques are available, but some of those are quite inconvenient and laborious, whereas the interpretation of the data may be equally confusing (radiolabeled precursor, antibodies, etc.). In this regard, a breakthrough was realized when several laboratories initiated work in the early 1980s, based upon the application of fluorescently- tagged lipid (-like) analogues (Klausner and Wolf, 1980; Struck and Pagano, 1980; Derzko and Jacobson, 1980; Spiegel et al., 1984).

The success of fluorescent lipid probes is due, on the one hand, to the great sensitivity and methodological simplicity of fluorescence techniques and, on the other, to the quite fast integration of the lipid probe into a membrane.

Fluorescent lipid probes can be divided into two main families:

1. probes that resemble the structural features of biological membrane constituents
2. probes that, though being amphiphilic molecules, do not mimic the natural lipid backbone.

The resemblance of the lipid probe structure to its biological counterpart is a necessary feature for the study of trafficking and sorting of lipids in cell biology, whereas this requirement is less crucial for the physicochemical characterization of both membrane models and biological membranes. In fact, a number of amphiphilic probes with different basic structures and tagged with every kind of dyes have been used to study physicochemical features of membranes such as the phase transition

temperature (Parasassi et al., 1991), the polarity and packing of the lipid bilayer (Bernik et al., 2001), the surface potential (Zuidam et Barenholz, 1993), and to follow some processes such as the formation of lipid domains and membrane fusion (Parasassi et al., 1994; Lei et MacDonald, 2003).

An important observation was that lipid analogues, prepared to mimic their natural counterparts, in which the fluorescent probe was attached to a hexadecyl (C6) spacer which replaced one of the fatty acids in phospholipids or the fatty acid in glycosphingolipids, displayed a lower degree of hydrophobicity than their natural counterparts. This property made it possible to readily integrate such a lipid analogue into a target membrane by simple exogenous addition. This feature thus paved the way for the synthesis of a great number of fluorescently labeled lipid analogs, whose fate in cells could thus be specifically examined. Furthermore, depending on the nature of the fluorescent analogue, i.e. acyl chain versus head group labeled, assays were developed which allowed a characterization of biophysical properties of the lipids per se or the membranes (both artificial and biological) in which they were integrated, and these properties were then related to physiologically relevant processes like e.g. membrane fusion. Most importantly, in cellular events the flow of the lipid of interest could be monitored directly in live cells by fluorescence microscopy. However, as for every derivatized compound, fluorescent and spin-labeled alike, it is crucial to critically evaluate the reliability of the use of a given probe in terms of its ability to reflect the genuine properties of the natural compound. Clearly, with regard to the aqueous solubility, the fluorescent lipid analogues do not. Yet, in light of the avalanche of data produced in recent years, it is apparent that their application has led and will further lead to highly relevant insights, both with regard to fundamentally and biologically significant processes in which lipids play a role. This has only been possible by critically evaluating such data, taking into account their limitations, but at the same time exploiting their credible options.

Lipids analogues not resembling (or mimic) the natural counterpart, may be of different types: anionic, cationic, Gemini or bola ones.

In the field of model systems for liposome, the synthesis of novel unsymmetrical bolaamphipiles is object of many studies.

Unsymmetrical bolaamphiphiles are original classes of surface-eactive molecules that have been found as cell-membrane components of methanogenic and thermoacidophilic archaea (Sprott, 1992; Masuda and Shimizu, 2001; Fuhrhop and Wang, 2004). These bipolar amphiphiles are characterized by the presence of two different hydrophilic end groups connected by a hydrophobic spacer that has one or two alkyl chains. These materials often self-assemble into monolayer lipid membranes that are more tightly packed and less permeable than standard bilayer membranes (Ghiozzi et al., 2002). Unsymmetrical bola lipids with polar head groups of different sizes may

exhibit an unsymmetrical or a symmetrical type arrangement depending on a parallel or antiparallel molecular packing within the monolayer (Figure **1.3-1**). Another interest of the bolaamphiphiles is their capability to adopt various conformations in supramolecular assemblies, that is, U-shaped and stretched conformations (Meister and Blume, 2007). The aggregate morphologies of bolaamphiphiles include vesicles and lamellae, disks, rods, tubules, ribbons and fibres in a micro- and nanometer range (Kunitake et al., 1981). Despite the continuing emergence of novel synthetic structures and original highly ordered assemblies (Miyawaki et al., 2003; Grinberg et al., 2008), fundamental studies to establish the relationship between the morphology of the self-organized systems and the chemical structure of unsymmetrical monomers remain to be carried out. Over the past decade, the results obtained from synthetic molecules have demonstrated the existence of complex relationships between chain composition, spacers and head groups that considerably influence the structure of their supramolecular aggregates (Meister and Blume, 2007; Benvegnu et al., 2004; Roussel et al., 2006).

Consequently, the rational design of well-defined functional bolaamphiphiles continues to be challenging in order to analyze the mechanisms involved in molecular self-assembly and to develop new advanced materials.

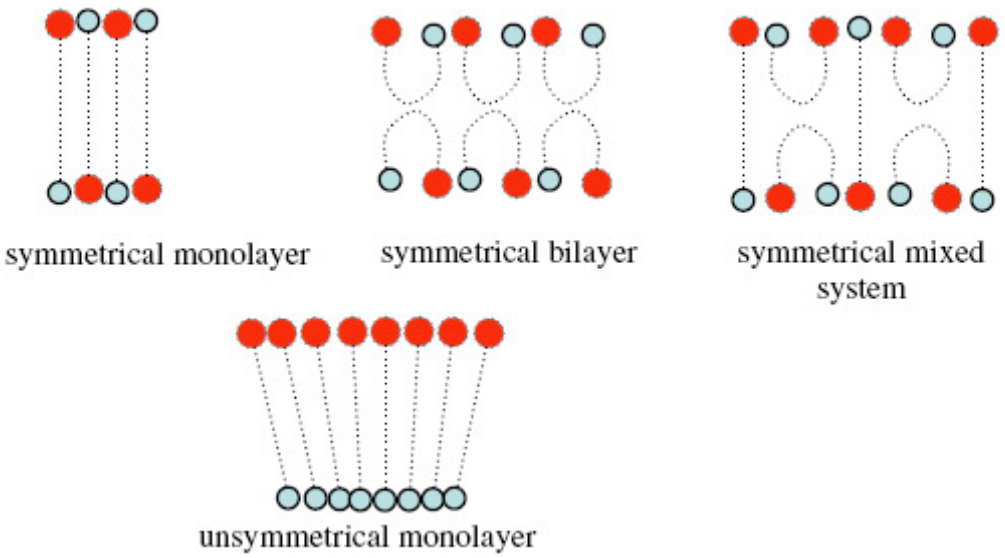

(Figure **1.3-1**): Symmetrical and unsymmetrical membranes based on unsymmetrical bolaamphiphile lipids.

Fluorescent lipid probes

Lipids are amphiphilic in nature and consist of a hydrophobic chain and a hydrophilic head group region. Accordingly, there are in principle two regions within the molecule to which fluorescent dyes can be covalently coupled. The intramolecular localization of the dye as well as the chemical nature of the dye itself (Figure **1.3-2**) are highly relevant, as they will determine the (biophysical) properties of the final fluorescent lipid analog as such, which in turn are relevant for the assay in which the probes will be eventually used. The majority of the fluorescent dyes that have been used in lipid derivatization, especially those emitting in the visible light region, are hydrophilic. When they are attached in the chain region, the dye will change the hydrophilic/hydrophobic balance of the lipid molecule. Evidently, such a perturbation may have considerable implications for the lipid's ability to integrate into membranes (Chattopadhyay, 1990). Thus, upon membrane integration, a mismatch with surrounding lipids may occur, causing a perturbation of the host membrane structure (Ashcroft et al., 1980), as reflected for example by leakage of entrapped aqueous dyes from liposomes. The imbalance can also lead to an undesirable increase in monomeric exchange rate of the lipid probes between membranes (Ohki et al., 1998). On the other hand, only chain-labeled lipid analogs are the probes of choice in case the research area of interest is focussed on issues in which the lipid head group may play a functional role, e.g. in lipid sorting (Van IJzendoorn and Hoekstra, 1998) and translocation (Raggers et al., 2000), and in specific events in sphingolipid dynamics and metabolism (Kok et al., 1998; Tepper et al., 2000; Ledesma et al., 1999).

Alternatively, head group labeled lipids can also be prepared and used in cases, when properties of the chain regions are important, e.g. for phase determination in biological membranes. Particularly in membrane fusion assays such probes have found a wide application, since the head group derivatives often show virtually non-exchangeable properties, given the hydrophilic nature of the probe itself and its localization, i.e. in this case the hydrophobic tails of the lipid are firmly anchored with the membrane in an unperturbed manner. Often, phosphatidylethanolamine (PE) has been employed as an anchor lipid for such, allowing their covalent attachment to the amine group. It should be taken into account that in this case the presence of the probe will change the shape of PE, which is known to be capable of displaying non-lamellar properties, thereby promoting negative bilayer curvature and membrane fusion (Chernomordik and Zimmerberg, 1995; Pecheur et al., 1999). Evidently, when derivatized, such polymorphic properties are no longer expressed by the tagged PE.

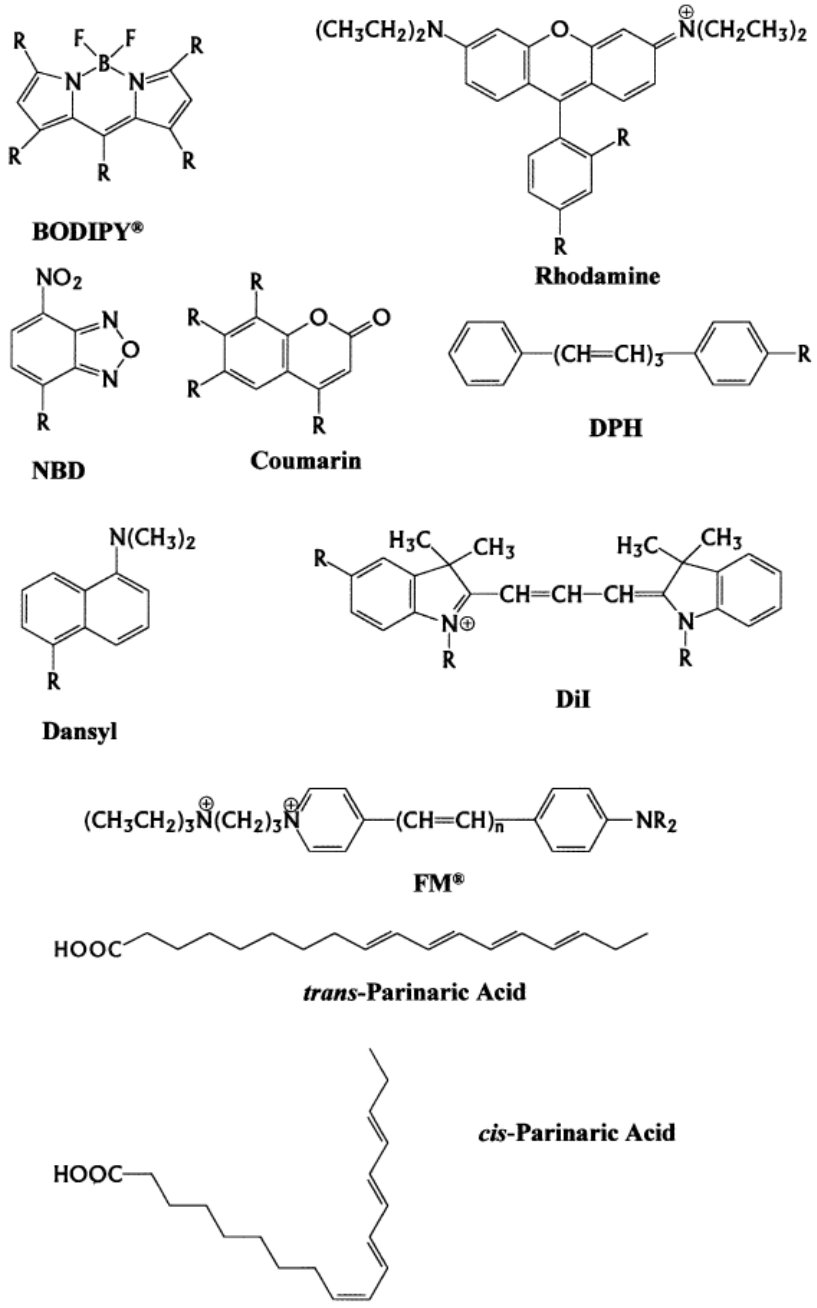

(Figure **1.3-2**): Basic structures of fluorescent dyes used for coupling to lipidic structures. R represents either lipidic anchors or other functional groups.

The quantum yield and fluorescence properties of the dyes are sensitive to their environment. Such environment-dependent changes can therefore be highly valuable in evaluating the fate and localization of the lipid and the nature of its interactions. The most simple feature is the decrease of the fluorescence yield, thereby leading to quenching. Quenching can be caused by different

mechanisms. It may for example involve an effect of an exogenous factor, e.g. a quenching molecule, but at a relatively high density, the dye can also readily interact with itself, which will lead to selfquenching. Quenchers can be used to determine the accessibility of a fluorophore in the membrane, e.g. the quenching of 7-nitrobenz-2-oxa-1,3-diazol-4-yl (NBD) in the chain region of lipid probes by the aqueous phase quencher sodium dithionite can be used to measure the density of the membrane packing (Huster et al., 2001), and the orientation of the derivatized chain in the core of the membrane. The faster the NBD is quenched, the more likely an enhanced exposure of the fluorophore towards the bilayer/water interphase. In this manner, insight can be obtained into the extent of lipid packing in membranes, which may be relevant for evaluating protein–lipid (membrane) interactions. By changing the length of the chain to which a fluorophore is attached, it is also possible to determine the depth to which the quencher can penetrate into the membrane, and thus determine partitioning parameters of the quencher itself (Langner and Hui, 1993).

Quenching of fluorescence may also occur as a result of selfquenching, which occurs most efficiently for fluorophores whose excitation and emission maxima are not that far apart (within 40–50 nm). The fluorescence of the selfquenching dye increases when the concentration of the fluorescent molecules in the membrane is decreased, or vice versa. An example for such a phenomenon is the use of octadecyl rhodamine B chloride (R18) as a membrane marker for the determination of membrane fusion (Hoekstra et al., 1984). In addition, selfquenching has also been exploited in detecting lipid phase separations, occurring under a variety of conditions in mixed membranes. In this case, when initially randomized, lipid clustering will result in an enhanced local concentration of the fluorescent lipid, leading to a decrease in fluorescence, a process that can also be monitored kinetically (Kok and Hoekstra, 1999).

Some fluorescence probes are able to interact with each other to form excimers. Excimers are excited-state dimers that exhibit altered emission spectra, compared to the monomers. A frequently used dye exhibiting this property because of the long lifetime of its excited state, is pyrene. Upon changing from the monomeric to excimeric state, the dimers (excimers) have a red-shifted fluorescence emission (Galla and Hartmann, 1980). Pyrene excimer formation can be utilized to follow membrane fusion or to detect lipid domain formation in artificial and natural membranes (Hinderliter et al., 1998). Excimers are formed when two pyrene molecules can interact during the excited state lifetime of a pyrene molecule. This will require a certain minimal level of probe concentration in a given membrane. The level of excimer formation decreases when probe dilution occurs, for example during fusion. Alternatively, in case of lipid domain formation, the local density of the probe will increase and accordingly, the incidence of excimer formation.

Pyrene fatty acids can be metabolically incorporated into phospholipids, di- and tri-acylglycerols

and cholesteryl esters, which opens possibilities to investigate living cells. In this manner it has thus been possible to investigate processes like lipid transport mechanisms and the action of lipid transfer proteins (Engelmann et al., 1998), to detect lipid–protein interactions, to monitor enzyme–substrate interaction.

Some fluorescent dyes are sensitive to changes in the environment. Environmental effects are parameters that are most important to studies utilizing lipid analogues.

Environmental effects can be probed by lipid analogues in which the fluorophore is attached at the alkyl chain. For example, the lateral properties of the chain labeled lipid analogues may be dictated by the environment of adjacent lipids. Specifically, as a function of its isomeric form, the auto-fluorescent parinaric acid (Figure **1.3-2**) only mixes in a preferred phase. Thus whereas cis-parinaric acid (Brewer and Matinyan, 1992) integrates into fluid phases, trans-parinaric acid prefers partitioning into more solid and rigid phases in the membrane.

Very recently it has been reported (Hongmei et al., 2012) the design and obtainment of fluorescent amphiphilic probes where the bisimidic perylene residue and dendritic polyethylene glycol (PEG) constitute the hydrophobic and hydrophilic regions, respectively, arranged in two different main architectures, the head-tail and the core-shell dyes. The first one is the architecture of a "conventional amphiphile" with a hydrophilic head group (the dendritic PEG) and a hydrophobic region (the perylene moiety), whereas in the core-shell architecture the bismidic perylene unit is linked in opposite directions to symmetric dendritic PEGs, thus resulting in a bola type (or bipolar) lipid. The architecture of the fluorescent amphiphiles have proved to influence the cellular uptake of the probes, in particular, the bola type lipid was internalized more efficiently by cells.

In another recently study (Yang and Zimmermann, 2012) the synthesis and photophysical properties of water-soluble, fluorescent polyglycerol-dendronized perylenediimides were reported (Figure **1.3-3**). The polyglycerol dendrons, which are known to be highly biocompatible, are found to confer high water-solubility on the perylenediimide in aqueous media while retaining its excellent fluorescent properties. Furthermore, intramolecular crosslinking of the polyglycerol dendrons using the ring-closing metathesis reaction not only enhances the photostability but also reduces the size of perylenediimidecored dendrimers.

Zhao and coworkers (2012), showed that by attaching two tetraphenylethene moieties to the 1,7-positions of PDIs, the aggragation-caused quenching characteristic was converted to an aggregation-induced emission characteristic molecule. The obtained PDI derivative exhibits several advantages over classical PDI derivatives, including pronounced fluorescence enhancement in aggregate state, red to near infrared emission, and facile fabrication into uniform nanoparticles.

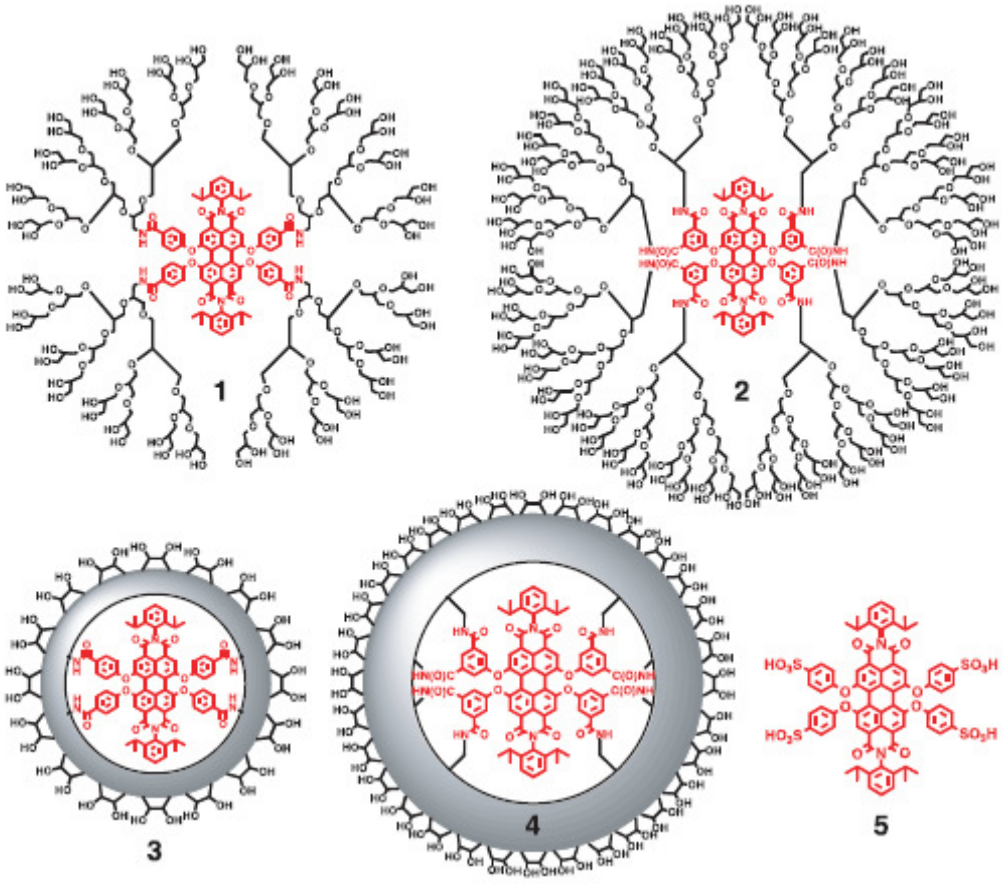

(Figure **1.3-3**): Structures of four PGD-PDIs (1-4) and PDI (5) (Yang and Zimmermann, 2012).

1.3.1 Use of Fluorescent lipid probes

Membrane fusion is a fundamental event in the life of a eukaryotic cell. Also processes like viral infections depend on the fusion of membranes, which represents the mechanism of their entry into host cells. To mimic such processes, artificial membranes are also used, and such studies have emphasized the added value of being able to monitor fusion in a kinetic and sensitive manner. To do so, fluorescent lipid analogues have been used as versatile tools to detect and quantify fusion, both in artificial and biological membrane systems. During fusion, the membranes merge concomitantly leading to the coalescence of the aqueous phases. Next to content mixing, which can often not be carried out in systems involving the fusion of a pure biological membrane system, lipid mixing has therefore often been taken as a simple measure of membrane fusion. Lipid mixing

assays are mainly based on two detection methods, i.e. either a change in resonance energy transfer (RET) or in fluorescence selfquenching. Whereas in artificial model systems the RET assays are most commonly used, fusion events involving biological membranes more frequently rely on the application of selfquenching assays (MacDonald, 1990) or the separation of an excimer forming compound (Stegmann et al., 1993). To monitor the lipid mixing in model systems, Struck et al. (1981) developed a convenient assay, based upon RET between N-NBD-PE and N- rhodamine(Rh)-PE, which is currently still one of the most popular assays employed for this purpose. In this assay, one population of the vesicles is labeled with both fluorescently-tagged lipid analogues in such a concentration, that their density results in efficient energy transfer. In addition, the concentration should be such that a change in energy transfer is directly proportional to the extent of lipid mixing, i.e. fusion. This is the case at lipid analogue concentration of approx. 0.8 mol% each. Thus upon fusion with an unlabeled vesicle population, the energy transfer decreases proportionally, which can be monitored continuously by registering an increase in the fluorescence of the donor (while exciting the donor at its excitation wavelength). Simultaneously, the energy transfer efficiency decreases, implying that when exciting the donor, the acceptor emission fluorescence will decrease.

Energy transfer has also become a powerful tool in detecting close approach of two bilayers. However, in this case the probes are incorporated into distinct vesicle populations, and aggregation is monitored as an increase in transfer efficiency. For example, using coumarin-PE and N-Rh-PE as RET couple, membrane aggregation was monitored and energy transfer allowed the detection of 'membrane changes upon approach', like undulations, prior to physical contact of both membranes (Niles et al., 1996). Indeed, fluorescent lipid probes are quite versatile in detecting changes in the aqueous environment between bilayers during such an aggregation event. By using dansyl-PE, changes of hydrophobicity during the approach of two phospholipids bilayers were measured and it was shown that the increase in hydrophobicity between the two bilayers is an essential step in the process that precedes vesicle fusion (Ohki and Arnold, 1990).

The transport of proteins and lipids to the plasma membrane of eukaryotic cells as well as the transport between cellular organelles is mainly mediated by small membrane-bound vesicles that bud from the donor organelle and fuse specifically with the acceptor compartment. Lipids are integral components of these vesicles and a variety of fluorescent lipid or lipid-like probes has been employed to analyze vesicle-mediated transport pathways. The possibility to follow the routes taken by these probes in living cells by fluorescence microscopy has been an invaluable tool for the analysis of the biosynthetic and endocytotic transport pathways of these cells as well as for the characterization of the involved organelles. In addition, by making proper use of other specific

biophysical features of these probes, further qualitative and quantitative information has been obtained. One example is the ability of several fluorescent molecules to convert diamino benzidine to an osmiophilic product of high electronic density (Sandell and Masland, 1988). Since some molecules as hexadecyl-NBD-ceramide accumulate in the Golgi-apparatus, this property can be used to characterize functional and structural aspects of the Golgi apparatus by electron microscopy (Pagano et al., 1989).

2. AIM OF THE THESIS

The central topic of the work described in this thesis is the synthesis of some dibromoperylene diimides and the study of their spectroscopic features, especially fluorescence, when they are inserted in specific biological-inspired systems.

These characteristics have been considered from two different points of view: as a model for the synthesis of stable DNA aptamers and as a target for the synthesis of fluorescent probes adequate to the introduction in phospholipids bilayers or "model membrane systems".

The first part of my work was inspired by the knowledge that G-quadruplex aptamers stability is strictly correlated with their biological activity as well as potentially nano-technological properties. Such a stability can be improved by the presence of aromatic substituents at the end of oligonucleotide strands (Hotoda et al. 1998, D'Onofrio et al. 2007).

Perylene derivatives are well studied G-quadruplex ligands, able to induce and stabilize these structures (Franceschin 2009), so we decided to try improving the stability of quadruplex forming dibromoperylene Phosphoramidite Building Block incorporated at the 5'-end of a G-Quadruplex forming oligonucleotides. Therefore the target of this part of my work was the synthesis of perylene units opportunely functionalized and the incorporation at the 5'-end of the selected GGGTTAGGG (HTR2) human telomeric repeat sequence. Furthermore, the structural behaviour of the conjugated PEOEBr-GGGTTAGGG (HTRp2) human telomeric repeat was investigated by using CD, UV and fluorescence techniques in desalted water and in K^+- and Na^+-containing buffers. In fact, the spectroscopic properties of perylene make these conjugated particularly interesting for the development of fluorescent nanodevices.

The main problem in using perylene derivates in biological-inspired systems is the poor water solubility. Some successful conjugations of duplex-forming ONs have been reported in aqueous solutions (Bevers et al. 2000), but the insertion of typical protective groups of DNA solid phase synthesis on these molecules was very difficult and the yields were so low (< 10%) to make unsuitable the whole synthetic strategy, due to the low solubility. Hence, the importance of developing a new methodology for the synthesis of conjugated perylene-GROs.

Following these results, the aim of my work became the synthesis of perylene derivatives opportunely modified in order to improve their solubility to be inserted in the oligonucleotides solid phase synthesis. To reach this aim I followed the strategy to insert substituents on the bay area improving the solubility and allowing the introduction of the solid phase synthesis protective group

in order to obtain phosphoramidite building-blocks (Figure **1**) (in collaboration with prof. Mayol's group at the Università di Napoli Federico II).

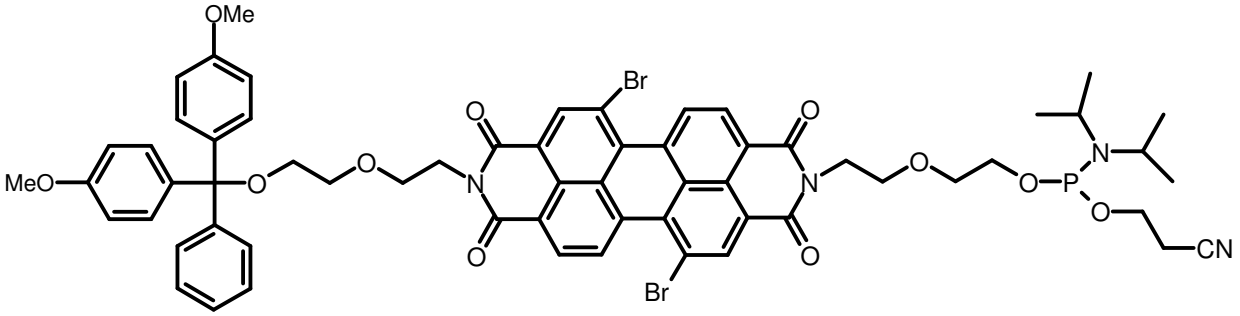

Figure **1**: DMT-PEOEBr-Phoshoramidite building-blocks

On the basis of our previous knowledge of the physico-chemical properties of perylene derivatives modified on the bay-area by bromination, we have synthesized bromine-substituted perylene diimides with oxydryl-ended side chains.

Only one of the derivates synthesized (DMT-PEOEBr-Phoshoramidite) was incorporated at the 5'-end of the selected GGGTTAGGG (HTR2) human telomeric repeat sequence. The choice of the PEOEBr moiety was due to our previous observation (Alvino et al., 2007; Franceschin et al, 2004) that

perylene bisimide derivatives containing suitable groups on the carbocyclic scaffold (known as "bay-area") exhibited greater solubility in aqueous solution.

UV, CD, fluorescence, and gel electrophoresis techniques were used in order to investigate the self-assembly properties of the resulting molecule, in which two types of association forces, i.e., strand organization in G-quadruplexes and perylene derivative aggregation, are potentially involved.

The subject of the second part of my thesis work was to find new perylene derivates opportunely modified to insert in phospholipids bilayers or "model membrane systems". However, given the size of an average lipid molecule, special care is needed for the selection of probes, since if the size and intramolecular localization of the probe is not specifically taken into account, it may dramatically affect the properties of the lipids. Perylene core, modified with side chains, should show amphiphilic characteristics required for the interaction with phospholipids bilayers: hydrophobic chain and a hydrophilic head group region. The final aim was to obtain a fluorescently-tagged lipid (-like) analogues (Klausner e Wolf 1980, Spiegel, et al. 1984, Struck e Pagano 1980, Derzko e Jacobson 1980). Basing on our experience on low solubility of perylene not

only in water but also in common organic solvents, we used perylene derivatives modified on the bay-area by bromination, analogously to the first part of this work described above. It was possible to synthesize two different perylene derivatives with side chains in order to mimic phospholipids bilayers: 1,8-diaminooctane and 1,12-diaminododecane (perylene-Br-C8 and perylene-Br-C12). These chains have the right length to take place inside phospholipids bilayers (Figure **2**).

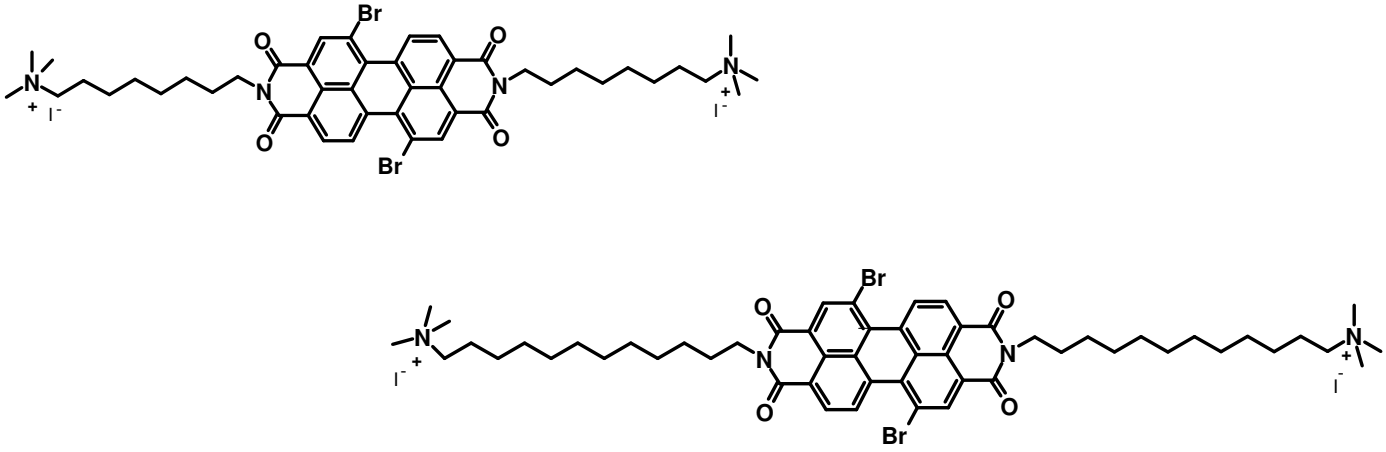

Figure **2**: perylene-Br-C8 and perylene-Br-C12 derivates

To study the dynamics of lipids, a variety of techniques are available, but some of those are quite inconvenient and laborious, whereas the interpretation of the data may be equally confusing. Fluorescent probes attached to a spacer which replaced one of the fatty acids in phospholipids or the fatty acid in glycosphingolipids are a very interesting way to study the dynamics of lipids. The quantum yield and fluorescence properties of perylene derivates (Kohl, et al. 2004) are sensitive to their environment. Such environment-dependent changes can therefore be highly valuable in evaluating the fate and localization of the lipid and the nature of its interactions. The most simple feature is the decrease of the fluorescence yield, thereby leading to quenching.

3. RESULTS AND DISCUSSION

3.1. Perylene conjugated oligonucleotides

3.1.1. Synthesis of phosphoramidite building-blocks

Among the great number of molecules potentially suitable for conjugation to G-rich oligonucleotides, perylene bisimide and its derivatives are of particular interest because their presence could add desired features such as chemical resistance and the propensity to form higher-ordered aggregates, as well as favourable fluorescence and electronic properties (Würthner, 2004; Imahori et al., 2009; Chen et al., 2009). Although a variety of DNA structures formed by linked perylene-oligonucleotides including duplexes,(Baumastark et al., 2008) triplexes,(Bevers et al., 2000) and hairpins, have been discussed extensively in many papers, to the best of our knowledge only one perylene bisimide-conjugated G-rich oligonucleotide has been reported to date (Saha et al., 2010). For this reason, in this work we explore the properties of DNA Quadruplexes formed by perylene-conjugated G-rich oligonucleotides.

We decided to take advantage of our experience on the physico-chemical properties of the perylene derivatives (Alvino et al. 2007) to allow the insertion of the functional groups commonly utilized for the solid phase synthesis of the oligonucleotides: DMT and phosphoramidite. In this way, phosphoramidite building-blocks would be obtained to be covalently bound to DNA during the solid phase synthesis. The resulting conjugated oligonucleotides are expected to show a better stability of the G-quadruplex structure with respect to unmodified sequences. To reach this aim we decided to synthesize bromine-substituted perylene diimides. The use of bromine-substituted perylene is a way to improve the solubility of these derivatives in organic solvents and to allow the next synthetic steps.

The bromination of the perylene bay area was carried out starting from 3,4,9,10-perylenetetracarboxylic dianhydride (**1**) (Scheme **3.1.1-1**). Four positions (1, 6, 7 and 11) of the perylene moiety are reactive, but electronic, and steric reasons, together with the moderate strength of the electrophile, allow only two dibromo derivatives to be obtained, whose ratio is determined by the reaction conditions: the major isomer is always 1,7-Dibromoperylene-3,4:9,10-tetracarboxylic dianhydride (**2**) and the minor one the corresponding 1,6-derivative (**3**) (Würthner et al. 2004, Franceschin et al. 2004) which is not separable from the 1,7-isomer in this step of the synthesis.

Temperature and reaction time have been shown to be key parameters in determining the ratio between the two isomers. In particular, keeping the temperature at 100°C for 4-6 hours, the highest amount of the major isomer was obtained, approximately in a 6:1 ratio with respect to the minor 1,6-isomer. A small amount of the 1,6-isomer was always present, as could be determined by analyzing the ^{1}H NMR spectra.

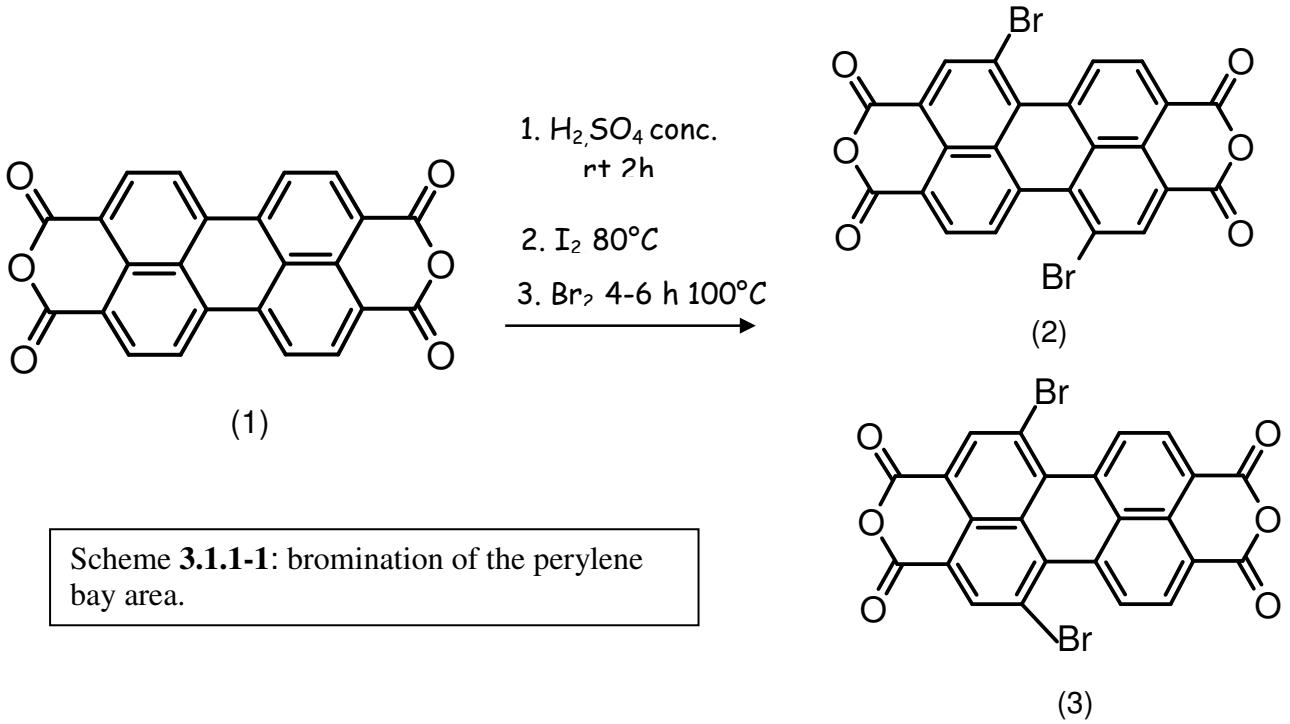

(1) (2) (3)

Scheme **3.1.1-1**: bromination of the perylene bay area.

Dibromo-perylenetetracarboxylic dianhydride was reacted with a series of commercially available aminoalcohols to obtain the bisimides: ***N,N*'-Bis(2-hydroxyethyl)-1,7-dibromoperylene-3,4:9,10-tetracarboxylic diimide (4), *N,N*'-Bis(3-hydroxypropyl)-1,7-dibromoperylene-3,4:9,10-tetracarboxylic diimide (5), *N,N*'-Bis(5-hydroxypentyl)-1,7-dibromoperylene-3,4:9,10-tetracarboxylic diimide (6)**, ***N,N*'-Bis(5-hydroxy-3-oxapentyl)-1,7-dibromoperylene-3,4:9,10-tetracarboxylic diimide (7) (PEOEBr),** in a yield between 82% and 95% (Scheme **3.1.1-2**).

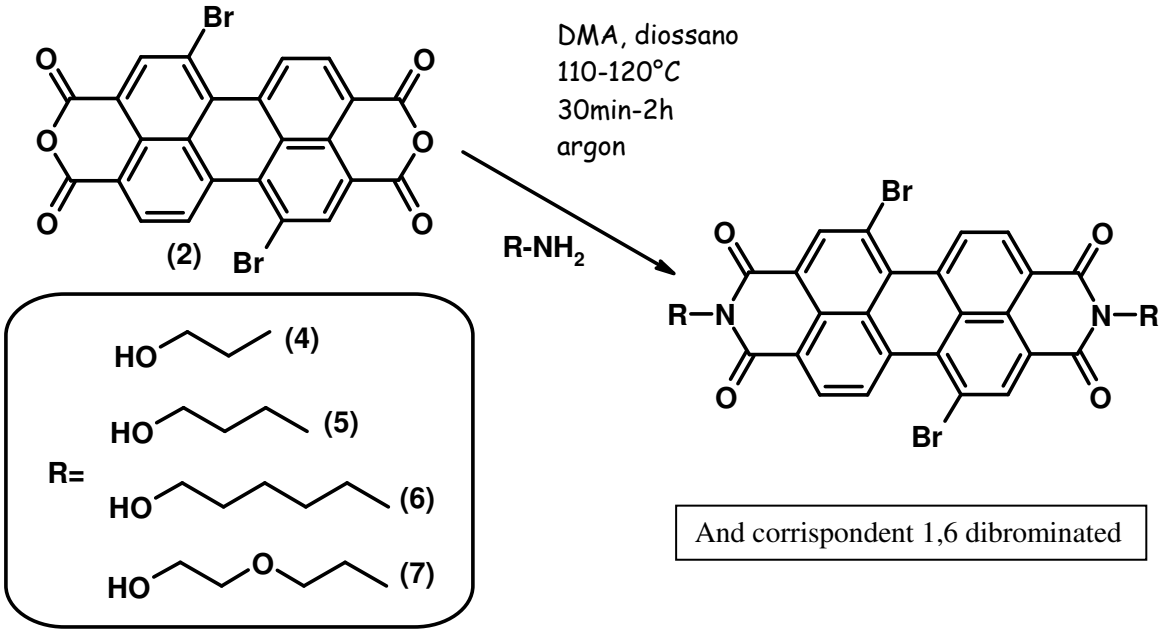

Scheme **3.1.1-2**: insertion of hydroxyl ending side chains on the perylene major axis.

No more than 10% excess of reactants was used to avoid side reactions at the brominated positions, which can occur at higher ratios. It is worth noting that, in principle, undesired reactions of the hydroxyl groups could occur, but this was not the case. On the contrary, substituition of bromine atoms by the primary amine of the amino-alcohols can actually occur even at this stoichiometric ratio. In our experience, this can be avoid strictly controlling the temperature and the time of reaction, following on TLC the appearance of any blue-green spot. If such spots appear, the reaction must be stopped and the products can be purified by column chromatography.

Each compound **4-7** was obtained as a mixture of 1,7 and 1,6 dibrominated regioisomers, which, similar to previous reports by Wurthner et al. 2004 and Rajasingh et al. 2007, were resolved by selective precipitation. The mixtures of regioisomers 4-7 were first acetylated and then purified by repetitive precipitation. The purity of the 1,7 regioisomers was ascertained by ^{1}H and ^{13}C NMR. The ^{1}H NMR signals of the aromatic portion of the acetylated **4-7** compounds before and after the purification steps (Figure **3.1.1-1**) indicated that the mixtures were efficiently resolved . The acetyl groups were then removed by treatment with a mixture of aqueous NH_3 and MeOH to obtain the 1,7 dibrominated regioisomers 4-7 (about 90% purity, ascertained by ^{1}H NMR) (Scheme **3.1.1-3**).

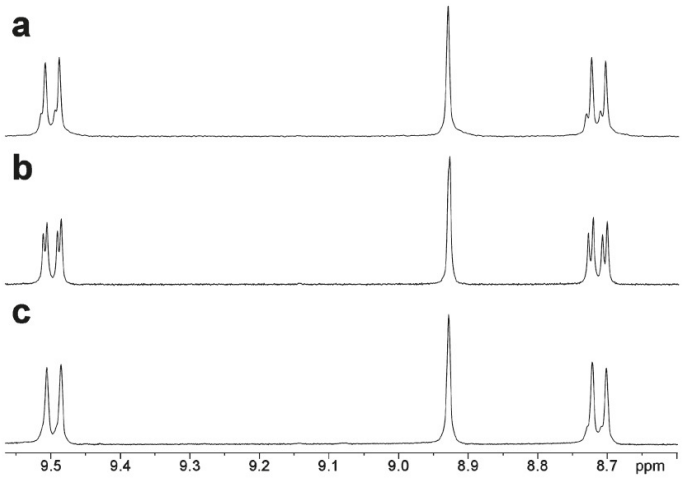

Figure **3.1.1-1**: expanded aromatic regions of ^{1}H NMR spectra in $CDCl_3$ of (a) a mixture 6:1 of 1,7 and 1,6 regioisomers of acetylated 7; (b) mother liquor enriched with the 1,6 regioisomer after precipitation; (c) 1,7 regioisomer of acetylated 7. All spectra were registered after two precipitation steps.

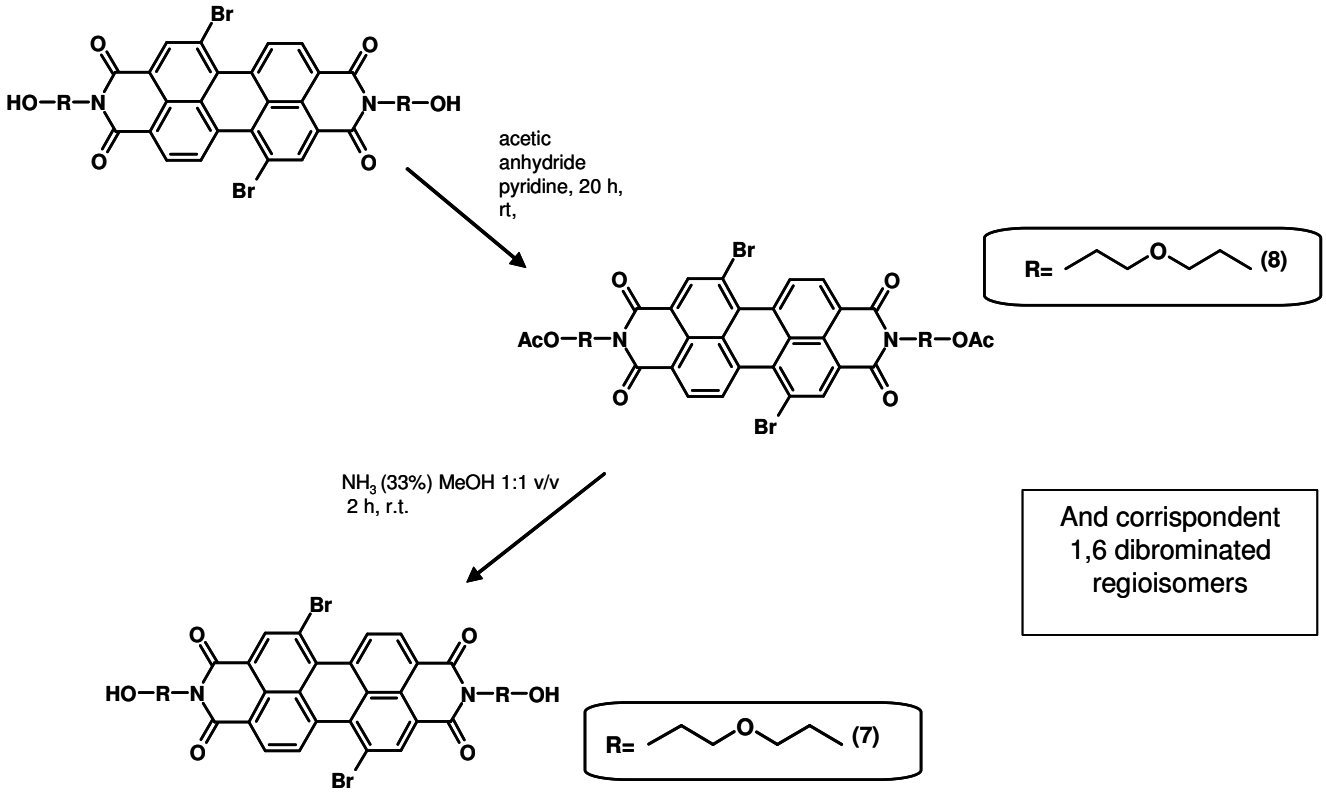

Scheme **3.1.1-3**: an example of synthesis of acetyl-derivative and successively remotion of acetyl group

These compounds show enough solubility in common organic solvents to allow the following

reactions at the terminal hydroxyls to insert the DMT and phosphoramidite groups. These reactions were performed by Prof. Mayol's group at the Università di Napoli Federico II. Due to the presence of two equivalent hydroxyls, the reaction of diimides **4-7** with DMT-Cl was performed at a molar ratio of 0.6 with respect to the substrate.

The solubility of derivatives **4-7** was properly related to the length of the side chains, and it was always higher than that for the corresponding non-brominated bisimides. The selective introduction of a DMT group was performed by the reaction of 4-7 with DMT-Cl in the presence of dimethylaminopyridine as a catalyst and a mixture of pyridine-acetonitrile as solvent. Compounds 12-15 were isolated with yields from 15 to 45%. The reaction yields (Table **3.1.1-1**) were not particularly influenced by the length of the side chains of the perylene bisimides, whereas the presence of an intrachain oxygen significativelly affected the reactivity of the hydroxyl group, as suggested by the opposite behaviour of **6** and **7** compounds.

Starting compound	Reaction with DMT-Cl	
	products	Yield (%)
4	9	< 20
5	10	20
6	11	15
7	12	45

Table **3.1.1-1**: Yields of reactions of **4-7** with DMT-Cl. The yields reported are referred to reactions conducted in a mixture of pyridine-acetonitrile 3:1 v/v.

On the basis of these results, compound **12** was selected for the conversion in the corresponding phosphoramidite derivative **13**. The synthesis was carried out by using the classical procedure (95% yields; Sinha et al. 1984) (Scheme **3.1.1-4**).

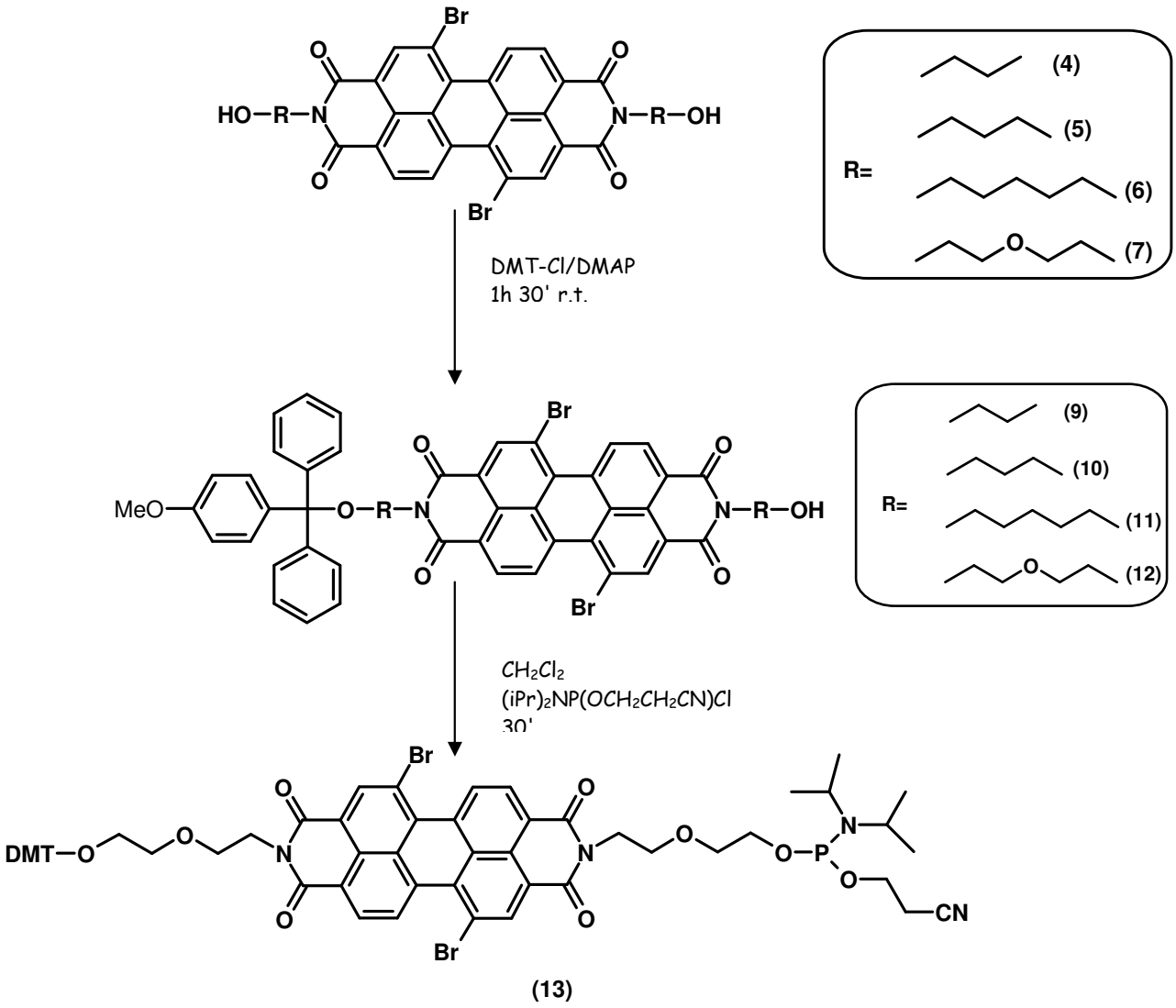

Scheme **3.1.1-4**: insertion of solid phase synthesis protective groups.

3.1.2. Synthesis of perylene conjugated oligonucleotides

The total yield for the synthesis of the phosphoramidite building-block **13** was about 40%, which is quite good with respect to the preparations reported in the literature for this kind of compounds (Bevers et al. 2000, Rahe et al. 2003). This compound was used in the subsequent conjugation to growing oligonucleotides by Prof. Mayol's group at the Università di Napoli Federico II. In all cases, sequences are grown from 3' to 5' on the solid support.

In order to select the best conditions for the coupling step in oligonucleotide solid phase synthesis, building block **13** was manually reacted with the commercially available IcaaCPG high-loading solid support functionalized with A, C, G, or T. Upgraded yields were obtained by increasing the time of each coupling cycle from 2 (standard condition) to 20 min (Table **3.1.2-1**).

Sequence (5'→3')	1° coupling cycle		2° coupling cycle	
	Reaction time (min)	Yield (%)	Reaction time (min)	Yield (%)
IcaaCPG-X-PEOEBr (X=A, G, C or T)	2	15	2	17
	10	30	10	45-48
	20	40-45	20	65-70
	40	42-45	60	65-70
IcaaCPG-GGGATTGGG-PEOEBr (HTRp2)	20	52	20	73

Table **3.1.2-1**: Yields of the coupling steps of DMT-PEOEBr-Phosphoramidite **13** on functionalized solid supports. The yields were almost insensitive to the nature of the nucleotide linked to the solid support (A, G, C, or T).

No further improvements were observed by extending the coupling time above 20 min. The selected sequence HTR2 was first synthesized by automated solid phase synthesis, then manually coupled with **13** by using two 20 min coupling cycles (Table 3.1.2-1), and finally detached from the solid support by treatment with 33% aqueous ammonia at room temperature
for 48 h. After HPLC purification, HTRp2 was checked for successful conjugation by MALDI-TOF analyses (Figure **3.1.2-1**).

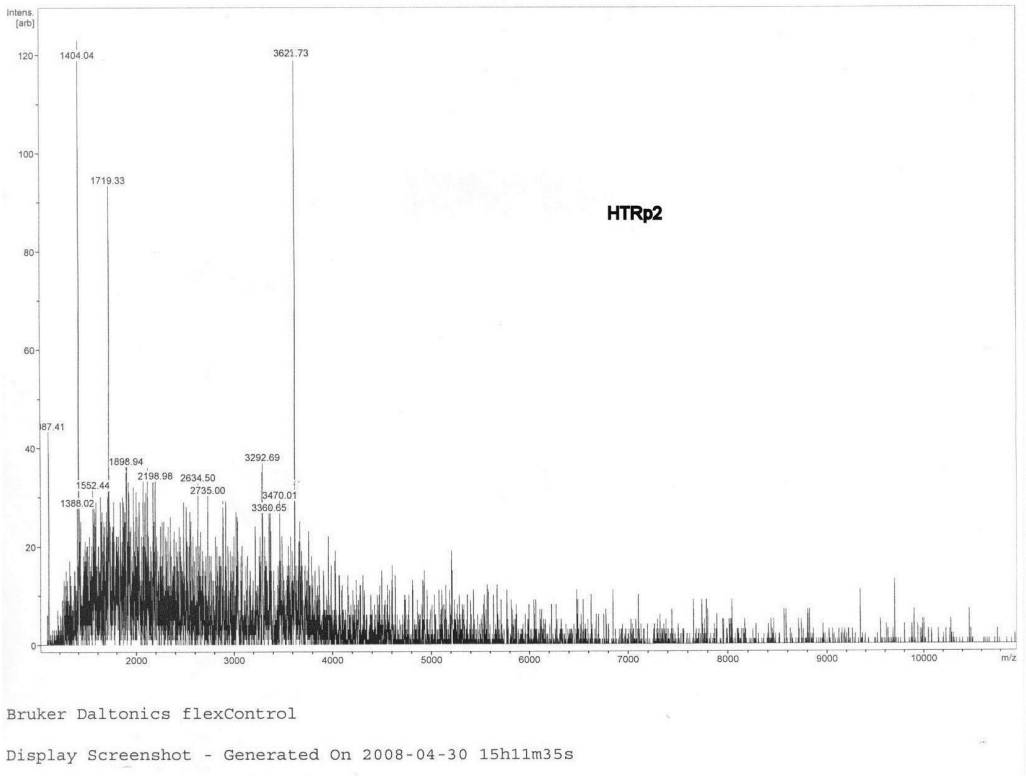

Figure **3.1.2-1**: MALDI-TOF mass spectrum of HTRp2 (positive mode). The sample was prepared using a mixture of picolinic/3-hydroxypicolinic acids as the matrix.

3.1.3. Study of spectroscopic characteristics of perylene conjugated oligonucleotides

The structural behaviour of the truncated human telomeric sequence HTR2 has been previously well characterized by using UV, CD, gel electrophoresis, NMR, and X-ray techniques (Mergny et al., 1998; Parkinson et al., 2002). In K+-containing buffer (hereafter in K+), HTR2 can form both parallel and antiparallel G-quadruplex structures, which differ by the spatial arrangement of lateral TTA loops (Figure **3.1.3-1**).

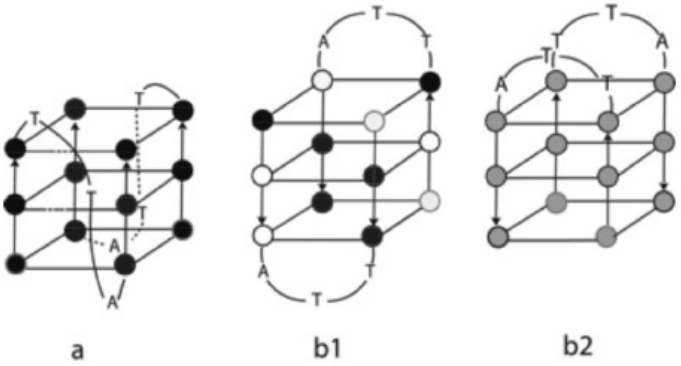

Figure **3.1.3-1**: Schematic representation of parallel (a) and antiparallel (b1 and b2) Q structures formed by unmodified HTR2. Black and white balls are used to indicate anti and syn conformations of dG residues, respectively.

NMR and CD studies (Vorličcková et al., 2002 ; Zheng et al., 2005) evidenced that the two structures can coexist and interconvert in solution. It was also demonstrated that the antiparallel Q arrangement is kinetically favoured, while the parallel one corresponds to the thermodynamical one (Vorličcková et al., 2002 ; Zheng et al., 2005). CD spectra of HTR2 in K^+ give rise to two positive dichroic bands centered at 263 and 295 nm, which can be ascribed to the formation of a mixture of both parallel and antiparallel Q structures (Vorličcková et al., 2002). Furthermore, in Na+-containing solution (hereafter in Na^+), only antiparallel Q arrangements were observed (b1 and b2, Figure **3.1.3-1**) (Vorličcková et al., 2002 ;Balagurumoorthy et al., 1994). In the latter case, HTR2, possessing a run of guanines at both ends of the sequence, can form at high strand concentration the b2 antiparallel structure (Figure **3.1.3-1**), in which the two lateral loops are located on the same side of the G-quadruplex. Two of these arrangements can mutually interact by π-stacking, forming a dimer of dimers (Balagurumoorthy et al., 1994). The two-repeat human telomeric sequence carrying additional bases at the ends of the sequence can form only the antiparallel G-quadruplex in which the two lateral loops TTA are located at opposite sides of the Q-structure (b1, Figure **3.1.3-1**) (Mergny et al., 2005). In both cases, CD spectra in Na+ give rise to a positive dichroic band centered at 295 nm and a negative one at about 260 nm. In order to verify the effect of perylene conjugation on G-quadriuplex typologies formed by HTR2, CD analyses were performed both in K^+ and in Na^+.

Figure **3.1.3-2** shows the CD profiles obtained from HTRp2 and HTR2 at 10°C in K^+.

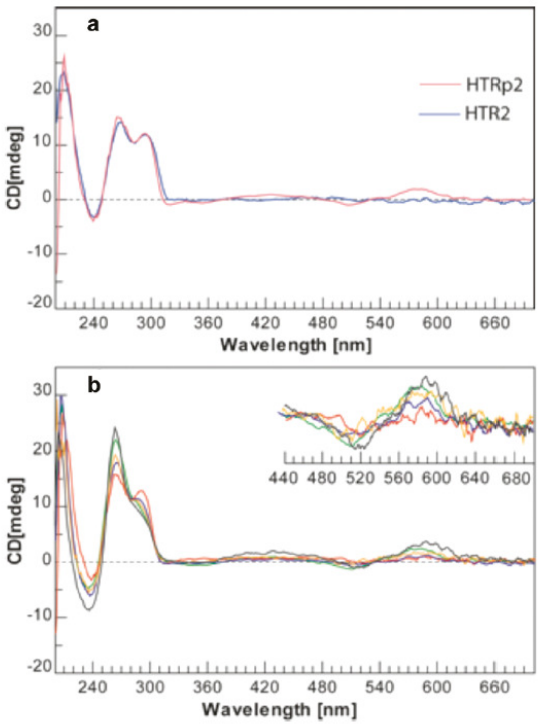

Figure **3.1.3-2**: (a) CD profiles of HTRp2 (red, 2 μM) and HTR2 (blue, 2 μM) in 10mMphosphate buffer (pH 7.4) containing 100mMof KCl. Both spectra were registered after 12 h from the annealing. (b) Time dependence of CD spectra of HTRp2 (2 μM) in 10 mM phosphate buffer (pH 7.4) containing 100 mM KCl. The sample was heated at 90°C for 5 min then slowly cooled (12 h) at room temperature, stored at 25°C, and the CD spectra registered at 25°C after 12 h (red), and 3 (blue), 5 (green), 7 (orange), and 10 (black) days.

Looking at the similarity of the shape and intensities of dichroic bands observed in the CD spectra of either HTR2 or HTRp2, it appears that the conjugation with the perylene moiety does not significantly affect the topology of resulting G-quadruplexes. Similarly to HTR2 (Vorličcková et al., 2005) the CD profiles of HTRp2 also showed different time-dependent contributions of the two dichroic bands at 262 and 295 nm (Figure **3.1.3-2,** b), with a constant increase of the first band associated with a constant decrease of the second one. However, according to CD melting experiments (Figure **3.1.3-3**, a), the conjugation provides a strong stabilizing effect on the parallel G-quadruplex structure, allowing an increase of the melting temperature of about 30°C.

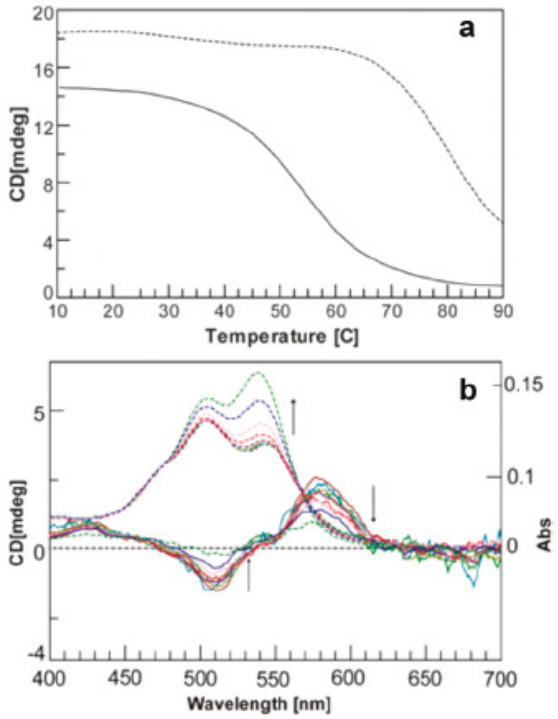

Figure **3.1.3-3**: (a) CD melting profiles (at 263 nm) of structures formed by HTR2 (2 μM) (continuous) and HTRp2 (2 μM) (outlined) in 10 mM phosphate buffer (pH 7.4) containing 100 mM of KCl. (b) Temperature- dependent CD and UV profiles in the long wavelength region for HTRp2 in 10 mM phosphate buffer (pH 7.4) containing 100 mM KCl. The arrows indicate the changes in UV and CD bands by increases in the temperature from 10 up to 90°C with steps of 10°C.

Furthermore, in K^+, HTRp2 exhibits strong long-wavelength features in CD profiles (Figure **3.1.3-3**, b) with a Cotton effect centred at 542 nm (a negative band at 500 nm and a positive band at 565 nm). By increasing the temperature, these CD bands progressively decrease in intensity, completely disappearing at 90°C, whereas the corresponding UV band at 542 nm (Figure **3.1.3-3**, b) undergoes a strong increase in intensity. The comparison between CD and UV data suggests the existence of exciton coupling between dibromo-perylene moieties (Zheng et al., 2005). Interestingly, the CD profile of HTRp2 in Na^+ changed significantly depending on the oligonucleotide concentration (Figure **3.1.3-4,** a) and on the time elapsed from annealing (Figure **3.1.3-4,** b).

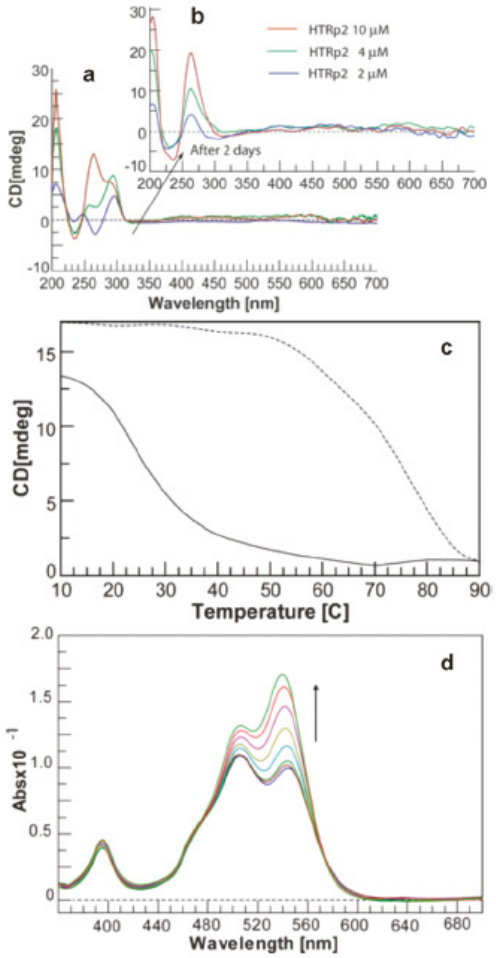

Figure **3.1.3-4**: (a) CD spectra of HTRp2 in 10 mM phosphate buffer (pH 7.4) containing 100 mM of NaCl, registered by using different strand concentrations (2, 4, and 10 µM). (b)CDspectra registered by using the same samples after two days. (c) CD melting profiles of structures formed by HTR2 (10 µM) (continuous) and HTRp2 (10 µM) (outlined) in 10 mM phosphate buffer (pH 7.4) containing 100 mM NaCl, registered by positioning the wavelength at 295 and 263 nm, respectively. (d) Long wavelength portion of UV spectra at different temperatures (10-90°C) produced by HTRp2 (4 µM) in 10 mM phosphate buffer (pH 7.4) containing 100 mM of NaCl. The arrow indicates the changes in UV bands by raising the temperature from 10 to 90°C.

At low (2 µM) strand concentration, the CD profile showed a positive band at 295 nm and a negative one at 260 nm (Figure **3.1.3-4,** a, blue line), the same as those for the unmodified HTR2 (Vorličcková et al., 2005). By increasing the strand concentration, a new band at 263 nm appeared (Figure **3.1.3-4,** a, green and red lines). Furthermore, regardless of strand concentration, the band at 295 nm completely disappeared after two days from annealing (Figure **3.1.3-4,** b). However, in all cases, no significant visible CD bands were observed. The CD melting profile (Figure **3.1.3-4,** c) obtained by monitoring the intensity of the CD band at 263 nm (ΔT=0.5°C/min) showed a strong enhancement in the stability of quadruplex structures formed by HTRp2. The long-wavelength region of UV profiles (Figure **3.1.3-4,** d) showed twoUV-visible bands produced by the dibromo-perylenemoieties. By increasing the temperature from 10 up to 90°C, the band at 542 nm shifted to 538 nm, increasing its intensity. At the same time, its red-broadening disappeared producing an isosbestic point at 570 nm. These observations suggest the existence of exciton coupling between chromophores (Baumastark et al., 2008; Zheng et al., 2006 and 2005). Furthermore, the ability of HTRp2 to associate in G-quadruplexes structures in desalted water has also been evaluated. The CD

spectra registered after heating at 80°C and rapidly cooling at 10°C displayed a positive band at 295 and a negative one at 246 nm (Figure **3.1.3-5,** a, blue line).

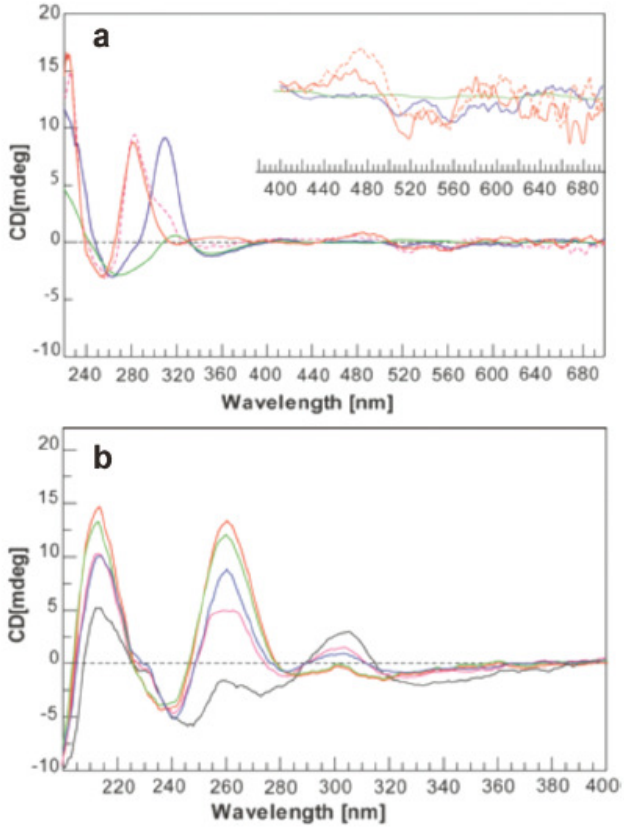

Figure **3.1.3-5:** CD and UV spectra of HTRp2 in desalted water. (a) Time dependent CD spectra. The sample was heated at 80 °C, rapidly cooled at room temperature (10 min), and kept at 20°C. The spectra were than registered after 1 h (blue line) and 3 days (dashed red line) and 10 days (red line). In green is reported the CD profile of the same sample heated at 80°C. (b) Temperature dependent CD spectra of HTRp2 in water of a sample kept for 10 days at 10°C. The spectra were registered at 10 (red), 20 (green), 40 (blue), 50 (violet), and 80°C (black).

At 25°C, the two bands slowly converted, leading after 10 days to the disappearance of the band at 295 nm and to the formation of a new band at 263 nm (Figure 3.1.3-5, a continuous red line). By increasing the temperature, the intensity of the new CD band decreased, and CD profiles showed a mixture of folded and unfolded structures (Figure **3.1.3-5,** b). These data strongly suggest the formation of G-quadruplex structures. It is noteworthy that HTR2 did not produce significant CD signals in desalted solution, in agreement with previously reported data (Figure **3.1.3-6**) (Vorličcková et al., 2005).

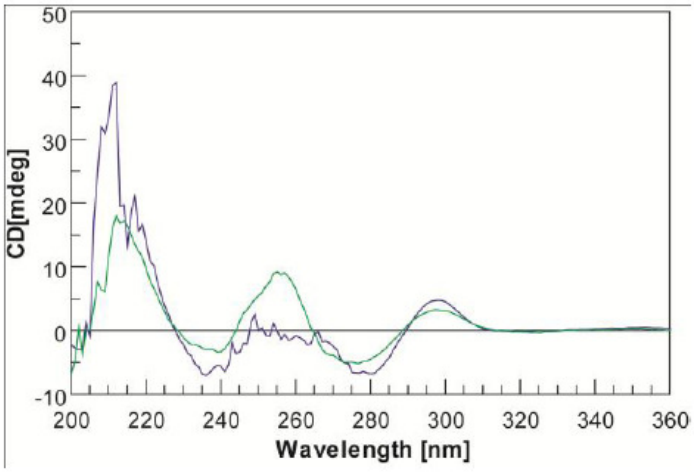

Figure **3.1.3-6:** CD spectra of 4 μM (green line) and 6 μM (blue line) HTR2 in desalted water (HPLC grade). The spectra were registered after heating at 90 °C and rapid cooling at 10 °C.

Finally, the short wavelength UV profiles of HTRp2 (Figure **3.1.3-7**), in all explored experimental conditions, showed an isosbestic point at 285 nm according to the presence of G-quadruplex structures in K^+, Na^+, and in water solutions, in agreement with previously reported studies (Mergny et al., 2005).

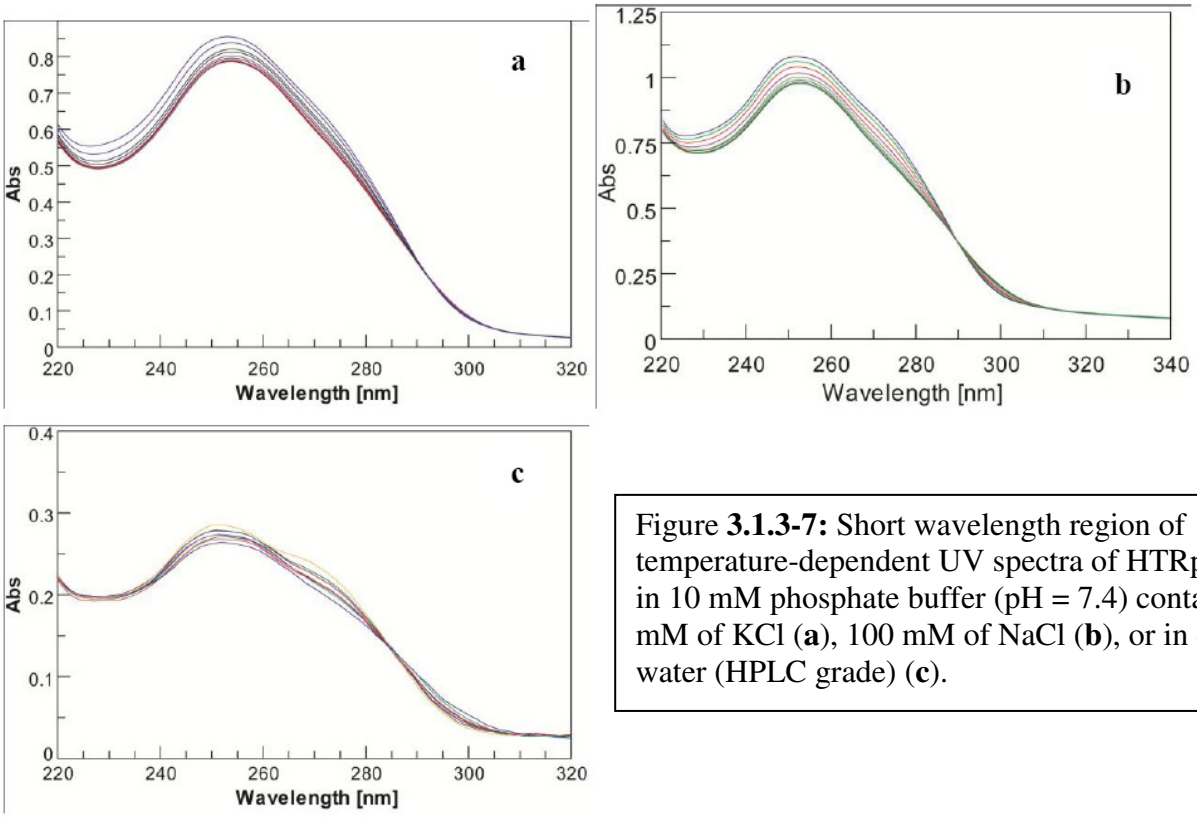

Figure **3.1.3-7:** Short wavelength region of temperature-dependent UV spectra of HTRp2 (2 μM) in 10 mM phosphate buffer (pH = 7.4) containing 100 mM of KCl (**a**), 100 mM of NaCl (**b**), or in desalted water (HPLC grade) (**c**).

Finally, fluorescence studies were conducted. Despite, the dibromo-perylene derivative showed significant fluorescence in organic solvent (Figure **3.1.3-8**), in all explored conditions, the conjugated oligonucleotide, showed only a weak fluorescence with a maximum at 560 nm (Figure **3.1.3-9**), and the quantum yield greatly increased when arising the temperature. This effect is known for such systems, and it can be explained as a consequence of quenching by neighboring DNA bases which decreases with temperature increasing. (Hariharan et al., 2009).

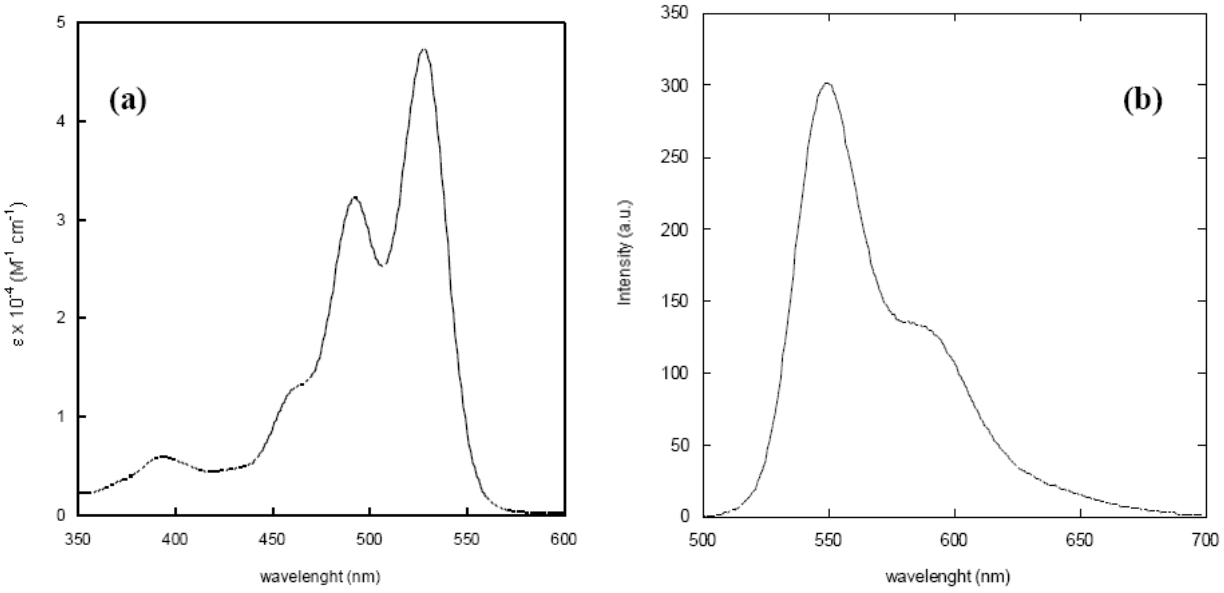

Figure **3.1.3-8:** Absorption (**a**) and fluorescence spectra (**b**) of compound **7** in chloroform. The excitation wavelength was 505 nm, the excitation and emission slits width were set to 5 nm and the emission PMT detector voltage to 600 V.

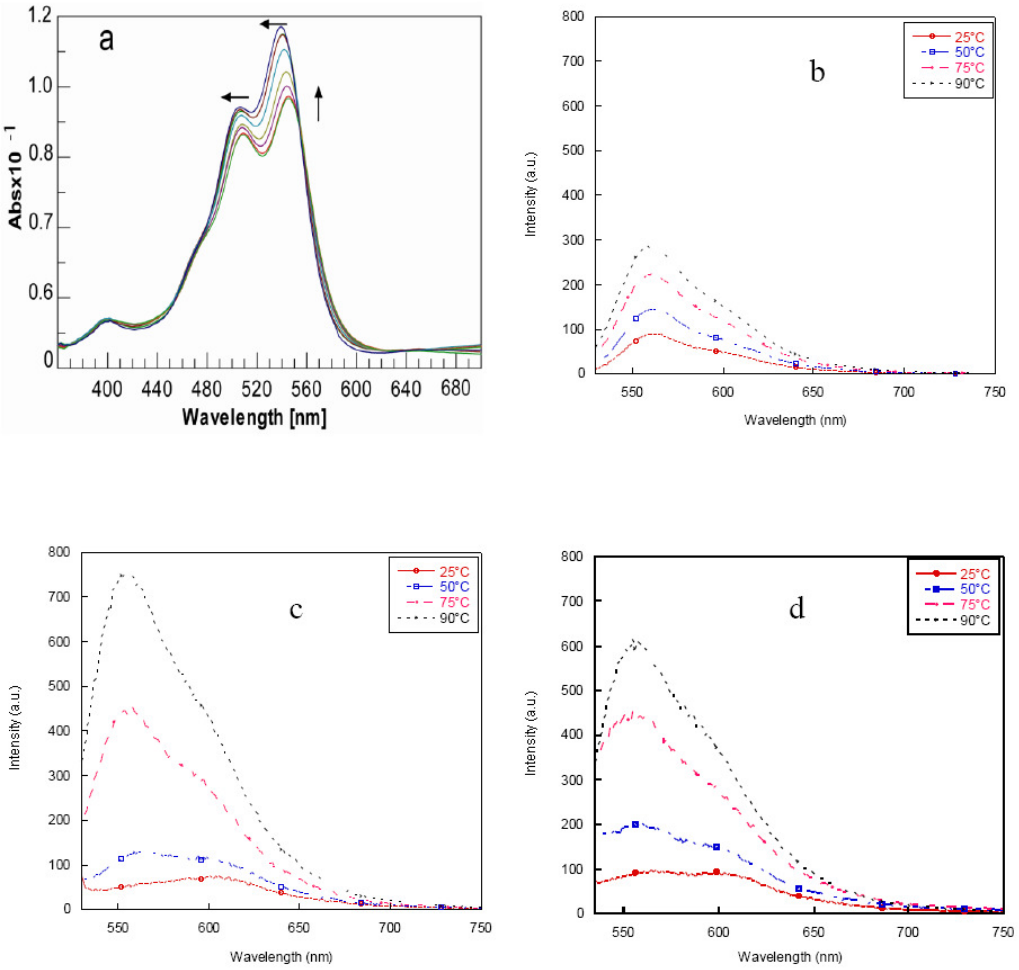

Figure **3.1.3-9:** a) long wavelength region of UV spectra registered from 10 up to 80 °C in desalted water. The arrows indicate the changes in the UV bands by increasing the temperature. b), c) and d) fluorescence spectra of HTRp2, respectively, in deionized water solution, in 10 mM phosphate buffer (pH 7.4) containing KCl 100 mM and in 10 mM phosphate buffer (pH 7.4) containing NaCl 100 mM. The spectra were acquired at different temperature by positioning ex.= 505 nm , ex. slit = 20, emission slit = 10, Voltage= 800 V, [HTRp2] = 3 μM.

3.2. Perylene as fluorescently-tagged lipid (-like) analogue

3.2.1. Synthesis of perylene derivates as fluorescent lipid analogues

Our design strategy in this part of my work starts from the research of an amphiphilic molecule with fluorescent characteristics, in order to use it as a probe in different application, as the study of the dynamic of lipids in cell biological studies or in biophysical applications.

The ideal new derivate should have hydrophobic chains ending with a polar hydrophilic head, suitable for the interaction with phospholipids bilayers, including a fluorescent hydrophobic core.

Perylene anhydride is an excellent candidate for creating the desired probe, since the insertion of side chains on the major axis of perylene is a well studied procedure (Würthner et al., 2004; Franceschin et al., 2004). Moreover perylene bisimide dyes are known for their high molar absorption coefficients 30,000– 90,000 cm^{-1} M^{-1} (Kohl et al., 2004; Langhals et al., 2000), fluorescence quantum yields close to unity (Seybold et al., 1989) and excellent photostability (Rademacher et al, 1982). Also in this case we used perylene derivatives modified on the bay-area by bromination (**2**), due our experience on perylene solubility.

In order to obtain a compound with the desired properties described above, we chose to insert as side chains on the dibromoperylene core two diammines with a long aliphatic chain: 1,8 diaminooctane (**14**) and 1,12-diaminododecane (**15**). This compound has the right length to take place inside phospholipids bilayers and presents two amino groups which are suitable for the reaction with the anhydride function, leaving a polar group at the opposite end of the chain.

On the other hand, the simultaneous presence of two equivalent groups on the same molecule represents the second main challenge of the proposed synthetic route.

Initially, based on a previous work of ours (Franceschin et al. 2008) we tried to conduct the reaction at 1:10 ratio (compound **1**: aliphatic chain **2**). The excess of reactant should avoid polymerization to occur. On the other hand we couldn't use a large excess of amine to avoid undesired side reaction of bromine substitution.

Unfortunately the main products obtained in these conditions were perylene mono-imides and not the di-substituted derivatives (Scheme **3.2.1-1**).

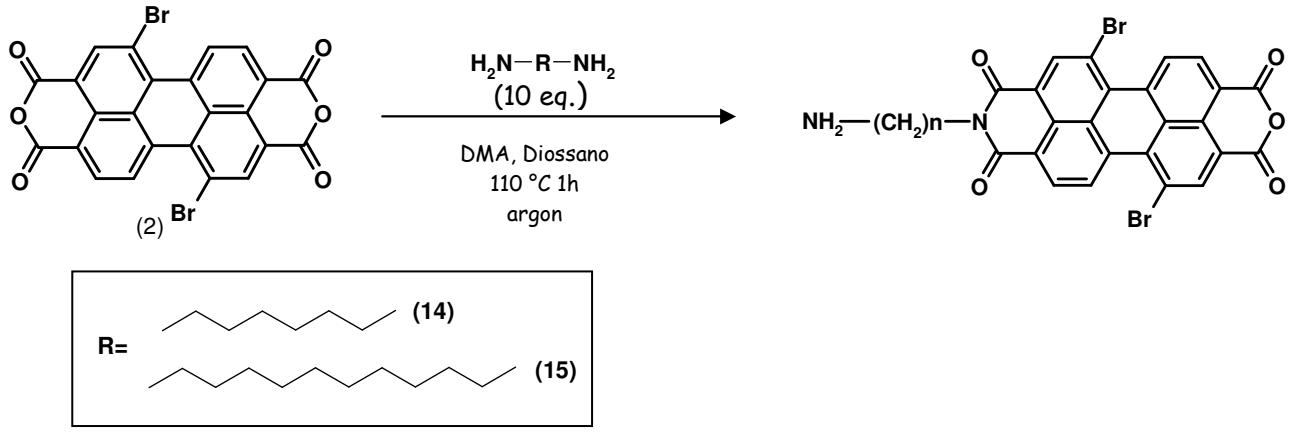

Scheme **3.2.1-1:** failed synthetic pathways experimented in order to obtain diimmide derivates

So we developed a different synthetic strategy: the first modification we made to the structure of compounds **14** and **15** was the protection of one of the two aminic groups with boc-anhydride (Scheme **3.2.1-2**). The addition of classical amino protecting group BOC led to asymmetrical compounds where the two amino groups present a different reactivity. In this reactions it is not useful to operate in stoichiometric conditions, considering that a high amount of unrecoverable di-protected derivatives would be obtained. So the reaction was conducted using BOC reactant at 0.3:1 ratio with respect to the amine (Ji et al., 2009), in dichlorometane at room temperature for 3 days, to obtain the desired compounds **16** and **17**. The mono-protected product **16** and **17** were efficiently purified by column chromatography on silica gel ($CHCl_3$/MeOH (90/10)). Even though due to the use of a small amount of boc-anhydride a big percentage of the unreacted amines remained in the reaction mixture, it was possible to recover by the same column chromatography the purified starting compounds, which could be again utilized.

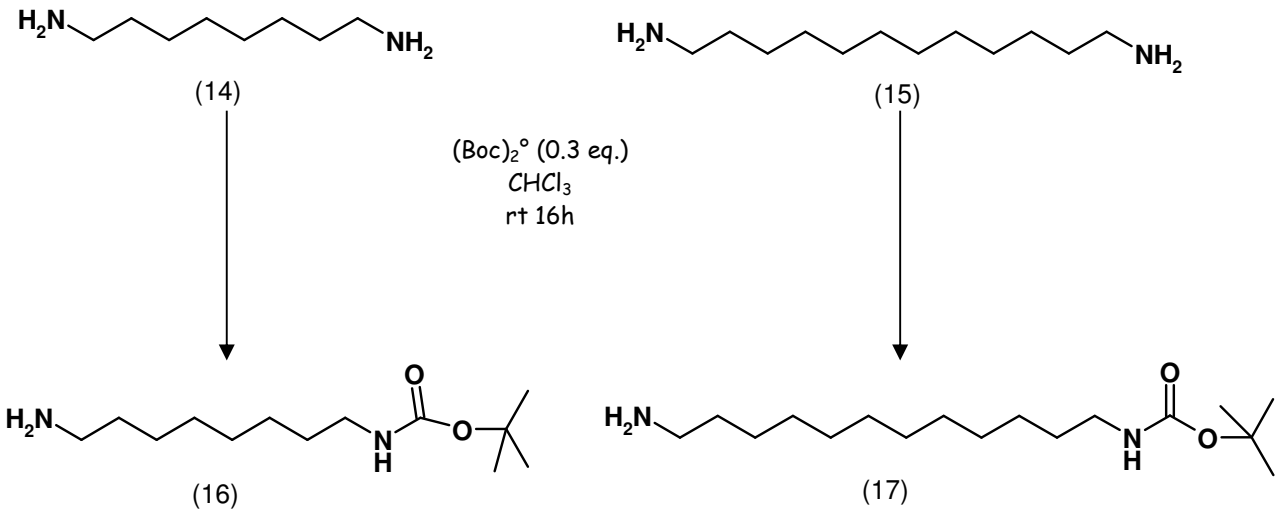

Scheme **3.2.1-2:** protection of amino groups with boc-anhydride

Once the asymmetrical compounds **16** and **17** were synthesized, perylene diimides **18** and **19** were easily obtained by treatment of the perylene anhydride **2** with an almost stoichiometric amount of **16** and **17**, in DMA/dioxane under argon, in a similar way as reported previously by our group (Rossetti et al. 2005).

No more than 10% excess of reactants was used to avoid side reactions at the brominated positions, which can occur at higher ratios. It is worth noting that, in principle, substitution of bromine atoms by primary amine can actually occur even at stoichiometric ratio. In our experience, this can be avoid strictly controlling the temperature and the time of reaction, following on TLC the appearance of any blue-green spot. If such spots appear, the reaction must be stopped and the products can be purified by column chromatography. Considering these aspects, the best conditions for this reaction were found to be heating for 6 h under reflux (Scheme **3.2.1-3**), after which the reaction was quenched by ice and brine and the mixture was cooled at 4 °C overnight. The precipitate was then filtered, washed repeatedly with water and dried under vacuum.

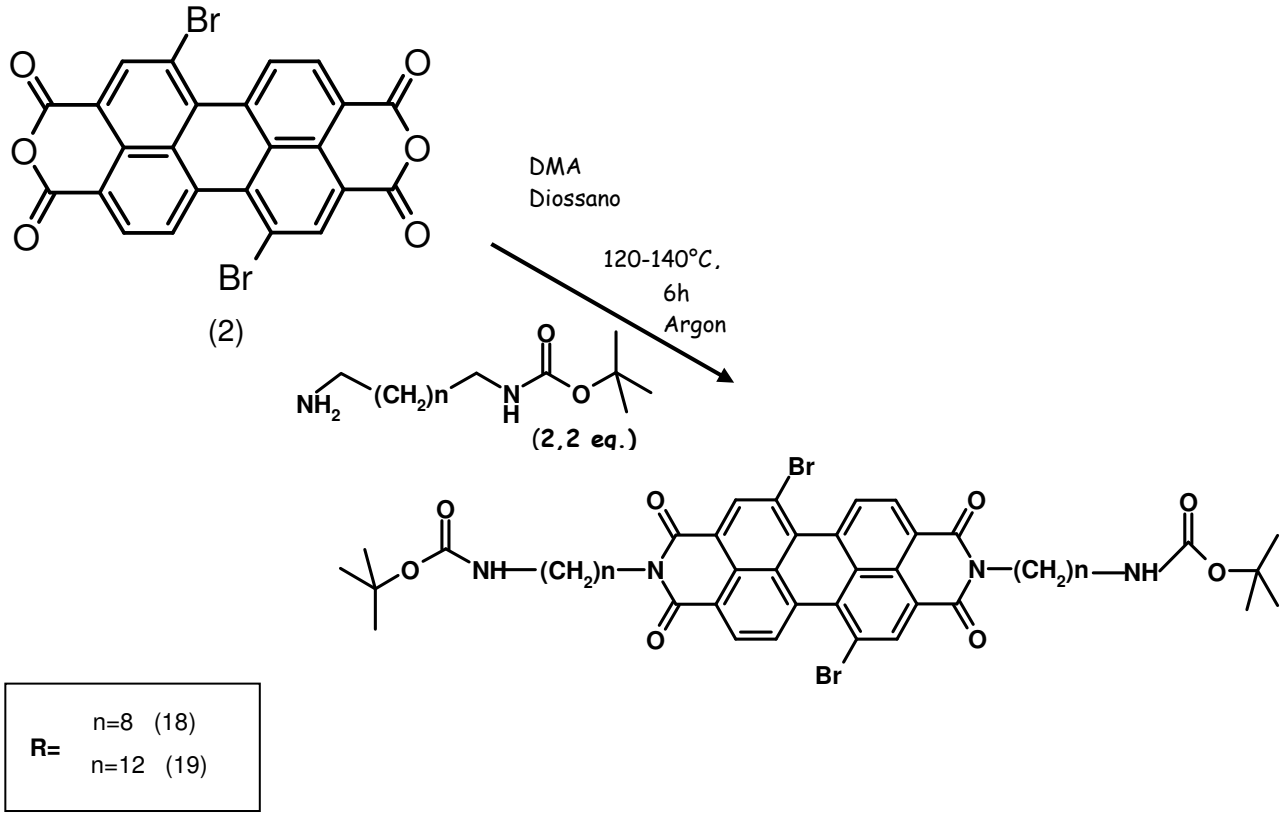

Scheme **3.2.1-3:** insertion of amminic ending side chains on the perylene major axis

The deprotection of pure compounds **18** and **19** were conducted in dichloromethane adding TFA dropwise. The mixture was stirred for 12 hours at 0°C, to transform tert-butyl ester in the free amines to obtain the pure compounds **20** and **21**.

Finally, to obtain a *bola* type molecule, the polar hydrophilic heads were subjected to exhaustive methylation in order to obtain a positively charged ending group. In particular, **N,N'-Bis(8-** t**rimethylammonium-octane) 1,7-dibromoperylene-3,4:9,10-tetracarboxylic diimide iodide** (perylene-Br-C8, compound **22)** and **N,N'-Bis(12-** t**rimethylammonium-dodecane) 1,7-dibromoperylene-3,4:9,10-tetracarboxylic diimide iodide** (perylene-Br-C12, compound **23)** were obtained by adding CH_3I to perylene bisimide previously dissolved in dioxane. After filtration, the desired compound: perylene-Br-C8 and perylene-Br-C12 were obtained in quantitative yield **(**Scheme **3.2.1-4)**.

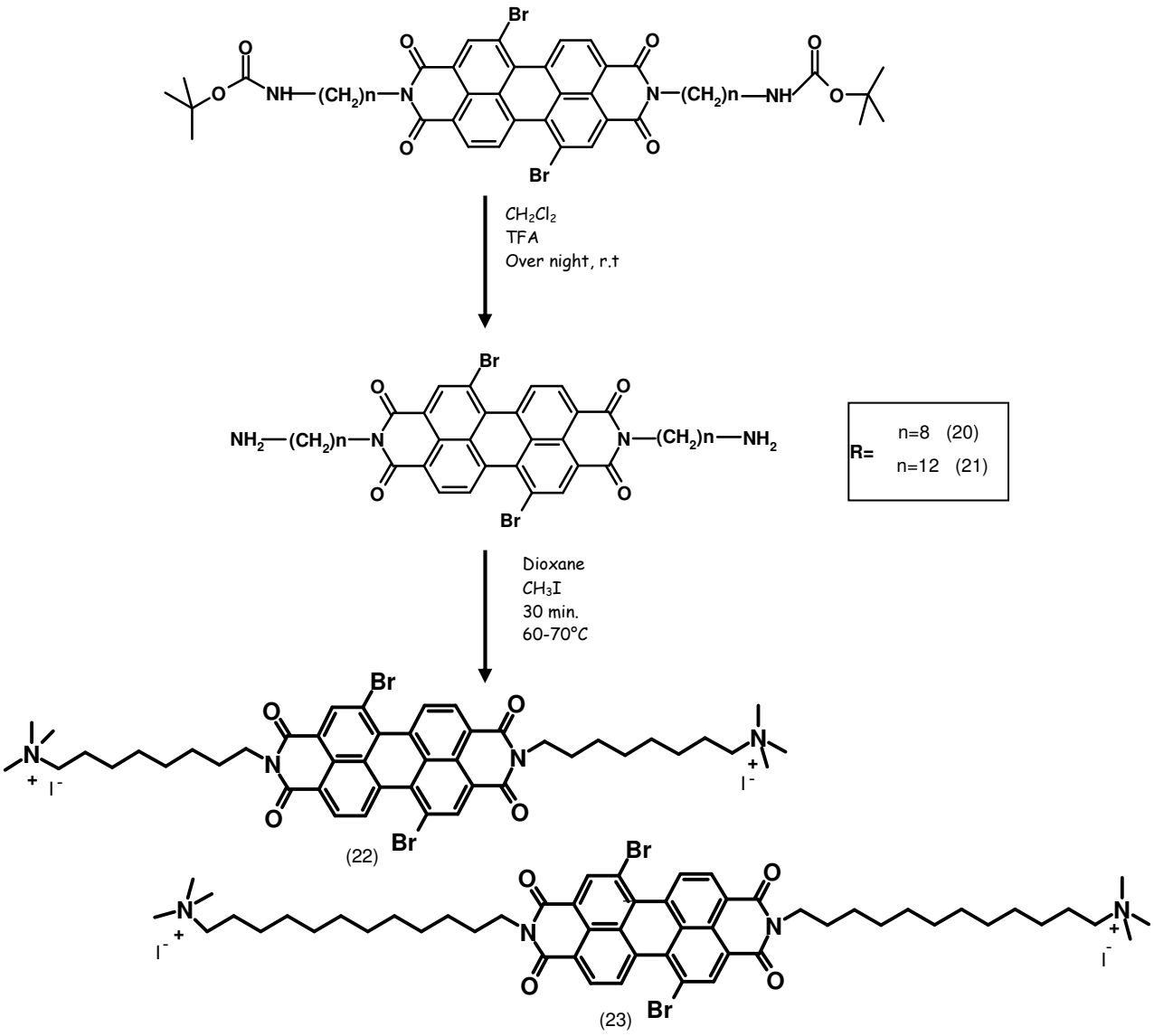

Scheme **3.2.1-4:** deprotection of amminic groups amd exhaustive methylation

3.2.2. Introduction of perylene in liposome

Between the two synthesized compounds, we decided to insert in phospholipids bilayers only perylene-Br-C12 . Unfortunately perylene-Br-C8 showed limited solubility, both in water and in common organic solvents and the operation of introduction in liposome could be difficult with a molecule as perylene-Br-C8. Moreover the length of major axe for perylene-Br-C12 (50 Å) was more adequate to take place inside phospholipids bilayers (80-100 Å).

The liposome used was the DMCP one (Dimyristoyl-*sn*-glycero-phosphocoline).

In collaboration with Dott.ssa Mancini's group at the CNR, the aqueous dispersion of DMPC/ perylene-Br-C12 liposomes was prepared according to the procedure described by Hope et al. A solute unentrapped in liposomes, as general rule, remains in solution after the extrusion and is removed from the liposome dispersion by filtration on exclusion chromatography column. In some cases the unentrapped solute can associate in solution to give large aggregates; in this case, it can be removed also in the extrusion procedure by the polycarbonate membrane. Therefore, the amount of unentrapped perylene-Br-C12 excluded by extrusion and/or gel filtration is mainly dependent on its aggregation state and water solubility.

Briefly, a film of lipid was prepared by evaporation of $CHCl_3$ solution in order to obtain the desired percentage mixture of DMPC/ perylene-Br-C12 500/1.

To the obtained film were added PBS buffer solution in order to obtain a final concentration of $2{,}5x10^{-2}$ M in DMPC and $5x10^{-5}$ M in perylene-Br-C12. The dispersion was then extruded at 307 K, well above the transition temperature of DMPC (297.2 K).

The unentrapped perylene-Br-C12 in extruded DMPC liposomes was separated from the liposomes on gel column Sephadex.

In Table **3.2.2-1** the molar percentages of perylene-Br-C12 in DMPC liposome dispersions at each stage of the preparation are reported. These values indicate that the percentage of perylene-Br-C12 in liposome solutions decreases only after extrusion, whereas does not change after gel filtration, thus suggesting that the polycarbonate membrane filters off all unentrapped perylene-Br-C12. This evidence suggests that the unentrapped perylene-Br-C12 is present in the buffer in the shape of large aggregates.

Table **3.2.2-1** Molar percentages of perylene-Br-C12 in DMPC liposome dispersions at each stage of the preparation.

	before extrusion	after extrusion	after gel filtration
% perylene-Br-C12	100%	80%	80%

3.2.3. Study of spectroscopic characteristics of perylene-bola lipids

UV and Fluorescent techniques were used to preliminary study the behaviour of perylene derivate. Absorption spectra were conducted both in DMSO and in water, in function of concentration.
All the spectra in DMSO show two main maxima in the UV/vis range, one of high intensity at 528 nm and the other at 494 nm (Figure **3.2.3-1**). Moreover, a shoulder at higher energy (458 nm) can be detected. The observed pattern (Gvishi et al., 1993; Sadrai et al., 1992), is due to the vibronic fine structure of the S0-S1 transition of the perylene moiety; in particular, the lower energy band, corresponding to the 0-0 transition, is more intense with respect to the higher energy band, corresponding to the 0-1 transition, and the shoulder can be assigned to the 0-2 transition. As expected, the vibronic peak are not well resolved as in other perylene derivatives without substituents in the "bay" positions. Qualitatively, this broadening originates from the loss of planarity of the perylene ring due to the presence of a bromine atom in the bay area. (Mahin et al., 1992). However, little changes of maxima absorption wavelengths are observed with respect to pure perylene, as expected in the presence of electron-withdrawing substituents in the "bay" positions. Moreover, the maxima absorption wavelengths of the bands do not shift with concentration and the ratio of the two main vibronic bands is constant in all the explored concentration range. Thus, in DMSO, the overall features of the spectra suggest the absence of aggregation involving a π- π interaction between the perylene rings.

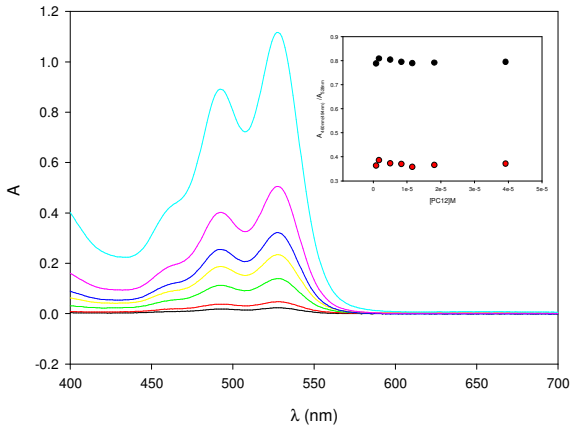

Figure **3.2.3-1:** Absorption spectra at increasing concentration of perylene-Br-C12 in DMSO are reported (concentration range 8.5x10-^{7} M – 4x10-^{5} M).

In aqueous solution perylene-Br-C12 shows the typical absorption spectrum of aggregated perylene dyes (Figure **3.2.3-2**); in fact, the absorption intensities of all bands decrease, and the 0-1 transition becomes more intense than the 0-0 one. The intensity reversal observed for the 0–0 and 0–1 bands indicates that in water the Franck–Condon factors favour the higher (0–1) excited state, (Yagai et al., 2008; Wang et al., 2010) suggesting the formation of H-type π- π stacking aggregates. By heating the sample (PC12 1x10^{-5} M) up to 55°C the relative intensity of the perylene absorption peaks does not change. (Figure **3.2.3-2**, see inset).

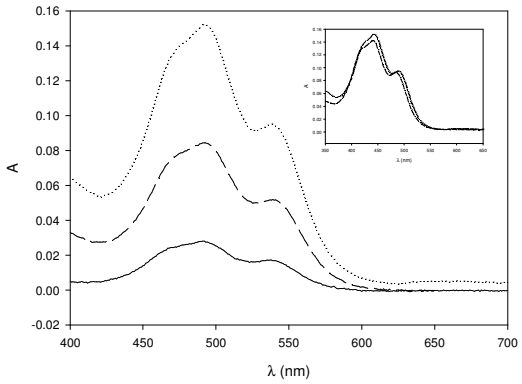

Figure **3.2.3-2:** Absorption spectra at different concentrations of perylene-Br-C12 in water are reported (concentration range 6x10-^{6} M – 1x10-^{5} M).

As UV-VIS spectra, also the study of fluorescence emission of perylene derivate alone was conducted in DMSO and in water as a function of temperature (25°C-60°C).

The emission spectrum in DMSO (Figure **3.2.3-3**) shows a broad band with a maximum at 555 nm and a shoulder at 595 nm, that is the mirror image of the absorption spectrum, as previously observed for other perylene derivatives. However, differently from other perylene dyes, the quantum yield of perylene-Br-C12 is very low, and the determination of its absolute value by the

standard method was not possible. The reason of this low quantum yield can be ascribed mainly to the nature of the substituent at the imide group (Würthner 2004). The alkyl chains on the nitrogen are not fixed in an orthogonal conformation and are characterized by a high conformational freedom, the vibronic motions ('loose bolt effect') (Rademacher et al., 1982) are responsible for a drop in the quantum yield of perylene. Another cause could be the nature of the counterion, i.e. iodide, that is a well known fluorescence quencher.

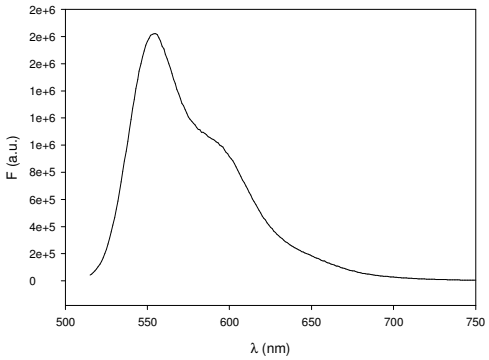

Figure **3.2.3-3:** Fluorescence emission spectrum of perylene-Br-C12 in DMSO ($6x10^{-6}$ M).

The emission spectrum in water shows, as in DMSO, a broad band with a maximum at 562 nm and 595 nm (Figure **3.2.3-4 a**). However, the aggregation behaviour of perylene-Br-C12 in this solvent is responsible for the decrease in the fluorescence quantum yield with respect to DMSO. In fact, with increasing temperature, the intensity of the fluorescence emission increases, suggesting a temperature driven disaggregation process. Note that, as expected, the fluorescence emission of perylene-Br-C12 as a function of temperature in DMSO decreases with increasing temperature, as obvious for a fluorophore in the absence of aggregation (Figure **3.2.3-4 b**).

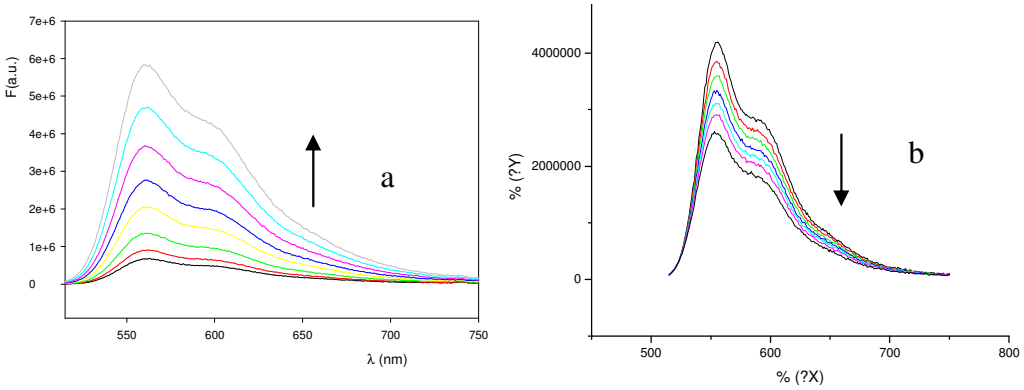

Figure **3.2.3-4:** Fluorescence emission spectra of perylene-Br-C12 ($6x10^{-6}$M) as a function of temperature (25°C-60°C) are reported: a) in water, b) in DMSO

The fluorescence intensity of perylene-Br-C12 entrapped in liposomes is very high with respect to perylene derivate at the same concentration ($6X10^{-6}$ M) in the buffer (Figure **3.2.3-5a**), suggesting that the perylene dye molecules are included in the lipid bilayer in the monomeric form.

Moreover, all the fluorescence spectrum is blue shifted, with the maximum at 543 nm (Figure **3.2.3-5b**). The maximum is 562 nm in water and 555 nm in DMSO, respectively, therefore, this shift suggests that the perylene dyes are located in a less polar environment. These evidences point out that, as expected from its lack of solubility in water, perylene-Br-C12 is embedded in the liposome bilayer, and, probably the dye molecules are not aggregated. This hypothesis is strengthened by the behaviour of the perylene-Br-C12 liposome solution with increasing temperature from 25 up to 60 degrees (Figure **3.2.3-6**): no increasing in intensity of fluorescence emission, suggestive of a disaggregation process, is observed, whereas, a slightly decrease of fluorescence emission is detected.

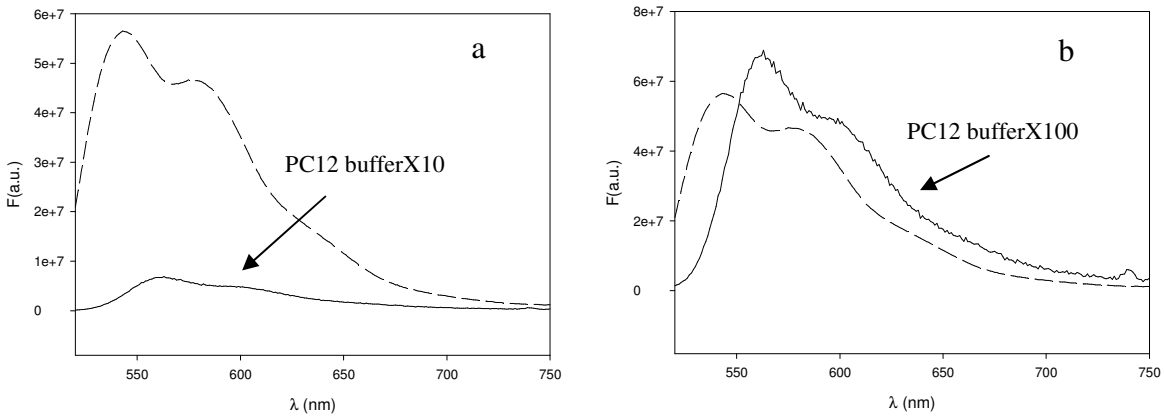

Figure **3.2.3-5:** Emission fluorescence spectrum of perylene-Br-C12 entrapped in liposomes after gel filtration.

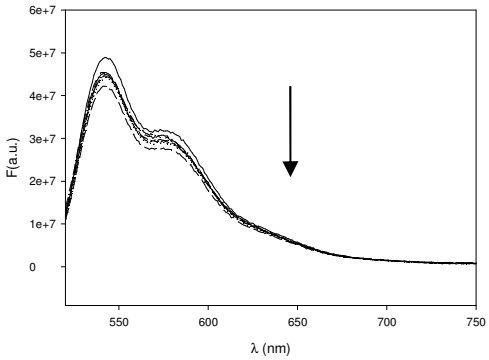

Figure **3.2.3-6:** Emission fluorescence spectrum of perylene-Br-C12 entrapped in liposomes in function of temperature.

Finally, the interactions of perylene-Br-C12 with cellular structures were studied in order to evaluate the potential of the newly synthesized compound as a fluorescent lipid probe. In particular, intracellular localization of perylene-Br-C12 administered either in DMSO or entrapped in liposomes was analyzed by laser scanning confocal microscopy (LSCM) in both human (LN229) and murine (C6) glioblastoma cells. As visualized in Figures **3.2.3-7 a-b** and **3.2.3-8 a-b**, after 5 and 27 h of treatment with a DMSO solution of the probe, perylene-Br-C12 stained preferentially cellular membranes of both C6 and LN229 cells. Plasma membrane and intracytoplamic organelles appeared strongly fluorescent, while no significant signal was revealed inside the nuclei. The cellular distribution of perylene-Br-C12 completely changed when it was entrapped in DMPC liposomes. After 5 h of incubation it completely failed to stain C6 and LN229 cells, as demonstrated by the lack of fluorescent signal in treated glioblastoma cultures (data not shown).
On the contrary, after 27 h of incubation, strongly fluorescent clusterized on the plasma membranes were revealed on both C6 and LN229 cells, whereas no intracytoplasmic signal could be observed (Figures **3.2.3-7 c** and **3.2.3-8 c**).

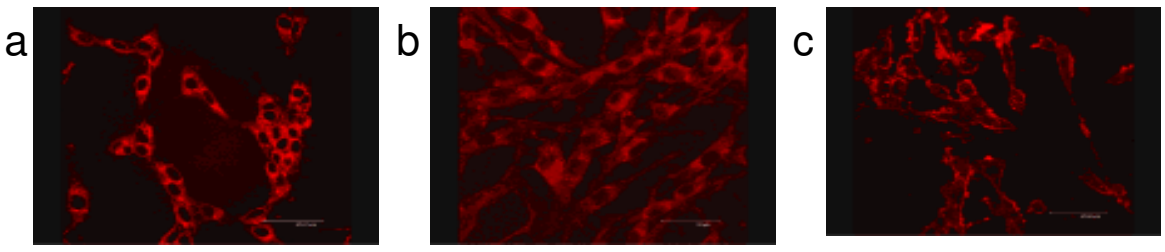

Figure **3.2.3-7**: LSCM data in membranes of murine (C6) cells: **a**, perylene-Br-C12 after 5 h; **b**, perylene-Br-C12 after 27 h; **c**, perylene-Br-C12 loaded in liposomes after 27 h.

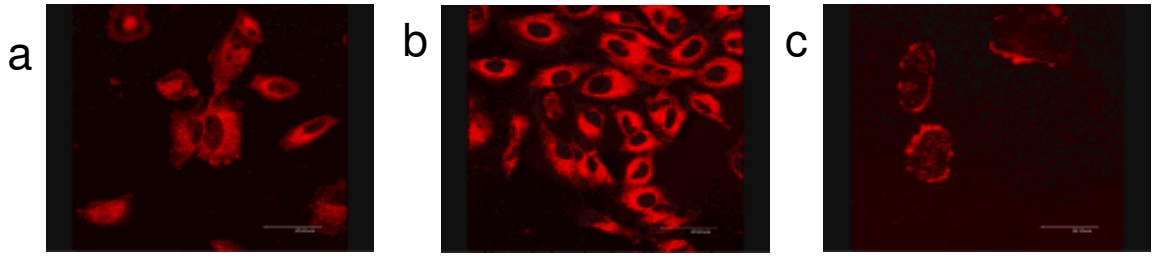

Figure **3.2.3-8**: LSCM data in membranes of human (LN229) glioblastoma cells: **a**, perylene-Br-C12 after 5 h; **b**, perylene-Br-C12 after 27 h; **c**, perylene-Br-C12 loaded in liposomes after 27 h.

4. CONCLUSIONS

Perylene bisimide derivatives show very interesting physical properties that render them useful for a high number of possible technical applications. The main aim of my thesis work was the synthesis of some dibromoperylene diimides suitable for study of fluorescence when they are inserted in biological-inspired systems:

- conjugation with quadruplex-forming G-rich oligonucleotides, to investigate the effect of such conjugation on the formation of G-quadruplexes species and to obtain nanostructures based on fluorescent G-quadruplex;
- insertion in phospholipids bilayers to study their dynamic, intramolecular and intracellular localization of the probe and the way of action of the probe during liposome assembling.

In the first case I have performed the synthesis of a new dibromoperylene phosphoramidite building block, suitable for conjugation with quadruplex-forming G-rich oligonucleotides, to investigate the effect of such conjugation on the formation of G-quadruplex species. While in the other case I synthesized suitable ligands to be included in phospholipids bilayers, to investigate the dynamic of these systems.

In particular, in order to obtain DNA aptamers, I tried improving the stability of quadruplex forming oligonucleotides covalently binding a perylene derivative to the DNA chain.

Therefore the target of this part of my work was the synthesis of perylene units opportunely functionalized to be inserted in the oligonucleotides solid phase synthesis.

The key problem with these molecules was their low solubility that didn't allow the insertion of the solid phase oligonucleotides synthesis protective groups.

To solve this problem I followed the strategy to insert substituents on the bay area improving the solubility in order to obtain phosphoramidite building-blocks.

By the first way I synthesized four bromine-substituted perylene diimides: N,N'-Bis(2-hydroxyethyl)-1,7-dibromoperylene-3,4:9,10-tetracarboxylic diimide (**4**), N,N'-Bis(3-hydroxypropyl)-1,7-dibromoperylene-3,4:9,10-tetracarboxylic diimide (**5**), N,N'-Bis(5-hydroxypentyl)-1,7-dibromoperylene-3,4:9,10-tetracarboxylic diimide (**6**) and N,N'-Bis(5-hydroxy-3-oxapentyl)-1,7-dibromoperylene-3,4:9,10-tetracarboxylic diimide (**7**).

Differently from not-brominated perylene diimides (Franceschin et al. 2004, Bevers et al. 2000), these compounds show enough solubility in common organic solvents to allow the following reactions at the terminal hydroxyls to insert the DMT and phosphoramidite groups. So in collaboration with prof. Mayol's group at the Università di Napoli Federico II it was possible to obtain with a good yield perylene derivatives as "phosphoramidite building-blocks", presenting the

two typical groups of the nucleotide precursors (DMT and phosphoramidite), useful for the solid-phase synthesis of conjugated oligonucleotides.

Between all the synthesized compounds the first selected in order to synthesize modified oligonucleotides, due to its good yield was 7. This compound was efficiently inserted in the desired step of the oligonucleotides solid-phase synthesis, according to well-established procedures. By modifying the coupling times, coupling yields have been optimized up to 70%, while following nucleotides show a coupling yield comparable to that of canonical nucleotides. This synthetic pathway is very interesting, due to the really higher yield with respect to the other previously reported in the literature, also for different applications, like obtaining fluorescent probes.

In this way one conjugated oligonucleotide was obtained: 5'-end conjugated PEOEBr-GGGTTAGGG (HTRp2).

First of all fluorescent studies were carried out. Despite, the dibromo-perylene derivative showed significant fluorescence in organic solvent, in all explored conditions, the conjugated oligonucleotide, showed only a weak fluorescence with a maximum at 560 nm , and the quantum yield greatly increased when arising the temperature. This effect is known for such systems, and it can be explained as a consequence of quenching by neighboring DNA bases which decreases with temperature increasing.

The G-quadruplex assembly properties of HTRp2, were evaluated in different conditions using UV, CD and fluorescence methods.

These studies were performed to obtain information about the influence of the perylene moiety on the folding properties of the sequences comparing the ability to form G-quadruplex structures of conjugated HTRp2 with the unmodified HTR2 in Na^+ or K^+ containing solutions. The structural behaviour of HTR2 incorporating PEOEBr at its 5'-end seems to be responsible for both the accelerating effect on quadruplex assembly of the resulting molecule in desalted solution and for the strong stabilizing effect of G-quadruplexes structures formed both in Na^+ and in K^+.

In the presence of Na^+ ions, as previously described by Hamilton and co-workers–for a perylene-conjugated G-rich oligonucleotide, the presence of the dibromoperylene moiety promotes the structuration in parallel G-quadruplexes. However, the decrease in the size of aggregates formed by dibromoperylene moieties, allows also the formation of antiparallel G-quadruplex species, which have been found to convert into the parallel one in a time- and concentration-dependent manner.

On the other hand, in the presence of K^+ ions, both HTR2 and HTRp2 give rise to similar CD profiles, which can be related to the formation of both parallel and antiparallel G-quadruplex structures. It is interesting that in K^+ the antiparallel G-quadruplex formed by HTRp2 slowly

switched to the parallel one in agreement with previously reported data by Vorlikova and co-workers.

The feature of HTRp2 of assuming different conformation (parallel/antiparallel) in the presence of Na^+ or K^+ ions, can be used in nano-technology field, based on the G-quadruplex. In fact nanostructures is a new fields of application of G-quadruplex structures with open synthetic challenges. For example one of the possible application of the new perylene conjugated oligonucleotides, is a quadruplex probe for the fluorimetric detection of K^+ ions (Nagatoishi et al., 2007). Another application of HTRp2 is to use perylene conjugated oligonucleotides as an "aptamer" with potential anti-HIV activity. In fact there are several different G-quartet oligonucleotides proposed and studied for their ability to inhibit HIV. One of the most efficient resulted to be the 17-mer oligonucleotide, 5'-GTGGTGGGTGGGTGGGT, referred to as T30177 (AR177 or Zintevir). In particular the biological activity of DNA-aptamers is correlated with the strong interaction with HIV-1 integrase in vitro and the ability to inhibit the integration of viral DNA into host DNA (Jing et al. 2000).

At the same time I synthetized new dibromoperylene derivates, fluorescently labelled lipid analogues.

In my work I performed the synthesis of perylene derivates suitable for the insertion in liposome. So we decided to modified perylene bay-area with suitable chains, in order to obtain molecules with right length and with amphiphilic characteristics required for the interaction with phospholipids bilayers.

As a first result, we obtained two new bromine-substituted perylene diimides: perylene-Br-C8 (**22**) and perylene-Br-C12 (**23**).

After examination of chemico-physical characteristics of the two derivates, we decided to insert in phospholipids bilayers only perylene-Br-C12. In fact perylene-Br-C8 showed limited solubility, both in water and in common organic solvents. Moreover the length of major axe for perylene-Br-C12 (50 Å) was more adequate to take place inside phospholipids bilayers (80-100 Å).

In collaboration with Dott.ssa Mancini's group at the CNR, it was possible to insert perylene-Br-C12 in liposome, with a good yield.

The liposome used was the DMCP one (Dimyristoyl-*sn*-glycero-phosphocoline).

According to a well established procedure, a film of lipid containing the proper amount of DMPC and perylene-Br-C12 (500/1) was prepared . The percentage of entrapped drug was 80 % .

Preliminary UV and fluorescent studies were performed in order to obtain information about the perylene-Br-C12 both alone and inside phospholipids bilayers.
UV spectra of perylene derivate demonstrated the classical opposite behaviour in organic solvent and in water: the absence of aggregation in DMSO and a typical spectrum of aggregated perylene in water.
Similarly emission spectra in function of temperature (25°C-60°C) show a increase in the fluorescence quantum yield in water, due to aggregation state as obvious for a fluorophore in the presence of aggregation.
The data collected for perylene-Br-C12 in liposomes suggest that perylene-Br-C12 is embedded in the liposome bilayer were the dye molecules are most probably in the monomeric form.

The different subcellular localization of free and liposome-entrapped perylene-Br-C12 could provide the basis for its different uses as fluorescent lipid probe. In fact, free perylene-Br-C12 was detectable both in plasma membrane and intracytoplasmatic organelles, whereas perylene-Br-C12 loaded in liposomes accumulates only on the plasma membrane of both C6 and LN229 cells. This difference suggests that perylene-Br-C12 when loaded in liposomes follows the same destiny of liposome itself in the cell cultures. Therefore, in the free form it could represent an aspecific lipid stain of cell membranes, particularly useful in multiple fluorescence experiments employing for example nucleus stains. In the liposome-entrapped form, since it follows the same destiny of liposome itself, it could be used to label specific cell subcompatments using liposomes specifically formulated for targeting defined compartments.

5. MATERIALS AND METHODS

5.1. Synthesis of perylene ligands

General. All commercial reagents and solvents were purchased from Fluka and Sigma-Aldrich and used without further purification. TLCs were run on Merck silica gel 60 F254 plates. Silica gel chromatography was performed by using Merck silica gel 60 (0.063-0.200 mm). ^{1}H and ^{13}C NMR spectra were performed with Varian NMR spectrometers running at 400 (Mercury Plus) and 500 (^{Unity}INOVA) MHz, Bruker 300 and Varian Mercury 300 instruments.
Elemental analyses (C, H, N) were carried out on a CE instrument EA1110 CHNSO (Thermo-Fischer).–API 2000 (Applied Biosystem) and the Micromass Q-TOF MICRO electrospray mass spectrometers were used to acquire the mass data of the intermediates and the monomer. ESI-MS spectra were recorded on a Micromass Q-TOF MICRO spectrometer.

1,7-Dibromoperylene-3,4:9,10-tetracarboxylic dianhydride (2). Commercial available 3,4:9,10-perylenetetracarboxylic dianhydride (**1**) (5 g) was initially dissolved in 96% sulphuric acid (100 ml) and stirred for 2 hours at room temperature. Elemental iodine (113 mg) was subsequently added and the mixture was heated. When a temperature of 80°C was reached, elemental bromine (1.65 ml) was added drop wise. The reaction mixture was stirred at 100°C for 4-6 hours. After cooling, it was added drop wise to ice and then filtered and washed with a 5% sodium metabisulfite solution to provide a red solid (6 g), which was dried and characterized (yield: 87%). In addition to the major (1,7) isomer, a small amount of the 1,6-Dibromoperylene-3,4:9,10-tetracarboxylic dianhydride (**3**) was also obtained. The two isomers could not be separated, so the mixture was used in the following steps without further purification. ^{1}H NMR (200MHz, D2SO4): δ 10.71 (d, J = 8Hz, 2H, aromatic H), 10.04 (s, 2H, aromatic H), 9.82 (d, J = 8Hz, 2H, aromatic H) ppm. The signals of the minor (1,6) isomer are mainly superimposed with those reported for (**2**). Elemental analyses: $C_{24}H_6O_6Br_2$: calcd C 52.4 %, H 1.1 %; found C 51.6 %, H 1.1 %.

General Procedures for 4-7. Starting material **2** (500 mg, 0.91 mmol), synthesized as a mixture of the two possible isomers, was dissolved in anhydrous N,N-dimethylacetamide (10 mL) and 1,4-dioxane (10 mL). The appropriate commercially available amino-alcohol (2 mmol) was added, and the reaction mixture was stirred at 120°C under argon, for 2 h (2-aminoethanol and 3-amino-1-propanol), 30 min (5-amino-1-pentanol), or 15 min (2-(2-aminoethoxy)ethanol). Upon cooling and water addition, the red solid was washed repeatedly with water, separated by filtration, and dried.

To remove the 1,6- from 1,7-dibromo-perylene derivatives, each product **4-7** was first converted into the corresponding acetylderivative, by treatment with acetic anhydride in dry pyridine. The resulting mixtures were dried under vacuum, dissolved in DCM, and washed three times with water. Each organic layer was dried and the residue dissolved in DCM/MeOH (9:1; v/v), from which the 1,7-dibromo-perylene derivatives were selectively precipitated. After three reprecipitations, the desired products were obtained as pure solids, as ascertained by ^{1}H and ^{13}C NMR. Finally, the acetyl groups were removed by treatment with a mixture of aqueous NH_3 (33%) and MeOH (1:1 v/v, 2 h, r.t.) to give the pure bisimides **4-7**.

N,N'-Bis(2-hydroxyethyl)-1,7-dibromoperylene-3,4:9,10-tetracarboxylic diimide (4): Reaction yield was 82% (70% after purification of the 1,7 regioisomer). Anal. found C 52.6%, H 2.6%, N 4.3% (calcd for $C_{28}H_{16}Br_2N_2O_6$: C 52.8%, H 2.5%, N4.4%). In order to achieve an affordable NMR characterization, acetylation of a portion of (**4**) was performed (pyridine, 20 h, rt, acetic anhydride) with a yield of 100%:

^{1}H NMR (400MHz, $CDCl_3$): δ 9.46 (d, J=8.1 Hz, 2H, aromatic H), 8.91 (s, 2H, aromatic H), 8.69 (d, J=8.1 Hz, 2H, aromatic H), 4.50 (m, 8H, N-CH2-CH2-O), 2.03 (s, 6H, acetyl) ppm. MS (ESI) m/z: 740.9466 [$(M+Na)^+$] (Calcd for $C_{32}H_{20}Br_2N_2O_8Na$: 740.9484).

N,N'-Bis(3-hydroxypropyl)-1,7-dibromoperylene-3,4,9,10-tetracarboxylic diimide (5): Reaction yield was 89% (75% after purification of 1,7 regioisomer).

^{1}H NMR (400MHz, $CDCl_3/CD_3OD$ 9:1): δ 9.42 (d, J=8.1 Hz, 2H, aromatic H), 8.83 (s, 2H, aromatic H), 8.61 (d, J=8.1 Hz, 2H, aromatic H), 4.24 (t, J=6.7 Hz, 4H, N_{imidic}-CH_2), 3.60 (t, J=6.7 Hz, 4H, C*H*$_2$-OH), 1.90 (m, 4H, CH_2-C*H*$_2$-CH_2-OH) ppm. ^{13}C NMR (8:2 $CDCl_3$:CD_3OD): δ (referred to $CDCl_3$) 163.2, 162.8, 138.3, 133.0, 132.8, 130.3, 129.1, 128.5, 127.1, 123.1, 122.0, 121.0, 59.5, 37.7, 30.8 ppm. MS (ESI) m/z: 684.9589 [$(M+Na)^+$] (Calcd for $C_{30}H_{20}{}^{79}Br_2N_2O_6Na$: 684.9586).

N,N'-Bis(5-hydroxypentyl)-1,7-dibromoperylene-3,4,9,10-tetracarboxylic diimide (6): Reaction yield was 92% (80% after purification of 1,7 regioisomer).

^{1}H NMR (400MHz, $CDCl_3$): δ 9.47 (d, J=8.1 Hz, 2H, aromatic H), 8.91 (s, 2H, aromatic H), 8.69 (d, J=8.1 Hz, 2H, aromatic H), 4.23 (t, J=7.4 Hz, 4H, N_{imidic}-CH_2), 3.69 (t, J=6.3 Hz, 4H, CH_2-OH), 1.8-1.4 signals superimposed to water; this region has been detailed by ^{1}H NMR (300MHz, $CDCl_3/CD_3OD$ 9:1): 1.8-1.2 (m, 12H, CH_2-CH_2-CH_2) ppm. ^{13}C NMR (100 MHz, $CDCl_3$): δ 163.2,

162.5, 138.4, 133.2, 131.3, 130.9, 128.8, 128.5, 123.2, 122.4, 121.9, 121.0, 63.0, 40.5, 33.2, 28.0, 23.2. MS (ESI) m/z: 741.0234 [$(M+Na)^+$] (Calcd for $C_{34}H_{28}{}^{79}Br_2N_2O_6Na$: 741.0212).

N,N'-Bis(5-hydroxy-3-oxapentyl)-1,7-dibromoperylene-3,4,9,10-tetracarboxylic diimide (7): Reaction yield was 95% (75% after purification of 1,7 regioisomer).
^{1}H NMR (400MHz, $CDCl_3$): δ 9.38 (d, J=8.1 Hz, 2H, aromatic H), 8.84 (s, 2H, aromatic H), 8.62 (d, J=8.1 Hz, 2H, aromatic H), 4.49 (t, J=5.5 Hz, 4H, N-CH_2), 3.91 (t, J=5.5 Hz, 4H, O-CH_2), 3.72 (m, 8H, O-CH_2) ppm. ^{13}C NMR ($CDCl_3$): δ 163.2, 162.8, 138.3 , 133.0, 132.9, 130.3, 129.2, 128.6, 127.1, 123.1, 122.7, 121.0, 72.6,68.5, 62.0, 40.2 ppm. MS (ESI) m/z: 744.9830 [$(M+Na)^+$] (Calcd for $C_{32}H_{24}{}^{79}Br_2N_2O_8Na$: 744.9797). Anal. found C 53.3% , H 3.2%, N 3.8% (Calcd for $C_{32}H_{24}Br_2N_2O_8$: C 53.1 %, H 3.3%, N 3.9%). UV ($CHCl_3$) λ_{max}, nm (ε x10^{-4}, $M^{-1}cm^{-1}$) : 492 (3.2), 528 (4.7); UV (DMSO) λ_{max}, nm (ε x10^{-4}, $M^{-1}cm^{-1}$) : 492 (3.2), 527 (4.6).

N,N'-Bis(5-ACETYL-3-oxapentyl)-1,7-dibromoperylene-3,4,9,10-tetracarboxylic diimide (8): The mixture of regioisomers (**7**) was dissolved in pyridine, 20 h, rt, with acetic anhydride. The reaction mixture was then purified by repetitive precipitation from dichloromethane/methanol (9:1 v/v), with a yield of 100%.
^{1}H NMR (200MHz, $CDCl_3$): δ 9. 38 (d, J=8.1 Hz, 2H, aromatic H), 8. 84 (s, 2H, aromatic H), 8.62 (d, J=8.1 Hz, 2H, aromatic H), 4.51 (t, J=5.5 Hz, 4H, N-CH_2), 4.21 (t, J=5.5 Hz, 4H, Ac-CH_2) 3.93 (t, J=5.5 Hz, 4H, O-CH_2), 3.71 (t, J=5.5 Hz, 4H, O-CH_2), 2.04 (s, 6H, acetyl) ppm

General Procedures for 9-12: Compounds **4-7** were dried on anhydrous $MgCl_2$ under vacuum (three days). To each compound (0.5 mmol, 1 equiv), 0.280 mmol of 4,40-dimethoxytrityl chloride (0.6 equiv) and 0.024 mmol of 4-dimethylaminopyridine (0.05 equiv) were added. The corresponding 5 mL of the desired mixture of solvents (Py/ACN3:1 v/v) was added and the solution stirred at room temperature under argon for 1 h. The residual of reactant was then disrupted by the addition of dry methanol. After 10 min, the solvents were removed by vacuum and the crude product dissolved in DCM/TEA (99:1, v/v) and chromatographed on a silica gel column eluted with DCM/MeOH/TEA (99:1:0.5, v/v/v).

N-2-[(2-O-4,4'-Dimethoxytrytilethoxy)ethyl]-N'-2-(2-ethoxy)-ethyl-1,7-dibromoperylene-3,4:9,10-tetracarboxylic Diimide (12): Yield = 48%. Rf = 0.4 (92:8DCM/MeOH).

^{1}H NMR (400 MHz, $CDCl_3$): δ 9.43 (d, J = 8.0 Hz, 2H), 8.89 (s, 2H), 8,67 (d, J = 8.0 Hz, 2H), 7.27 (5H overlapped by solvent signal), 7.16 (d, J = 8.8 Hz, 4H), 6.82 (d, J = 8.8 Hz, 4H), 4.48 (t, J = 5.5 Hz, 4H), 3.89 (t, J = 5.5 Hz, 4H), 3.80 (s, 6H), 3.70 and 3.68 (m, 8H) ppm. ^{13}C NMR ($CDCl_3$): δ 163.0, 162.6, 158.5, 147.0, 139.4, 138.0, 133.0, 132.8, 130.2, 130.0, 129.1, 128.5, 128.0, 127.7, 127.0, 122.8, 122.4, 120.8, 113.1, 72.2, 68.2, 61.8, 55.2, 45.7, 39.9 ppm. ESI MS m/z: 1063.1 $[M+K]^+$ (calcd for $C_{53}H_{42}{}^{79}Br_2$-$N_2O_{10}K$: 1063.1).

N-2-[(2-O-4,4'-Dimethoxytrytilethoxy)ethyl]-N'-2-{[(2-cyanoethyldiisopropylphosphino) ethoxy]ethyl}-1,7-dibromoperylene-3,4:9,10-tetracarboxylic Diimide (13): Perylene derivative **12**

(0.270 g, 0.241 mmol) was dried in vacuo overnight before being dissolved in anhydrous CH_2Cl_2 (6 mL) and 180 μL of diisopropylethylamine (1 mmol, 4 equiv). To this solution, 90 μL (0.380 mmol, 1.5 equiv) of 2-cyanoethyl diisopropylchlorophosphoramidite was added. After 30 min, the reaction mixture was quenched by the addition of dry methanol, diluted with ethyl acetate (10 mL), and washed with 10% sodium carbonate solution (10 mL) and brine (10 mL). The organic layer was dried on magnesium sulfate and concentrated in vacuo. The residue was purified on a silica gel column eluted with 80:10:10 v/v/v CH_2Cl_2/ethyl acetate/TEA. Yield = 95%.

^{1}H NMR (200 MHz, $CDCl_3$) δ 9.47 (br. d, 2H), 8.90 (br. d, 2H), 8,69 (br. d, 2H), 7.31-7.27 (broad, 5H), 7.17 (4H), 6.83 (4H), 4.47 (4H), 4.33-4.23 (m, 2H,OCH_2CH_2CN), 3.89 (m, 4H), 3.63 (s, 6H, OCH_3), 3.62-3.58 (8H), 3.40 (m, J = 6.60 Hz, 1H, $CH(CH_3)_2$), 3.12 (m, 1H, CH_2CH_2CN), 2.80 (m, 1H, CH_2CH_2CN), 1.28 (d, J = 6.60 Hz, 6H, $CH(CH_3)_2$). ^{13}C NMR ($CDCl_3$): δ 162.9, 162.5, 158.5, 145.2, 144.9, 139.4, 138.1, 138.0, 137.7, 135.5, 135.4, 131.0, 130.2, 130.1, 129.6, 129.2, 129.1, 129.0, 128.5, 127.9, 127.8, 127.7, 127.6, 127.0, 126.9, 123.0, 122.5, 120.8, 116.1, 113.1, 112.9, 72.2, 69.5, 68.2, 67.9, 65.4, 63.5, 61.8, 59.6, 55.3, 55.2. 53.0, 45.8, 39.8, 39.5, 29.6, 22.5, 22.3, 20.0, ppm. $[M+H]^+$ (calcd for $C_{62}H_{59}{}^{79}Br_2N_2O_{11}PH$: 1225.2).

8-(amino-octyl)-carbamic acid tert-butyl ester (16): To a solution of 500 mg (3.47 mmol) of compound (**14**) in 5 ml of CH_2Cl_2 and 5 ml of chloroform at 0°C was added 168 mg (0.77 mmol) of boc-anhydride in dichloromethane dropwise. The reaction was stirred at room temperature for a week. The residue was taken up with ethyl acetate, washed with brine (10 ml, 3X), dried over Na_2SO_4 and evaporated to obtain an oil. The residual oil was subjected to column cromatography using $CHCl_3$/MeOH (90/10) to obtain 153,4 mg (66.5%) of 12-(amino-dodecyl)-carbamic acid tert-butyl ester as a colourless oil.

^{1}H NMR (300 MHz, $CDCl_3$): δ 4.60 (br, s, 1H, N*H*-BOC), δ 3.05 (m, 2H, NH_{BOC} -CH_2), δ 2.64 (t, J=7 Hz, 2H, $NH_{2AMMINIC}$-CH_2), δ 1.46-1.41 (br, 13 H, CH_2- β $NH_{2AMMINIC}$, CH_2- β NH_{BOC} , (CH_3) $_3$-

C), δ 1.26 (br, 8H, -C*H*$_2$- alkyl chain); ^{13}C NMR ($CDCl_3$): δ 142.5, δ 42.5, 48.9, 34.0, 30.3, 29.8, 29.7, 29.5, 28.6, 27.1. ESI MS m/z 245 $[M+H]^+$ and m/z: 267 $[(M+Na)^+]$ (calcd for $C_{13}H_{28}N_2O_2$: 244).

12-(amino-dodecyl)-carbamic acid tert-butyl ester (17): To a solution of 505 mg (2.52 mmol) of 1,12-diaminododecane in 5 ml of CH_2Cl_2 and 5 ml of chloroform at 0°C was added 168 mg (0.77 mmol) of boc-anhydride in dichloromethane dropwise. The reaction was stirred at room temperature for a week. The residue was taken up with ethyl acetate, washed with brine (10 ml, 3X), dried over Na_2SO_4 and evaporated to obtain an oil. The residual oil was subjected to column cromatography using $CHCl_3$/MeOH (90/10) to obtain 153,4 mg (66.3%) of 12-(amino-dodecyl)-carbamic acid tert-butyl ester as a colourless oil.

^{1}H NMR (300 MHz, $CDCl_3$): δ 4.53 (br, s, 1H, N*H*-BOC), δ 3.08 (m, 2H, NH_{BOC} -C*H*$_2$), δ 2.67 (t, J=7 Hz, 2H, $NH_{2AMMINIC}$-C*H*$_2$), δ 1.43 (br, 13 H, C*H*$_2$- β $NH_{2AMMINIC}$, C*H*$_2$- β NH_{BOC} , (C*H*$_3$) $_3$-C), δ 1.31-1.18 (br, 16 H, -C*H*$_2$- alkyl chain); ^{13}C NMR ($CDCl_3$): δ 142.5, δ 42.5, 48.9, 34.0, 30.3, 29.8, 29.7, 29.5, 28.6, 27.1.

N,N'-Bis[(amino- octyl)-8-carbamic acid tert-butyl ester]-1,7-dibromoperylene-3,4:9,10-tetracarboxylic diimide (18): To 212.5 mg of compound (**2**) (0.39 mmol) and 207.6 mg of compound (**16**) (0.85 mmol) was added anhydrous dioxane (4 ml) and anhydrous DMA (4 ml). The reaction mixture was then refluxed, stirring under argon for 6 h. Successively, ice and brine were added and the solution was stored at 4°C for a night. Then the solution was filtered on Hirsh imbute, washing with water. After drying in oven the precipitate, 340.6 mg of compound (**18**) was obtained (87% yield).

^{1}H NMR (300 MHz, $CDCl_3$): δ 9,47 (d, J = 8 Hz, 2H, ar. H), δ 8.90 (s, 2H, ar. H), δ 8.69 (d, J = 8 Hz, 2H, ar. H), δ 4.20 (t, J = 7 Hz, 4H, , N_{imidic}-C*H*$_2$), δ 3.10 (t, J = 7 Hz, 4H, NH_{BOC} -C*H*$_2$), δ 1.74 (br, 4H, NH_{BOC} -CH_2-C*H*$_2$), δ 1.50-1.38 (broad, 18H, (C*H*$_3$)$_3$-C), δ 1.60-1.37 (m, 20H, alifatyc C). MS (ESI) m/z: 1025 $[(M+Na)^+]$ (calcd for $C_{50}H_{58}Br_2O_8N_4$ M =1002).

N,N'-Bis[(amino-dodecyl)-12-carbamic acid tert-butyl ester]-1,7-dibromoperylene-3,4:9,10-tetracarboxylic diimide (19): To 257.6 mg of compound 1 (0.47 mmol) and 309 mg of compound 3 (1.03 mmol) was added anhydrous dioxane (2.5 ml) and anhydrous DMA (2.5 ml). The reaction mixture was then refluxed, stirring under argon for 6 h. Successively, ice and brine were added and

the solution was stored at 4°C for a night. Then the solution was filtered on Hirsh imbute, washing with water. After drying in oven the precipitate, 449.4 mg of compound 4 was obtained (85% yield).

^{1}H NMR (300 MHz, CF_3COOD): δ 9.81 (d, J = 8 Hz, 2H, ar. H), δ 9.16 (s, 2H, ar. H), δ 8.94 (d, J = 8 Hz, 2H, ar. H), δ 4.44 (t, J = 8 Hz, 4H, , N_{imidic}-CH_2), δ 3.35 (t, J = 8 Hz, 4H, NH_{BOC} -CH_2), δ 1.93 (br, 4H, NH_{BOC} -CH_2-CH_2), δ 1.72 (broad, 18H, (CH_3)$_3$-C), δ 1.60-1.37 (m, 40H, alifatyc C); ^{13}C NMR (CF_3COOD): δ 165.7, δ 165.7, δ 139.6, δ 134.5, δ 134.3, δ 131.5, δ 129.3, δ 129.1, δ 127.0, δ 122.3, δ 121.8 , δ 121.5, δ 100.3, δ 42.1, δ 41.7, δ 29.3, δ 29.2, δ 29.0, δ 28.6, δ 27.7, δ 27.1, δ 26.8, δ 25.8. MS (ESI) m/z: 1137 [(M+Na)+] (calcd for $C_{58}H_{74}Br_2O_8N_4$ M =1114).

N,N'-Bis(8-aminooctane) 1,7-dibromoperylene-3,4:9,10-tetracarboxylic diimide (20)

334.6 mg of compound (**19**) was dissolved in dichloromethane (12 ml) and TFA (0.5 ml) was added dropwise. The reaction mixture was stirring for 12 hours, at 0°C. Then, the reaction mixture was poured into ice and neutralized carefully with NH_3 (solution at 10%) until pH 8. The residue was extracted with dichloromethane or chloroform, washed with brine (5 ml, 3X), dried over Na_2SO_4 and evaporated to obtain 208.8 mg of the desired product (**19**) (78.9 % yield).

^{1}H NMR (300 MHz, CF_3COOD): δ 9.84 (d, J = 8 Hz, 2H, ar. H), δ 9.18 (s, 2H, ar. H), δ 8.95 (d, J = 8 Hz, 2H, ar. H), δ 4.45 (t, broad 4H, N_{imidic}-CH_2), δ 3.37 (br, 4H, $NH_{2amminic}$ -CH_2), δ 1.95 (broad, 8H, $NH_{2AMMINIC}$ -CH-CH_2 and N_{imidic}-CH-CH_2), δ 1.60-1.30 (br, 16H, alifatyc C). MS (ESI) m/z: 803 [(M+H)$^+$] and m/z: 825 [(M+Na)$^+$] (calcd for $C_{40}H_{42}O_4Br_2N_4$ M =802).

N,N'-Bis(12-aminododecane) 1,7-dibromoperylene-3,4:9,10-tetracarboxylic diimide (21)

372.1 mg of compound 4 was dissolved in dichloromethane (12 ml) TFA (0.5 ml) was added dropwise. The reaction mixture was stirring for 12 hours, at 0°C. Then, the reaction mixture was poured into ice and neutralized carefully with NH3 (solution at 10%) until pH 8. The residue was extracted with dichloromethane or chloroform, washed with brine (5 ml, 3X), dried over Na2SO4 and evaporated to obtain 171.8 mg of the desired product 5 (57.0 % yield).

^{1}H NMR (300 MHz, CF_3COOD): δ 9.84 (d, J = 8 Hz, 2H, ar. H), δ 9.18 (s, 2H, ar. H), δ 8.96 (d, J = 8 Hz, 2H, ar. H), δ 4.47 (t, broad 4H, N_{imidic}-CH_2), δ 3.37 (br, 4H, $NH_{2amminic}$ -CH_2), δ 1.95 (broad, 8H, $NH_{2AMMINIC}$ -CH-CH_2 and N_{imidic}-CH-CH_2), δ 1.60-1.30 (br, 32H, alifatyc C); ^{13}C NMR (CF_3COOD): δ 165.3, δ 139.6, δ 137.4, δ 134.6, δ 134.4, δ 131.6, δ 129.3, δ 129.1, δ 127.1, δ 122.4, δ 121.9, δ 47.9, δ 29.3, δ 29.2, δ 29.1, δ 28.7, δ 27.7, δ 27.2, δ 26.8, δ 25.9. MS (ESI) m/z: 915 [(M+H)$^+$] and m/z: 937 [(M+Na)$^+$] (calcd for $C_{48}H_{58}O_4Br_2N_4$ M =914).

N,N'-Bis(8- t*rimethylammonium-octane) 1,7-dibromoperylene-3,4:9,10-tetracarboxylic diimide iodide (22): To 203.3 mg of compound **(20)** (0.25 mmol) 6 mL of anhydrous 1,4-dioxane was added. The reaction mixture was stirred at 120°C to favourite the complete dissolution of compound (**20**). Then the reaction mixture was cooled down, CH_3I (1.5 mL) was added and the reaction was heated to 65 ºC for 30 minutes. The solid was separated by filtration to obtain 241.8 mg of the desired compound (yield 84.7%). MS (ESI) m/z: 444 $[(M)^{2+}]$ (calcd for $C_{46}H_{56}O_4Br_2N_4$ M =1000).

N,N'-Bis(12- trimethylammonium-dodecane) 1,7-dibromoperylene-3,4:9,10-tetracarboxylic diimide iodide (23): To 84.7 mg of compound **(21)** (0.09 mmol) 3 mL of anhydrous 1,4-dioxane was added. The reaction mixture was stirred at 120°C to favourite the complete dissolution of compound (**21**). Then the reaction mixture was cooled down, CH_3I (1 mL) was added and the reaction was heated to 65 ºC for 30 minutes. The solid was separated by filtration to obtain 113.9 mg of the desired compound (yield 98%).

^{1}H NMR (300 MHz, DMSO-d6): δ 9.35 (d, J = 8 Hz, 2H, ar. H), δ 8.60 (s, 2H, ar. H), δ 8.56 (d, J = 8 Hz, 2H, ar. H), δ 4.03 (t, J= 7Hz, 4H, , N_{imidic}-C*H*$_2$), δ 3.27 (br, 4H, $NH_{2amminic}$ -C*H*$_2$), δ 3.03 (s, 18H, $NH_{2amminic}$ -C*H*$_3$), δ 1.66 (br, 8H, $NH_{2amminic}$ -CH-C*H*$_2$ and N_{imidic}-CH-C*H*$_2$), δ 1.40-1.20 (br, 32H, alifatyc C); ^{13}C NMR (DMSO-d6): δ 163.0, δ 162.4, δ 137.3, δ 132.7, δ 132.4, δ 130.3, δ 129.2, δ 129.0, δ 127.0, δ 123.6, δ 123.3, δ 120.9, δ 66.1, 52.9, 39.5, 22.7-22.6 MS (ESI) m/z: 500 $[(M)^{2+}]$ (calcd for $C_{54}H_{72}O_4Br_2N_4$ M =1000).

5.2. Conjugated perylene-DNA solid phase synthesis

Materials

Reagents and phosphoramidites for DNA synthesis were purchased from Glenn Research. ON syntheses were performed on a PerSeptive Biosystem Expedite DNA synthesizer. HPLC analyses and purifications were carried out using a JASCO PU-2089 Plus HPLC pump equipped with a JASCO BS-997-01 UV detector. A Purospher-STAR RP-18 end-capped (5-μm) HPLC column was used to purify the sequences. Both conjugated and unmodified ONs were dialyzed using Slide-ALyzer Dialysis Cassettes, with a 3500 molecular weight cutoff, manufactured by Thermo-

Scientific. MALDI-TOF experiments were performed on a Bruker Autoflex I mass spectrometer using a picolinic/3-hydroxypicolinic acid mixture as the matrix.

Synthesis of oligomers

The ON sequences were synthesized with automated DNA synthesizer using a controlled pore glass support (100 mg, IcaaCPG high loading, loaded with G nucleotide) following the standard β-cyanoethyl phosphoramidite method (DMT-on protocol). After the elongation of the sequence, the solid support was charged in a small column supplied with a stopcock and a glass filter on the bottom, washed with dry ACN, fluxed by argon (5 min), and finally treated with three cycles of deblock solution (a solution of dichloroacetic acid in ACN; 5 mL of each cycle) to detach the 4,40-dimethoxytrityl groups. All of the acidic washing solutions were collected, and the quantitative spectrophotometric 4,40-dimetoxytrityl cation test (Sinha et al., 1984) was used to evaluate the yields of each conjugation step. The solid support was washed three times with anhydrous ACN, fluxed by argon (5 min), and then reacted for 20 min with a solution of 5d in dry DCM, in the presence of the activator solution (5-ethylthio-1H-tetrazole in ACN). After five washing cycles with a 1:1 mixture of dry ACN/DCM, the solid support was dried by argon (5 min) and submitted to the second coupling cycle. The support was washed from the residual excess of reactants by using four swelling cycles in dry solvents under argon flow (2 mL each, for 2 min). The subsequent capping and oxidation cycles were performed manually by using the same conditions of a standard automated synthesis. Finally, the solid support was treated with the deblock solution (five cycles, 5 mL each) to detach the 4,40-dimethoxytrityl groups. The solid support was then washed with ACN, dried under argon, charged in a vial supplied with a cap, and treated with aqueous ammonia (33%) at room temperature for 24 h to detach the ON. The combined filtrates and washings were concentrated under reduced pressure, dissolved in a basic aqueous solution (2% NH_3), and purified by HPLC by using a C18 reverse phase column [H_2O/ACN 98:2 v/v for 10 min and then by a gradient of CAN inH_2O (from 2 to 20% in 30 min)]. The peaks were identified by setting the UV detector at 260 and 540 nm in two different courses (the conjugated sequence produced a peak at 540 nm). To remove undesired ions, the ON aqueous solutions were subjected to three dialysis treatments (3500 MW cutoff). The concentration of samples used in CD, UV and fluorescence experiments were determined by measuring the UV absorbance (at 260 nm, 80°C) of the aqueous ON solutions, using the extinction coefficient calculated according to the method of Gray et al. The absorbance contribution of the dibromo-perylene moiety was calculated by using the molar extinction coefficient measured in $CHCl_3$ (29,500 for the band at 265 nm).

5.3. Occlusion of perylene derivates in liposome

Materials

Dimyristoyl-sn-glycero-phosphocoline (DMPC) was purchased from Avanti Polar Lipids (Alabaster, AL), exclusion gel Sephadex G-50 and Phospate Buffer PBS tablets from Sigma-Aldrich; RPE- and HPLC-grade solvents (chloroform, ethanol, bidistilled water) were purchased from Carlo Erba Reagenti (Milano, Italy).

Liposome preparation

The aqueous dispersion of DMPC/PC12 liposomes was prepared according to the procedure described by Hope et al. Briefly, a film of lipid was prepared on the inside wall of a round-bottom flask by evaporation of $CHCl_3$ solution containing the proper amount of DMPC and PC12 to obtain the desired percentage mixture (DMPC/PC12 500/1). To the obtained film stored in a desiccator overnight under reduced pressure were added 10 mL of PBS buffer solution (Aldrich, 10-2 M pH 7.4) in order to obtain a final concentration of 2,5x10-2 M in DMPC and 5x10-5 M in PC12. The dispersion was vortex-mixed and then freeze-thawed six times from liquid nitrogen to 313 K. Dispersion was then extruded (10 times) through a 100 nm polycarbonate membrane (Whatman Nucleopore). The extrusion procedure was carried out at 307 K, well above the transition temperature of DMPC (297.2 K), using a 10 mL extruder (Lipex Biomembranes, Vancouver, Canada).

Determination of Entrapped PC12 Percentage

The unentrapped PC12 in extruded DMPC liposomes was separated from the liposomes on a Sephadex G-50® gel column, equilibrated in PBS buffer solution. PC12 concentration in liposome preparations before and after extrusion and before and after Sephadex filtration was determined by measuring the absorbance maximum (at 521 nm) of 3 mL of PC12/liposomes before and after extrusion, (and also before and after filtration) disrupted by complete evaporation of water and dissolution of the residue in absolute ethanol. The percentage of entrapped drug was calculated using the equation (Hwang et al., 1999):

$$\%PC12 = 100 \text{ X } (M^{a}_{PC12}\, M^{b}_{lip})/(M^{b}_{PC12}\, M^{a}_{lip})$$

where **M**a PC12 and **M**b PC12 are the perylene derivative concentration in liposome dispersion, respectively, before and after extrusion and before and after gel filtration and **M**a lip and **M**b lip are the total lipid concentration before and after extrusion and before and after gel filtration, respectively.

5.4. CD, UV and fluorescence: spectroscopic studies

5.4.1. CD and UV experiments of conjugated perylene-GROs

Materials

The UV thermal experiments were carried out using a JASCO 530 spectrophotometer equipped with ETC-505 T temperature controller. CD experiments were performed on a JASCO 715 spectropolarimeter equipped with a PTC-348 temperature controller.

UV and CD experiments

UV and CD experiments were carried out on DNA samples at concentrations of 2, 4, and/or 10 μM. The buffers used contained 100 mM NaCl and 10 mM NaH_2PO_4 at pH 7.4, or 100mMKCl and 10mM KH_2PO_4 at pH 7.4. The samples were annealed by heating at 90°C for 5 min and then slow cooling at room temperature (12 h). The UV and CD spectra were registered at increasing temperatures, from 10 to 90°C with heating steps of 10°C, from 200 to 700 nm. Before each spectrum, the sample was equilibrated for 20 or 30 min, respectively, at the specific temperature. The samples used for the CD measurements of ONs in desalted water (HPLC-grade water, Merck) were not submitted to the annealing procedure. Each reported spectrum is the background-subtracted average of three scans. The spectra were collected with the following conditions: response, 16 s; bandwidth, 1 nm; speed, 100 nm/min. CD melting curves were obtained by following the changes in the amplitude of CD bands at 263 nm as a function of temperature. ON solutions were heated from 10 to 90°C, at the rate of 0.5°C/min.

5.4.2. Fluorescence of perylene diimide in biological-inspired systems: G-quadruplexes and liposome

G-quadruplexes

Fluorescence emission spectra were recorded using a Varian Cary Eclipse Fluorescence spectrophotometer. Fluorescence emission spectra were performed at 298 K, if not otherwise

indicated. The fluorescence emission of compound **7** in chloroform was recorded setting the excitation and emission slits width to 5 nm and the emission PMT (PhotoMultiplier Tubes) detector voltage to 600 V. Fluorescence spectra of the perylene-conjugated oligonucleotide HTRp2 at different temperatures, were recorded setting the excitation and emission slits widths to 20 and 10 nm, respectively, and the emission PMT detector voltage to 700 V; the emission range was set from 530 to 750 nm.

Liposome

Steady-state fluorescence experiments were carried out on a HORIBA Jobin-Yvon Fluoromax 4 spectrofluorimeter. Spectrofotometric experiments were carried out on a Varian Cary 300 Bio using a cell of 1 cm path length*;* the excitation λ was set at 505 nm

Cell Culture

Human (LN229) and murine glioblastoma (C6) lines (kindly provided by Dr. S. Ciafre`, University of Rome "Tor Vergata", Italy) were grown as monolayer in DMEM medium supplemented supplemented with 1% non essential amino acids, 1% L-glutamine, 100 IU/ml penicillin, 100 IU/ml streptomycin, and 10% fetal bovine serum at 37°C in a 5% CO_2 humidified atmosphere in air.

Laser Scanning Confocal Microscopy

Glioblastoma cells were analyzed by laser scanning confocal microscopy (LSCM) in order to investigate the intracellular distribution of the perylene-Br-C12 administered to cells in DMSO or delivered by liposome formulation. Cells, grown on 12 mm glass coverslips, were inoculated with perylene-Br-C12 in DMSO or in liposome formulations. After 5 and 27 h of incubation at 37°C, cells were fixed in 3.7% paraformaldehyde in PBS, for 10 min at room temperature. Observations were performed by using a Leica TCS SP2 laser scanning confocal microscopy (Leica Microsystems, Mannheim, Germany).

6. REFERENCES

- Aboul-ela F, Murchie AI, Norman DG, Lilley DM, J. Mol. Biol. 1994; 243; 458-471.
- Aboul-ela F, Murchie AI, Lilley DM, Nature 1992; 360; 280-282.
- Alvino, A., Franceschin, M., Cefaro, C., Borioni, S., Ortaggi, G., and Bianco, A. Tetrahedron 2007; 63, 7858–7865.
- Ambrus A, Chen D, Dai J, Jones RA, Yang D, Biochemistry 2005; 44; 2048-2058.
- Ashcroft, R.G., Thulborn, K.R., Smith, J.R., Coster, H.G., Sawyer, W.H., Biochim. Biophys. Acta 1980, 602, 299–308.
- Balagurumoorthy, P., and Brahmachari, S. K., J. Biol. Chem. 1994, 34, 21858–21869.
- Bastiaens P. I. HSquire., A., Trends Cell Biol. 1999, 9, 48– 52.
- P. Bates, J. L. Mergny, D. Yang, EMBO Rep. 2007, 8, 1003– 1010.
- Baumastark, D., and Wagenknecht, H. A., Angew. Chem., Int. Ed. 2008, 47, 2612–2614.
- Bejugam M, Sewitz S, Shirude PS, Rodriguez R, Shahid R, Balasubramanian S, J. Am. Chem. Soc. 2007; 129; 12926-12927.
- Bell GI, Selby MJ, Rutter WJ, Nature 1982; 295, 31-35.
- Benvegnu, T.; Brard, M.; Plusquellec, D. Curr. Opin. Colloid Interface Sci. 2004, 8, 469–479.
- Bernik D. L, Zubiri D., Tymczyszyn E., Disalvo E. A., Langmuir, 2001, 17, 6438–6442
- Bevers S, Schutte S, McLaughlin LW, J. Am. Chem. Soc. 2000; 122; 25
- Blackburn EH Structure and function of telomeres. Nature 1991; 350; 569-573.
- Blokzijl, W.. Engberts, J. B. F. N Angew. Chem. 1993, 105, 1610 – 1650; Angew. Chem. Int. Ed. Engl. 1993, 32, 1545 – 1579.
- Bock LC, Griffin LC, Latham JA, Vermaas EH, Toole JJ Nature 1992; 355; 564 566
- Bourdoncle A., Estévez Torres A., Gosse C., Lacroix L., Vekhoff P., Le Saux T., Jullien L., Mergny J. L., J. Am. Chem. Soc. 2006, 128, 11094–11105.
- Brewer, G.J., Matinyan, N., Biochemistry 1992, 31, 1816–1820.
- Catasti P, Chen X, Moyzis RK, Bradbury EM, Gupta G, J. Mol. Biol. 1996; 264; 534-545.
- Chattopadhyay, A., Chem. Phys. Lipids 1990, 53, 1–15.
- Chen, Z., Lohr, A., Saha-Möller, C. R., Würthner, F., Chem. Soc. Rev. 2009, 38, 564–584.
- Chernomordik, L.V., Zimmerberg, J., Curr. Opin. Struct. Biol. 1995, 5, 541–547.

- Cheung I, Schertzer M, Rose A, Lansdorp PM, Nat. Genet. 2002; 31; 405-409.
- Chou S.H., Chin K. H.,. Wang A. H, Trends Biochem. Sci. 2005, 30, 231–234.
- Cogoi S, Xodo LE, Nucleic Acids Res. 2006; 34; 2536-2549.
- Coppola T, Varra M, Oliviero G, Galeone A, D'Isa G, Mayol L, Morelli E, Bucci MR, Vellecco V, Cirino G, Borbone N Bioorg. Med. Chem. 2008; 16; 8244–8253.
- Crabbe L, Verdun RE, Haggblom CI, Karlseder J, Science 2004; 3061; 1951-1953.
- D'Onofrio J, Petraccone L, Erra E, Martino L, Di Fabio G, De Napoli L, Giancola C, Montesarchio D, Bioconjugate Chem. 2007; 18; 1194-1204.
- Dai J, Dexheimer TS, Chen D, Carver M, Ambrus A, Jones RA, Yang D, J. Am. Chem. Soc. 2006; 128; 1096-1098.
- Dapic´ V, Abdomerovic´ V, Marrington R, Peberdy J, Rodger A, Trent JO, Bates PJ Nucleic Acids Res. 2003; 31; 2097–2107.
- Davis J. T., Angew. Chem. Int. Ed. 2004, 43, 668–698.
- Davis J. T., Spada G. P., Chem. Soc. Rev. 2007, 36, 296–313.
- de Armond R, Wood S, Sun D, Hurley LH, Ebbinghaus SW, Biochemistry 2005; 44; 16341-16350.
- De Cian A., Guittat L., Kaiser M., Sacca B., Amrane S., Bourdoncle A., Alberti P., Teulade-Fichou M. P., Lacroix L., Mergny J. L., Methods 2007, 42, 183–195.
- Deliggeorgiev, T., Zeneva D., Pektov, I. Timcheva Il. Subnis, R. Dyes Pigments, 1994, 24-75.
- Derzko, Z., Jacobson K., Biochemistry, 19 1980: 6050–6057.
- Ding H, Schertzer M, Wu X, Gertsenstein M, Selig S, Kammori M, Pourvali R, Poon S, Vulto I, Chavez E, Tam PP, Nagy A, Lansdorp PM, Cell 2004; 117; 873-886.
- Du X, Shen J, Kugan N, Furth EE, Lombard DB, Cheung C, Pak S, Luo G, Pignolo RJ, DePinho RA, Guarente L, Johnson FB, Mol. Cell. Biol. 2004; 24; 8437-8446.
- Eytan, G. D, Biochim. Biophys. Acta, **1982** 694: 185–202.
- Engelmann, B., Schaipp, B., Dobner, P., Stoeckelhuber, M., Kogl, C., Spiess, W., Hermetter, A.,. J. Biol. Chem. 1998, 273, 27800–27808.
- Ford W. E., Photochem J.. 1986, 34, 43 – 54
- Ford W. E., Photochem J.. 1987, 37, 189 – 204;
- Franceschin, M., Alvino, A., Ortaggi, G., and Bianco, A. Tetrahedron Lett. 2004; 45, 9015–9020.
- Franceschin M., Eur. J. Org. Chem. 2009, 2225–2238

- Franceschin, M., Lombardo, C., Pascucci, E., D'Ambrosio, D., Micheli, E., Bianco, A., Ortaggi G., Savino M., Bioorg. & Med Chem 2008, 162292–2304
- Fuhrhop, J.-H.; Wang, T. Chem. Rev. 2004, 104, 2901–2938.
- Galla, H.-J., Hartmann, W., Chem. Phys. Lipids 1980, 27, 199–219.
- Garcìa F., Sànchez L., Chem. Eur. J. 2010, 16, 3138 – 3146;
- Gliozzi, A.; Relini, A.; Chong, P. L. -G. J. Membr. Sci. 2002, 206, 131–147.
- Gomez D, O'Donohue MF, Wenner T, Douarre C, Macadre J, Cancer Res. 2006; 66; 6908–6912.
- Gonzàlez-Rodrìguez D., Schenning, A. P. H. J.Chem. Mater. 2011, 23, 310 – 325;
- Gray, D. M., Hung, S. H., and Johnson, K. M. Methods Enzymol. 1995, 246, 19–34.
- Grinberg, S.; Kolot, V.; Linder, C.; Shaubi, E.; Kas'yanov, V.; Deckelbaum, R. J.; Heldman, E. Chem. Phys. Lipids 2008, 153, 85–97.
- Gvishi R., Reisfeld R., Burshtein Z., Chem. Phys. Lett. **1993**, *213*, 338-344
- Han, H., Cliff, C. L., Hurley, L. H. Biochemistry 1999**,** 38, 6981–6986.
- Hariharan, M., Zheng, Y., Long, H., Zeidan, T. A., Vura-Weiss, J., Wasielewski, M. R., Schatz, G. C. and Lewis, F. D. J. Am. Chem. Soc. 2009, 131, 5920-5929
- Haugland R. P., Handbook of Fluorescent Probes and Research Chemicals, Molecular probes Inc., Eugene, 1989.
- Held D. M.,. Kissel J. D, Patterson J. T., Nickens D. G., Burke D. H., Front. Biosci. 2006, 11, 89–112.
- Hinderliter, A.K., Almeida, P.F., Biltonen, R.L., Creutz, C.E., Biochim. Biophys. Acta 1998, 1448, 227–235.
- Hoeben F. J. M,. Shklyarevskiy I. O, Pouderoijen M. J., Engelkamp H,. Schenning, A. P. H. J Christianen P. C. M., Maan J. C., Meijer E.W., Angew. Chem. 2006, 118, 1254 – 1258;
- Hoekstra, D., de Boer, T., Klappe, K., Wilschut, J., Biochemistry 1984, 23, 5675–5681.
- Hoekstra, D. (Ed.), 1994. Current Topics in Membranes; Cell Lipids, vol. 40. Academic Press, San Diego.
- Hongmei L., Yongli W., Chenghui L., Hongxia L., Baoxiang G., Zhang L., Fuli B., Qianqian B., Xinwu B J. Mater. Chem., 2012, 22, 6176
- Hope, M. J.; Nayar, R.; Mayer, L. D.; Cullis, P. R. In Liposome Technology, 2nd ed.; Gregoriadis, G.; Ed.; CRC Press: Boca Raton, FL, 1992; Vol. I, pp 123**-**139.
- Hope-Ross M., Yannuzzi L. A., Gragoudas E. S., Guyer D. R., Slakter J. S., Sorenson A., Ophthalmology 1994, 101, 529 –533.

- Hotoda H, Koizumi M, Koga R, Kaneko M, Momota K, Ohmine T, Furukawa H, Agatsuma T, Nishigaki T, Sone J, Tsutsumi S, Kosaka T, Abe K, Kimura S, and Shimada K, J. Med. Chem. 1998; 41; 3655-3663.
  Huber MD, Lee DC, Maizels N, Nucleic Acids Res. 2002; 30; 3954-3961.
- Hughes R. E.,. Hart S. P, Smith D. A., Movaghar B.,. Bushby R. J, Boden N., J. Phys. Chem. B 2002, 106, 6638 – 6645
- Hunter, C. A., Sanders J. K. M., J. Am. Chem. Soc. 1990, 112,5525 – 5534.
- Huppert JL, Balasubramanian S, Nucleic Acids Res. 2007; 35; 406-413.
- Huppert JL Hunting G-quadruplexes Biochimie 2008; 90; 1140-1148.
- Huster, D., Müller, P., Arnold, K., Herrmann, A., Biophys. J. 2001, 80, 822–831.
- Hwang; S H.; Maitani, Y.; Qi, X R.; Takayama, K.; Nagai, T Int. J. Pharm. 1999, 179, 85-95.
- Imahori, H., Umeyama, T., Ito, S. Acc. Chem. Res. 2009, 42, 1809–1818.
- J. N. Israelachvili in Intermolecular & Surface Forces, 2nd ed.,Academic Press, San Diego, 1991, pp. 122 – 394.
- Ji, Feng-Yuan, Zhu, L., Ma, X., Wang, Q., Tian, H., Tetrahedron Letters, 50 2009: 597–600.
- Jing N. Opin Investig Drugs. 2000a; 9; 1777-85.
- Jing N., De Clercq E., Rando R. F., Pallansch L., Lackman- Smith C., Lee S., Hogan M. E., J. Biol. Chem. 2000b, 275, 3421– 3430.
- Johnson JE, Smith JS, Kozak ML, Johnson FB, Biochimie 2008; 90; 1250-1263.
- Kang C, Zhang X, Ratliff R, Moyzis R, Nature 1992; 356; 126-131.
- Karimata H., Miyoshi D., Fujimoto T., Koumoto K., Wang Z. M., Sugimoto N., Nucleic Acids Symp. Ser. 2007, 51, 251–252.
- Kaucher M. S., Harrell Jr. W. A., Davis J. T., J. Am. Chem. Soc. 2006, 128, 38–39.
- Klausner, R.D., Wolf D.E., Biochemistry, 19 1980: 6199–6203.
- Kohl, C., T. Weil, J. Qu, e K. Mullen., 2004 Chem Eur J 10:5297–5310
- Kok, J.W., Babia, T., Filipeanu, C.M., Nelemans, A., Egea, G., Hoekstra, D., J. Cell Biol. 1998, 142, 25–38.
- Kok, J.W., Hoekstra, D., Mason, W.T. (Ed.), second ed. Academic Press, San Diego, 1999, pp. 136–155.
- Kraft A, Grimsdale AC, Holmes AB, Angew. Chem. Int. Edit. 1998; 37; 403.
- Kunitake, T.; Okahata, Y.; Shimomura, M.; Yasunami, S.; Takarabe, K. J. Am. Chem. Soc. 1981, 103, 5401–5413.

- Langhals H, Chem. Ber, 1985, 118, 4641
- Langhals H, Heterocycles, 1995-40, 477
- Langhals H, Ismael R, Yürük O 2000, Tetrahedron 56:5435–5441;
- Langhals H., Helv. Chim. Acta 2005, 88, 1309.
- Langner, M., Hui, S.W., Chem. Phys. Lipids 1993, 65, 23–30.
- Ledesma, M.D., Bru¨ gger, B., Bu¨nning, C., Wieland, F.T., Dotti, C.G., EMBO J. 1999, 18, 1761–1771.
- Lei G. et MacDonald R. C., Biophys. J., 2003, 85, 1585–1599.
- Liu H., Wang Y., Liu C., Li H., Gao B., Zhang L., Bo F., Baia Q., Ba X., J. Mater. Chem., 2012, 22, 6176
- MacDonald, R.I., J. Biol. Chem. 1990, 265, 13533–13539
- Macaya RF, Schultze P, Smith FW, Roe JA, Feigon J Proc. Natl. Acad. Sci. USA 1993; 90; 3745-3749.
- Maget-Dana, R. Biochim. Biophys. Acta, 1999**,** 1462 : 109–140.
- Mahin S., Hadel W a, Saws R., Husain S., Krogh-Jespemn K., Westbrook J. D.,, Bird G. R. J.Phys.Chem. 1992, 96, 7988-7996
- Marcu KB, Bossone SA, Patel AJ, Annu. Rev. Biochem. 1992; 61; 809-860.
- Marsh T. C., Vesenka J., Henderson E., Nucleic Acids Res. 1995, 23, 696–700.
- Masuda, M.; Shimizu, T. Chem. Commun. 2001, 2442–2443.
- Meister, A.; Blume, A. Curr. Opin. Colloid Interface Sci. 2007, 12, 138–147.
- Mergny, J. L., Phan, A. T., and Lacroix, L., FEBS Lett. 1998, 435, 74–78.
- Mergny J. L., Maurizot J. C., Chembiochem 2001, 2, 124–132;
- Mergny, J. L., Li, J., Lacroix, L., Amrane, S., and Chaires, J. B., Nucleic Acids Res. 2005, 33, e138/1–6
- Miyawaki, K.; Harada, A.; Takagi, T.; Shibakami, M. Synlett 2003, 349–353.
- Miyoshi D., Inoue M., Sugimoto N., Angew. Chem. Int. Ed. 2006, 45, 7716–7719.
- Miyoshi D., Karimata H., Wang Z. M., Koumoto K., Sugimoto N., J. Am. Chem. Soc. 2007, 129, 5919–5925.
- Moerner W. E., Orrit M., Science 1999, 283, 1670.
- Murat P., Cressend D., Spinelli N., Van der Heyden A., Labbé P., Dumy P., Defrancq E., ChemBioChem 2008, 9, 2588–91;
- Murchie AI, Lilley DM, Nucleic Acids Res. 1992; 20, 49-53.

- Nagatoishi, S. Nojima, T. Galezowska, E. Gluszynska, A. Juskowiak, B. Takenaka, S. Anal. Chim. Acta 2007, 581, 125– 131.
- Neidle S, Parkinson GN., Nature Review Drug Discovery 2002; 1: 383-93
- Niles, W.D., Silvius, J.R., Cohen, F.S., J. General Physiol. 1996, 107, 329–351.
- Ohki, S., Arnold, K., J. Membrane Biol. 1990, 114, 195–203.
- Ohki, S., Flanagan, T.D., Hoekstra, D., 1998, Biochemistry 37, 7496–7503.
- Oliviero G., Borbone N., Galeone A., Varra M., Piccialli G., Mayol L., Tetrahedron Lett. 2004, 45, 4869–4872;
- Oliviero G., Amato J., Borbone N., Galeone A., Petraccone L., Varra M., Piccialli G., Mayol L., Bioconjug. Chem. 2006, 17, 889–98;
- Paeschke K, Simonsson T, Postberg J, Rhodes D, Lipps HJ , Nat. Struct. Mol. Biol. 2005; 12; 847-854.
- Pagano, R.E., Sepanski, M.A., Martin, O.A., J. Cell Biol. 1989, 109, 2067–2079.
- Pagano B, Martino L, Randazzo A, Giancola C, J. 2008; 94; 562–569.
- Parasassi T., Di Stefano M., Loiero M., Ravagnan G., Gratton E., Biophys. J., 1994, 66, 120–132.
- Parasassi T., De Stasio G., Ravagnan G., Rusch R. M., Gratton E., Biophys. J., 1991, 60, 179–189
- Parkinson, G. N., Lee, M. P. H., Neidle, S., Nature 2002 417, 876–880.
- Pecheur, E.I., Sainte-Marie, J., Bienvenue, A., Hoekstra, D., J. Membrane Biol. 1999, 167, 1–17.
- Phillips K, Dauter Z, Murchie AI, Lilley DM, Luisi B, J. Mol. Biol. 1997; 273; 171-182.
- Pisano S., Varra M., Micheli E., Coppola T., De Santis P., Mayol L., Savino M., Biophys. Chem. 2008, 136, 159–163.
- Qin Y, Rezler EM, Gokhale V, Sun D, Hurley LH, Nucleic Acids Res. 2007; 35; 7698-7713.
- Rademacher A, Märkle S, Langhals H 1982, Chem Ber 115:2927–2934
- Raggers, R.J., Pomorski, T., Holthuis, J.C., Kalin, N., van Meer, G., Traffic 20001, 226–234.
- Rahe N, Rinn C, Carell Chem. Commun. 2003, 2119-21.
- Rajasingh, P., Cohen, R., Shirman, E., Shimon, L. J. W., Rybtchinski, B., J. Org. Chem. 2007, 72, 5973–5979.
- Rohr U, Kohl C, Mullen K, van de Craats A, Warman J., J. Mater. Chem. 2001; 11; 1789.

- Rohr U, Schlichting P, Bohm A, Gross M, Meerholz K, Brauchle C, Mullen K., Angew. Chem. Int. Ed. 1998, 37, 1434.
- Rossetti L, Franceschin M, Schirripa S, Bianco A, Ortaggi G, Savino M., Bioorganic & Medicinal Chemistry Letters 2005; 15: 413-420.
- Roussel, M.; Lognone, V.; Plusquellec, D.; Benvegnu, T. Chem. Commun. 2006, 3622–3624.
- Ryu J.-H., Hong D.-J., Lee M., Chem. Commun. 2008, 1043 –1054;
- Saha, S., Cai, J., Eiler, D., and Hamilton, A. D. Chem. Commun. 2010, 46, 1685–1687.
- Sandell, J.H., Masland, R., J. Histochem. Cytochem. 1988, 36, 555–559.
- Sandrai M, Hadel L, Sauers RR, Husain S, Krogh-Jespersen K, Westbrook JD, Bird FR., J. Phys. Chem. 1992; 96; 7988.
- Schaffitzel C, Berger I, Postberg J, Hanes J, Lipps HJ, Pluckthun A, Proc. Natl. Acad. Sci. U.S.A. 2001; 98; 8572-8577.
- Schnurpfeil, G. Stark J. Wohrle D., Dyes Pigments, 1995, 27-339.
- Schultze P, Macaya RF, Feigon J., J. Mol. Biol. 1994a; 235; 1532-1547.
- Schultze P, Smith FW, Feigon J., Structure 1994b; 2; 221-233.
- Sen D, Gilbert W A., Nature 1990; 344; 410-414.
- Sen D, Gilbert W., Nature 1988; 334; 364-366.
- Seybold G, Wagenblast G ,1989 Dyes Pigm 11:303–317
- Siddiqui-Jain A, Grand CL, Bearss DJ, Hurley LH, Proc. Natl. Acad. Sci. USA 2002; 99; 11593-11598.
- Simonsson T, Pecinka P, Kubista M., Nucleic Acids Res. 1998; 26; 1167-1172.
- Simonsson T, Sjöback R., J. Biol. Chem. 1999; 274; 17379-17383.
- Sinha, N. D., Biernat, J., McManus, J., Koster, H., Nucleic Acids Res. 1984, 12, 4539–4557.
- Smith FW, Feigon J., Nature 1992; 356; 164-168.
- Spiegel, S., Kassis S., Wilchek M., Fishman P.H.. J. Cell Biol. , 99 1984: 1575-1581.
- Sprott, G. D. J. Bioenerg. Biomembr. 1992, 244, 555–566.
- Stegmann, T., Schoen, P., Bron, R., Wey, J., Bartoldusy, I., Ortiz, A., Nieva, J.L., Wilschut, J., Biochemistry 1993, 32, 11330–11337.
- Struck, D.K., Pagano R.E., Biol. Chem., 255 1980: 5405-5410.
- Struck, D.K., Hoekstra, D., Pagano, R.E., Biochemistry 1981, 20, 4093–4099.
- Sun H, Karow JK, Hickson ID, Maizels N., J. Biol. Chem. 1998; 273; 27587-27592.
- Sun D, Pourpak A, Beetz K, Hurley LH., Clin. Cancer Res. (Supplement) 2003; 9; A218.

- Sun D, Guo K, Rusche JJ, Hurley LH, Nucleic Acids Res. 2005; 33; 6070-6080.
- Tamm, L. K., McConnell H. M.. Biophys. J. , **1985**, 47: 105–113
- Teng Y., Girvan A. C., Casson L. K., Pierce Jr W. M.., Qian M., Thomas S. D., Bates P. J., Cancer Res. 2007, 67, 10491– 10500.
- Tepper, A.D., Ruurs, P., Wiedmer, T., Sims, P.J., Borst, J., van Blitterswijk, W.J., J. Cell Biol. 2000, 150, 155–164.
- Tuesuwan, B., Kern, J. T., Thomas, P. W., Rodriguez, M., Li, J., David, W. M., Kerwin, S. M. Biochemistry **2008,** 47, 1896–1909.
- Van IJzendoorn, S.C.D., Hoekstra, D., J. Cell Biol. 1998, 142, 683–696.
- Vorličcková, M., Chládková, J., Kejnovská, I., Fialová, M., and Kypr, J., Nucleic Acids Res. 2005 33, 5851–5860.
- Wang Y, Patel DJ., Biochemistry 1992; 31; 8112-8119.
- Wang Y, Patel DJ., J. Mol. Biol. 1993a; 234; 1171-1183.
- Wang Y, Patel DJ., Structure 1993b; 1; 263-282.
- Wang KY, McCurdy S, Shea RG, Swaminathan S, Bolton PH A Biochemistry 1993c; 32; 1899-1904.
- Wang Y, Patel DJ., J. Mol. Biol. 1995; 251; 76-94.
- Wang J., Kulago A.,. Browne W. R., Feringa B. L., J. Am. Chem. Soc., 2010, 132, 4191.
- Williamson JR., Rev. Biophys. Biomol. Struct. 1994; 23; 703.
- Williamson JR Guanine quartets Curr. Opin. Struct. Biol. 1993; 3; 357.
- Würthner, F. Kaiser, T. E. Saha-Mçller, C. R. Angew. Chem. 2011, 123, 3436 – 3473; Angew. Chem. Int. Ed. 2011, 50, 3376 – 3410
- Würthner F, Schmidt R. Chem. Phys. Chem. 2006; 7; 793.
- Würthner, F. Chem. Commun., 2004, 14, 1564–1579.
- Würthner F., Thalacker C., Diele S., Tschierske C., Chem. Eur. J., 2001, 7, 2245–2253;
- Yagai S., Seki T., Karatsu T., Kitamura A., Würthner F., Angew. Chem., Int. Ed., 2008, 47, 3367;
- Yang S.K., Zimmermann S. C., Adv. Funct. Mater, 2012, 22, 3023-3028
- Zaug AJ, Podell ER, Cech TR, Proc. Natl. Acad. Sci. U.S.A. 2005; 102; 10864-10869.
- Zhang, G. Jin W., Fukushima T., Kosaka A., Ishii N., Aida T., J. Am. Chem. Soc. 2007, 129, 719 – 722
- Zhao, Q., Li, K., Chen, S., Qin, A., Ding, D., Zhang, S., Liu, Y., Liu, B., Sun, J. Z., Tang B. Z., J. Mater. chem.., 2012, 22, 15128-15135

- Zheng, Y., Long, H., Schatz, G. C., and Lewis, F. D., Chem. Commun. 2005, 38, 4795–4797.
- Zheng, Y., Long, H., Schatz, G. C., and Lewis, F. D., Chem. Commun. 2006, 29, 3830–3832.
- Zollinger H Color Chemistry, 2nd ed.; VCH: Weinheim, 1991
- Zollinger H., Color Chemistry, VCH Verlagsgesellschaft, Weinheim, 1987.
- Zuidam N. J. et Barenholz Y., Biochim. Biophys. Acta, Biomembr., 1997, 1329, 211–222